DD&T

Drug Discoveries & Therapeutics

IRCA
BSSA

IACMHR

www.ddtjournal.com

Drug Discoveries & Therapeutics is one of a series of peer-reviewed journals of the International Research and Cooperation Association for Bio & Socio-Sciences Advancement (IRCA-BSSA) Group and is published bimonthly by the International Advancement Center for Medicine & Health Research Co., Ltd. (IACMHR Co., Ltd.) and supported by the IRCA-BSSA and Shandong University China-Japan Cooperation Center for Drug Discovery & Screening (SDU-DDSC).

Drug Discoveries & Therapeutics publishes contributions in all fields of pharmaceutical and therapeutic research such as medicinal chemistry, pharmacology, pharmaceutical analysis, pharmaceutics, pharmaceutical administration, and experimental and clinical studies of effects, mechanisms, or uses of various treatments. Studies in drug-related fields such as biology, biochemistry, physiology, microbiology, and immunology are also within the scope of this journal.

Drug Discoveries & Therapeutics publishes Original Articles, Brief Reports, Reviews, Policy Forum articles, Case Reports, News, and Letters on all aspects of the field of pharmaceutical research. All contributions should seek to promote international collaboration in pharmaceutical science.

Editorial Board

Drug Discoveries & Therapeutics

Editorial and Head Office

Pearl City Koishikawa 603, 2-4-5 Kasuga, Bunkyo-ku, Tokyo 112-0003, Japan

Tel: +81-3-5840-9697, Fax: +81-3-5840-9698
E-mail: office@ddtjournal.com
URL: www.ddtjournal.com

Editorial Board Members

CONTENTS

Volume 6, Number 6, 2012

Review

Original Articles

CONTENTS   (*Continued*)

Letter

Index

Acknowledgements (online)

Guide for Authors

Copyright

Review of drugs for Alzheimer's disease

Xiaoting Sun[1], Lan Jin[2,*], Peixue Ling[1,3]

[1] *Institute of Biochemical and Biotechnological Drugs, School of Pharmaceutical Science, Shandong University, Ji'nan, Shandong, China;*
[2] *National Glycoengineering Research Center, Shandong University, Ji'nan, Shandong, China;*
[3] *Institute of Biopharmaceuticals of Shandong Province, Ji'nan, Shandong, China.*

ABSTRACT: Alzheimer's disease (AD) is the most common form of dementia in the elderly. The number of people affected by AD is rapidly increasing. AD is characterized by cerebral atrophy, cerebral senile plaques, intraneuronal neurofibrillary tangles, and neuronal cell loss. Medical treatment of AD has a long history and differing results. We will review the effectiveness and limitations of the drugs used to treat AD.

Keywords: Alzheimer's disease, treatment, drugs

1. Introduction

Many age-related neurodegenerative diseases such as Alzheimer's disease (AD), amyotrophic lateral sclerosis (ALS), and Parkinson's disease represent a huge challenge for patients and caregivers (*1*). Of these, AD is the most common form of dementia in the elderly (*2*). AD is a progressive disorder (*3*) that affects 2% of the population in industrialized countries. More than 10% of the population over the age of 65 and 50% of the population over the age of 85 are suffering from AD (*4*). As the population ages, this number will double every twenty years, likely increasing to more than 80 million cases by the year 2040 (*5*).

　　AD is characterized by a series of neuropathologic changes, including cerebral atrophy, cerebral senile plaques containing extracellular deposits of β-amyloid peptide (Aβ), intraneuronal neurofibrillary tangles (NFTs) containing hyperphosphorylated tau protein, and neuronal cell loss (*6,7*). These result in patients suffering from memory loss, confusion, impaired judgment, disorientation, and trouble expressing themselves. The symptoms worsen over time and the disease is fatal.

*Address correspondence to:
Dr. Lan Jin, National Glycoengineering Research
Center, Shandong University, No 44, West Wenhua
Road, Ji'nan 250012, Shandong, China.
E-mail: lanjin@sdu.edu.cn

It disrupts the normal lives of patients and poses a substantial economic burden to family and society (*8*). Therefore, AD has garnered increasing attention in terms of its diagnosis, pathological mechanism, and therapeutic agents. The current article reviews the pathological mechanism of AD and drugs used to treat AD and it discusses the effectiveness and limitations of these drugs.

2. The neuropathology of Alzheimer's disease

The neuropathology of AD is very complex and has yet to be completely understood. There are several hypotheses that try to explain the pathological mechanism of the disease.

2.1. *Cholinergic dysfunction of the central nervous system*

Early studies showing loss of cholinergic activity in central nervous system (CNS) as AD progresses have been corroborated by numerous studies thus far. The brains of AD patients have very low levels of acetylcholine (ACh) (*9*). According to some pathophysiology research, the loss of cholinergic neurons usually occurs in brain areas associated with memory and learning, such as the hippocampus, nucleus basalis of Meynert, and cortex. A reduction in cholinergic activity is thus thought to be associated with cognitive deficits (*10*). This reduced activity affects synaptic transmission and initiates inflammatory processes. Some reactive oxygen species will be produced, resulting in cell death. Furthermore, Aβ can inhibit cholinergic neurons from absorbing choline and halt the action of cholinergic acetyltransferase (chAT), which inhibit the generation of ACh (*11*). However, whether the decrease in ACh is the cause of AD needs to be studied further.

2.2. *The amyloid cascade hypothesis*

2.2.1. *Amyloid precursor protein (APP) processing*

In humans, *APP* gene is located on chromosome 21. It has 3 major forms: APP695, APP751, and APP770.

The APP protein consists of 695-770 amino acids. It is a transmembrane glycoprotein that exists widely in human histiocytosis. It is widely expressed in the brain and functions as a membrane receptor (*12*). It undergoes cleavage by three types of enzymes: α-secretase, β-secretase, and γ-secretase (Figure 1). The sequential cleavage of APP by α-secretase and γ-secretase produces two soluble peptides, referred to as P3 and sAPPα. The sequential cleavage of APP by β-secretase and γ-secretase generates sAPPβ and insoluble Aβ, respectively. Under normal conditions, APP is cleaved *via* the first pathway. In contrast to Aβ, sAPPα has an important role in maintaining the activity of neurons. It can protect neurons against excitotoxicity and regulate neural stem cell proliferation (*13*).

2.2.2. *The structure of Aβ*

Aβ is an approximately 40-residue-long peptide. Its molecular weight is ~4,000. There are two main forms of Aβ, $Aβ_{40}$ and $Aβ_{42}$. $Aβ_{42}$ is more hydrophobic and more prone to aggregate and is considered to be the most neurotoxic form. The forms differ in their terminal carbon structures (Figure 2). $Aβ_{42}$ is the major component of

senile plaques (SP) (*14*). In a normal brain, the majority of Aβ produced is $Aβ_{40}$, while patients with AD have a high ratio of $Aβ_{42}/Aβ_{40}$. In the brain, Aβ exists in soluble and fibril forms. Formation of Aβ fibrils is a multi-step process that requires a conformational change from an α-helical to β-pleated sheet structure. Many studies have confirmed that the neurotoxicity of Aβ is largely dependent on its ability to form β-sheet structures (*15*).

2.2.3. *Aβ function*

Many studies have found that overproduction of Aβ results in a neurotoxic effect on neurons. It leads to synaptic dysfunction (*16*) and formation of intraneuronal fibrillary tangles (*17*) and eventually to neuron loss. Soluble Aβ can stimulate neurite growth in a short amount of time, which can increase neurons' survival rate. However, deposited Aβ has the opposite effect on neurons. It can cause the shrinkage of neurites and denaturing of neurons (*18*). Although the overproduction of Aβ has a negative effect on nerve cells, low levels of Aβ can increase hippocampal long-term potentiation and enhance memory.

2.2.4. *The mechanism of Aβ neurotoxicity*

Ca^{2+} is a second messenger in organisms. The extracellular concentration of Ca^{2+} is higher than that of intracellular Ca^{2+}. Aβ can disrupt the calcium channels in the cell membrane, enhancing Ca^{2+} influx and leading to the disequilibrium of calcium. An intracellular Ca^{2+} overload will impair the ability of mitochondria to buffer or cycle Ca^{2+}, resulting in cell toxicity and eventual cell death. The disruption in calcium homeostasis may in turn cause a variety of secondary effects such as lipid peroxidation and generation of free radicals. Over time, these related actions of Aβ will reduce synaptic integrity (*19,20*).
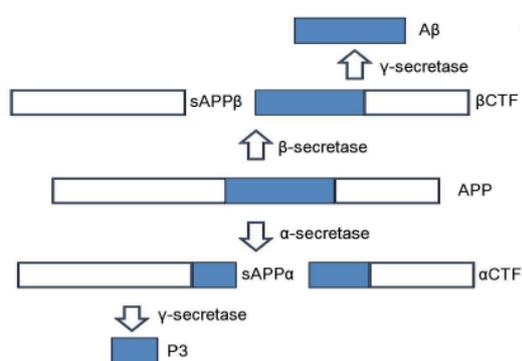

Figure 1. Diagram of APP processing.
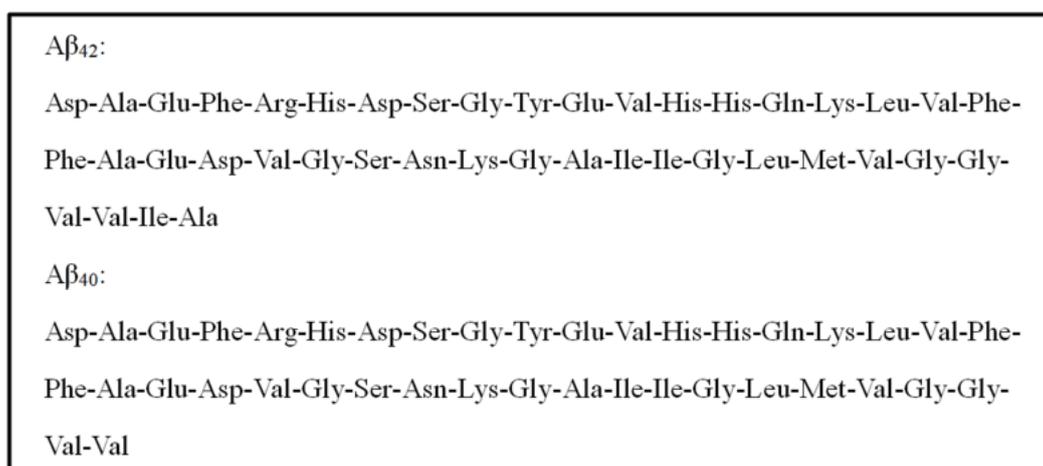
Figure 2. The structures of $Aβ_{42}$ and $Aβ_{40}$. $Aβ_{40}$ has two fewer amino acids than $Aβ_{42}$ at the C-terminal end.

2.3. *Neuroinflammation in AD*

Inflammation is one of the secondary effects of Aβ deposition. In the brain, it is characterized by activation of glial cells and expression of key inflammatory mediators. This inflammation is chronic. The cells participating in the action are mainly microglia and astrocytes. They participate in initiation and progression of neurological disorders by releasing cytotoxic molecules such as proinflammatory cytokines, reactive oxygen intermediates, proteinases, and complement proteins. In one form of attack, the activated glial cells kill neurons nearby by releasing reactive oxygen species (ROS), NO, and proteinase that cause neurotoxicity (*21*). In a second form of attack, an inflammatory reaction can stimulate the regeneration of Aβ, aggravating the inflammation and forming a vicious cycle (*22*).

2.4. *Other pathogeneses*

An increasing risk factor for AD is ApoE, which is a 34 kDa glycoprotein. It facilitates neuronal repair, it has anti-inflammatory properties, and it facilitates dendritic growth. In humans, there are three major forms of ApoE: ApoE2, ApoE3, and ApoE4. ApoE4 is reported to be associated with AD (*23*). It can promote amyloid deposition, neurotoxicity, oxidative stress, neurofibrillary tangle formation, and increasing brain inflammation. Previous studies have shown that ApoE4 causes mitochondrial damage, microvascular generation, and neural injury (*24*).

In addition, hypercholesterolemia is considered to be a risk factor for AD (*25*). People with a rare mutation in the *APP*, presenilin-1 (*PSEN1*), and presenilin-2 (*PSEN2*) genes are usually at greater risk for developing hypercholesterolemia (*26*). Additionally, several environmental agents, including metals (Al^{3+} (*27*), Hg^{2+} (*28*)), pesticides, dietary factors, and brain injuries, have been suggested as possible risk factors for AD.

3. Drugs used to improve cholinergic function

Many drugs have been approved for AD treatment in different stages of the disease, although they all have limited efficacy. The AD process has an apparent linear relationship to the pathological changes in the human brain, indicating that the disease can be halted by medication that interferes with the different stages. Many drugs have been used to improve cholinergic function in patients.

3.1. *Acetylcholinesterase inhibitors*

Acetylcholinesterase inhibitors were the first drugs approved by the FDA to treat AD, representing obvious progress in treatment of the disease. Tacrine, approved by the FDA in 1993, is the first drug used in AD treatment as an acetylcholinesterase inhibitor. The mechanism by which tacrine causes damage is not completely understood and it consistently causes a number of adverse reactions. Tacrine is now rarely used in AD treatment (*29*) due to its hepatotoxicity.

Donepezil is another acetylcholinesterase inhibitor. It is readily absorbed after oral administration. Compared to tacrine, its effects last longer (Table 1). It is better tolerated

Table 1. Comparison of pharmacological characteristics of 5 acetylcholinesterase inhibitors

	Tacrine	Donepezil	Rivastigmine	Galantamine	Huperzine A
Structure					
Target enzymes	AChE and BuChE	AChE	AChE and BuChE	AChE	AChE
Recommended dosage	160 mg/day (four times daily)	10 mg/day (once daily)	9.5 mg/24 h patch (once daily) 12 mg/day (twice daily)	24 mg/day (twice daily)	0.4 mg/day (twice daily)
Plasma half-life	2-4 h	About 70 h	About 3 h (patch) About 1 h (capsule)	About 7 h	About 60 h
Period of disease treatment	—	All stages of Alzheimer's disease	Mild to moderate Alzheimer's disease	Mild to moderate Alzheimer's disease	Mild to moderate Alzheimer's disease
AChE IC_{50} (nM)	190	22	48,000	800	47
BuChE IC_{50} (nM)	47	4.1	54,000	73,000	30
Adverse reactions	Hepatotoxicity	Diarrhea, nausea	Diarrhea, nausea	Nausea, weight loss	Nausea
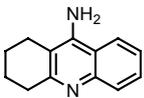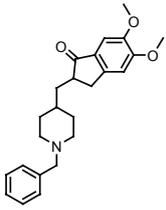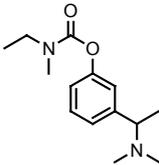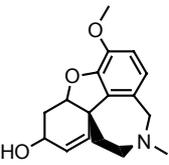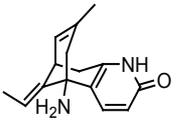
by patients and causes fewer adverse reactions. Adverse reactions to the drug are primarily nausea, dizziness, diarrhea, and anorexia. All of these are dose-dependent (*30*). A number of clinical trials suggest that it can effectively improve cognitive performance and stabilize the functional ability of patients. It is used to treat mild to moderate AD (*31*).

Rivastigmine is a carbamate derivative. It can reversibly inhibit both acetyl- and butyryl-cholinesterase (AChE and BuChE, respectively). After oral administration, it reaches its peak plasmatic concentration in one hour (*32*). It is the only drug in which cytochrome P450 isoenzymes are not involved in its metabolism, so it can minimize drug-drug interactions. Many clinical trials suggest that rivastigmine has a significant effect on memory and the praxis domains of cognition. Unlike rivastigmine capsules, rivastigmine patches have a significant effect on the language domain. These patches can be used to treat patients with mild to moderate AD (*33*).

Galantamine is an extract of the flowers and bulbs of lilies, daffodils, and related plants. It is a selective acetylcholinesterase inhibitor. It improves cognitive dysfunction and affords neuronal protection, preventing the cytotoxicity caused by aggregation of Aβ (*34*). It is also believed to enhance central neurotransmission. The clinical efficacy of galantamine is almost equivalent to that of donepezil (*35*).

Huperzine A is a plant-based alkaloid from a plant named *Huperzia serrata*. It is an effective AChE inhibitor that can cross the blood-brain barrier (BBB). Huperzine A provides neuroprotection against neuronal damage. It has stronger inhibition and better selectivity than tacrine and galantamine (*36*).

In addition to the aforementioned drugs, many acetylcholinesterase inhibitors are used to treat AD, such as metrifonate and physostigmine and its derivatives. These drugs may provide protection against oxidative stress and Aβ toxicity. Although they increase synaptic transmission, acetylcholinesterase inhibitors also have several limitations. They are expensive and usually provide limited benefits. They may damage the neuronal membrane and more guidance is needed regarding their clinical use.

3.2. *M₁ receptor agonists*

M_1 muscarinic receptors remain mostly intact in the brains of AD patients. Therefore, M_1 receptors are considered to be an attractive therapeutic target for AD treatment. M_1 receptor agonists ameliorate the symptoms of AD and also delay the disease's progression. Several such drugs are used to treat AD, such as xanomeline (*37*) and milameline.

Xanomeline is a function selective muscarinic M_1/M_4-preferring receptor agonist. It can cross the BBB. Many clinical studies have noted significant improvement in the cognitive function of patients

with AD. The drug's most common adverse effects are gastrointestinal response and cardiovascular adverse reactions.

4. Anti-Aβ drugs

β-Amyloid peptides are the main contributors to the pathology of AD. Many studies have found that overproduction of Aβ results in a neurotoxic effect on neurons. It leads to synaptic dysfunction, formation of intraneuronal fibrillary tangles (*17*), and eventually neuron loss. The deposited Aβ can cause the shrinkage of neurites and denaturing of neurons. Aβ can disrupt the calcium channels in the cell membrane, enhancing Ca^{2+} influx and leading to the disequilibrium of calcium. Therefore, anti-Aβ drugs may be the most effective drugs for AD treatment.

4.1. *Calcium antagonists*

An overload or insufficiency of calcium in nerve cells affects the production, transmission, and release of neurotransmitters. Drugs widely used in AD treatment as calcium antagonists are nimodipine, flunarizine, verapamil, and tetrandrine.

Nimodipine (*38*) is an L-type calcium channel antagonist. It is highly lipophilic and it can readily cross the BBB and effectively inhibit calcium influx, enhancing blood flow in the brain. It appears to be tolerated well by patients with fewer adverse reactions (*39*).

4.2. *Antioxidants*

Antioxidants can prevent the degeneration of nerve cells by eliminating active oxygen or preventing its generation. Vitamin E is the most commonly used antioxidant. It is a lipophilic vitamin. Many clinical trials have suggested that it can prevent oxidative action. It can decrease cellular death induced by Aβ and attenuate toxicity in neuroblastoma cells (*40*).

There are other common clinical antioxidant drugs, such as selegiline and melatonin. Selegiline is a selective monoamine antioxidant. It does help somewhat to improve the cognition, behavior, and mood of patients. However it does not globally benefit cognition, functional ability, and behavior (*41*). Melatonin functions by regulating circadian rhythms, clearing free radicals (*42*), improving immunity (*43*), and generally inhibiting the oxidation of biomolecules. It also has significant anti-amyloidogenic action. It prevents Aβ fibrillogenesis and aggregation by disrupting the imidazole-carboxylate salt bridge (*44*).

4.3. *Nonsteroidal anti-inflammatory drugs*

Many clinical studies have suggested that nonsteroidal anti-inflammatory drugs (NSAIDs) could be used

to prevent rather than treat AD. The mechanism of NSAIDs might be by inhibiting inflammation associated with the generation of SP (*45*). NSAIDs include indomethacin, tenidap, aspirin, ibuprofen, and naproxen (*46*). However, NSAIDs are known for their liver and kidney toxicity.

4.4. *Hypolipidemic drugs*

The expression of ApoE can lead to Aβ deposition and the formation of amyloid plaques. Nowadays, the use of ApoE isomers can effectively reduce the formation of amyloid plaques.

4.5. *Iron chelators*

High levels of iron have been found in both SP and NTFs in the brain. Ions may be involved in free radical formation and neuron degeneration. They may bind tightly to Aβ, possibly causing damage to neurons.

Treatment with iron chelators aims to remove excess iron that causes neurotoxicity in brain tissue. Iron chelators have a high affinity for iron. As an example, desferrioxamine, a natural iron scavenger, is a specific chelator with a high affinity for aluminum, copper, and zinc. Desferrioxamine is widely used in the treatment of AD (*47*). However, it requires continuous dosing due to its short circulating half-life. A drawback, however, is that it can cause serious adverse reactions such as injection site reactions and retinal toxicity (*48*).

5. Vaccines

Immunotherapy may be one of the most promising approaches to preventing the aggregation of Aβ (*49*). Many clinical trials have shown that anti-Aβ antibodies are effective in clearing Aβ deposits. Vaccination therapy for AD was invented by Dale Schenk and his colleagues in 1999 (*50*). They found that amyloid deposits were significantly reduced when they immunized young APP transgenic mice with Aβ and an adjuvant. The first clinical trial vaccine was AN-1792, which consisted of synthetic Aβ and adjuvant QS21. Patients who were suffering mild-to-moderate AD were treated with this vaccine. The trial was halted because 6% of patients developed subacute meningoencephalitis after one to three intramuscular injections of the vaccine. The meningoencephalitis was believed to be caused by a T cell-mediated autoimmune response. Many passive immunization clinical trials using anti-Aβ antibodies are now underway. There are many challenges to developing future Aβ vaccines. For example, a vaccine should help to prevent the disease in the early stages and it should be inexpensive; antigen targets should also be appropriately selected. Moreover, it should be efficacious in patients regardless of their immune status and it should facilitate compliance.

6. Conclusion and perspectives for the future

AD is a nervous system disease that exists in patients for many years. Many efforts are currently underway to explore the pathology of AD and develop appropriate treatments. These strategies focus on slowing disease progression and maintaining patients' quality of life. Nonetheless, there is no treatment that effectively stops the disease's progression. Accurate diagnosis of AD is problematic. Therefore, researchers need to recognize early signs of AD and explore new therapies to combat AD.

Acknowledgements

References

1. Hu WT, Chen-Plotkin A, Arnold SE, Grossman M, Clark CM, Shaw LM, McCluskey L, Elman L, Karlawish J, Hurtig HI, Siderowf A, Lee VM, Soares H, Trojanowski JQ. Biomarker discovery for Alzheimer's disease, frontotemporal lobar degeneration, and Parkinson's disease. Acta Neuropathol. 2010; 120:385-399.
2. Forlenza OV, Diniz BS, Gattaz WF. Diagnosis and biomarkers of predementia in Alzheimer's disease. BMC Med. 2010; 8:89-102.
3. Sabbagh M, Cummings J. Progressive cholinergic decline in Alzheimer's disease: Consideration for treatment with donepezil 23 mg in patients with moderate to severe symptomatology. BMC Neurol. 2011; 11:21-26.
4. Zhang YW, Thompson R, Zhang H, Xu H. APP processing in Alzheimer's disease. Mol Brain. 2011; 4:3-15.
5. Massoud F, Gauthier S. Update on the pharmacological treatment of Alzheimer's disease. Curr Neuropharmacol. 2010; 8:69-80.
6. Amatsubo T, Yanagisawa D, Morikawa S, Taguchi H, Tooyama I. Amyloid imaging using high-field magnetic resonance. Magn Reson Med Sci. 2010; 9:95-99.
7. Wang JM, Sun C. Calcium and neurogenesis in Alzheimer's disease. Front Neurosci. 2010; 4:194-198.
8. Coppede F. One-carbon metabolism and Alzheimer's disease: Focus on epigenetics. Curr Genomics. 2010; 11:246-260.
9. Wollen KA. Alzheimer's disease: The pros and cons of pharmaceutical, nutritional, botanical, and stimulatory therapies, with a discussion of treatment strategies from the perspective of patients and practitioners. Altern Med Rev. 2010; 15:223-244.
10. Mufson EJ, Counts SE, Perez SE, Ginsberg SD. Cholinergic system during the progressing of Alzheimer's disease: Therapeutic implications. Expert Rev Neurother. 2008; 8:1703-1718.
11. Watanabe T, Iwasaki K, Ishikane S, Naitou T, Yoshimitsu Y, Yamagata N, Ozdemir MB, Takasaki K, Egashira N, Mishima K, Fujiwara M. Spatial memory impairment without apoptosis induced by the combination of β-amyloid oligomers and cerebral ischemia is related to decreased acetylcholine release in rats. J Pharmacol Sci. 2008; 106:84-91.
12. Bekris LM, Yu CE, Bird TD, Tsuang DW. Genetics of

Alzheimer disease. J Geriatr Psychiatry Neurol. 2010; 23:213-227.

13. Pagani L, Eckert A. Amyloid-β interaction with mitochondria. Int J Alzheimers Dis. 2011; 10:1-11.

14. Li T, Zhao ZX. β-Amyloid and Alzheimer disease: Recent progress. Acad J Second Mil Med Univ. 2010; 31:1133-1137.

15. He H, Dong W, Huang F. Anti-amyloidogenic and anti-apoptotic role of melatonin in Alzheimer disease. Curr Neuropharmacol. 2010; 8:211-217.

16. Ondrejcak T, Klyubin I, Hu NW, Barry AE, Cullen WK, Rowan MJ. Alzheimer's disease amyloid β-protein and synaptic function. Neuromolecular Med. 2010; 12:13-26.

17. Giaccone G, Pedrotti B, Miqheli A, *et al*. βPP and Tau interaction. A possible link between amyloid and neurofibrillary tangles in Alzheimer's disease. Am J Pathol. 1996; 148:79-87.

18. Armstrong RA. The pathogenesis of Alzheimer's disease: A reevaluation of the "amyloid cascade hypothesis". Int J Alzheimers Dis. 2011; 10:1-6.

19. Supnet C, Bezprozvanny I. Neuronal calcium signaling, mitochondrial dysfunction, and Alzheimer's disease. J Alzheimers Dis. 2010; 20:487-498.

20. Itkin A, Dupres B, Dufrene YF, Bechinger B, Ruysschaert JM, Raussens V. Calcium ions promote formation of amyloid β-peptide (1-40) oligomers causally implicated in neuronal toxicity of Alzheimer's disease. PLoS One. 2011; 6:1-10.

21. Ramberg V, Tracy LM, Samuelsson M, Nilsson LN, Iverfeldt K. The CCAAT/enhancer binding protein (C/EBP) δ is differently regulated by fibrillar and oligomeric forms of the Alzheimer amyloid-β peptide. J Neuroinflammation. 2011; 8:34-60.

22. Lei LW, Wang Y. Progress of pathogenesy and inflammation in Alzheimer's disease. Med Recap. 2008; 14:3041-3043.

23. Nishitsuji K, Hosono T, Nakamura T, Bu G, Michikawa M. Apolipoprotein E regulates the integrity of tight junctions in an isoform-dependent manner in an *in vitro* blood-brain-barrier model. J Biol Chem. 2011; 286:17536-17542.

24. Altman R, Rutledge JC. The vascular contribution to Alzheimer's disease. Clin Sci. 2010; 119:407-421.

25. Bates KA, Sohrabi HR, Rodrigues M, *et al*. Association of cardiovascular factors and Alzheimer's disease plasma amyloid-β protein in subjective memory complainers. J Alzheimers Dis. 2009; 17:305-318.

26. Zhuang Y, Chen J. Research process on causes and mechanism of Alzheimer's Disease. J Jilin Med Col. 2008; 29:101-104.

27. Kawahara M, Kato-Negishi M. Link between aluminum and the pathogenesis of Alzheimer's disease: The integration of the aluminum and amyloid cascade hypotheses. Int J Alzheimers Dis. 2011; 10:1-17.

28. Mutter J, Curth A, Naumann J, Deth R, Walach H. Does inorganic mercury play a role in Alzheimer's disease? A systematic review and an integrated molecular mechanism. J Alzheimers Dis. 2010; 22:357-374.

29. Wu TY, Chen CP, Jinn TR. Alzheimer's disease: Aging, insomnia and epigenetics. Taiwan J Obstet Gynecol. 2010; 49:468-472.

30. Aranda-Abreu GE, Hernandez-Aquilar ME, Denes JM, Garcia Hernandez LI, Rivero MH. Rehabilitating a brain with Alzheumer's: A proposal. Clin Interv Aging. 2011; 6:53-59.

31. Benjamin B, Burns A. Donepezil for Alzheimer's disease. Expert Rev Neurother. 2007; 7:1243-1249.

32. Kurz A, Farlow M, Lefevre G. Pharmacokinetics of a novel transdermal rivastigmine patch for the treatment of Alzheimer's disease: A review. Int J Clin Pract. 2009; 63:799-805.

33. Grossberg GT, Schmitt FA, Meng X, Tekin S, Olin J. Reviews: Effects of transdermal rivastigmine on ADAS-cog items in mild-to-moderate Alzheimer's disease. Am J Alzheimers Dis Other Demen. 2010; 25:627-633.

34. Ago Y, Koda K, Takuma K, Matsuda T. Pharmacological aspects of the acetylcholinesterase inhibitor galantamine. J Pharmacol Sci. 2011; 116:6-17.

35. Seltzer B. Galantamine-ER for the treatment of mild-to-moderate Alzheimer's disease. Clin Interv Aging. 2010; 5:1-6.

36. Zheng R, Su YF. Research progress of clinical use of Huperzine A. Pract Pharm Clin Remedies. 2008; 11:107-108.

37. Jakubik J, Michal P, Machova E, Dolezal V. Importance and prospects for design of selective muscarinic agonists. Physiol Res. 2008; 57(Suppl 3):39-47.

38. Disterhoft JF, Oh MM. Pharmacological and molecular enhancement of learning in aging and Alzheimer's disease. J Physiol Paris. 2006; 99:180-192.

39. Lopez-Arrieta JM, Birks J. Nimodipine for primary degenerative, mixed and vascular dementia. Cochrane Database Syst Rev. 2002; 3:CD000147.

40. Mas E, Dupuy AM, Artero S, Portet F, Cristol JP, Ritchie K, Touchon J. Functional vitamin E deficiency in ApoE4 patients with Alzheimer's disease. Dement Geriatr Cogn Disord. 2006; 21:198-204.

41. DelaGarza VW. Pharmacologic treatment of Alzheimer's disease: An update. Am Fam Physician. 2003; 68:1365-1372.

42. Wang X. The anti-apoptotic activity of melatonin in neurodegenerative diseases. CNS Neurosci Ther. 2009; 15:345-357.

43. Esposito E, Cuzzocrea S. Antiinflammatory activity of melatonin in central nervous system. Curr Neuropharmacol. 2010; 8:228-242.

44. He H, Dong W, Huang F. Anti-amyloidogenic and anti-apoptotic role of melatonin in Alzheimer disease. Curr Neuropharmacol. 2010; 8:211-217.

45. Krause DL, Muller N. Neuroinflammation, microglia and implications for anti-inflammatory treatment in Alzheimer's disease. Int J Alzheimers Dis. 2010; 10:1-9.

46. Davies P, Koppel J. Mechanism-based treatment for Alzheimer's disease. Dialogues Clin Neurosci. 2009; 11:159-169.

47. Liu G, Men P, Perry G, Smith MA. Nanoparticle and iron chelators as a potential novel Alzheimer therapy. Methods Mol Biol. 2010; 610:123-144.

48. Oshiro S, Morioka MS, Kikuchi M. Dysregulation of iron metabolism in Alzheimer's disease, Parkinson's disease, and amyotrophic lateral sclerosis. Adv Pharmacol Sci. 2011; 10:1155-1163.

49. Xing XN, Zhang WG, Sha S, Li Y, Guo R, Wang C, Cao YP. Amyloid β 3-10 DNA vaccination suggests a potential new treatment for Alzheimer's disease in BALB/c mice. Chin Med J (Engl). 2011; 124:2636-2641.

50. Xing XN, Zhang WG, Sha S, Li Y, Guo R, Wang C, Cao YP. Amyloid β3-10 DNA vaccination suggests a potential new treatment for Alzheimer's disease in BALB/c mice. Chin Med J. 2011; 124:2636-2641.

Role of NPxY motif in Draper-mediated apoptotic cell clearance in *Drosophila*

Yu Fujita, Kaz Nagaosa, Akiko Shiratsuchi, Yoshinobu Nakanishi*

Graduate School of Medical Sciences, Kanazawa University, Kanazawa, Ishikawa, Japan.

ABSTRACT: Draper, a receptor responsible for the phagocytosis of apoptotic cells in *Drosophila*, possesses atypical epidermal growth factor (EGF)-like sequences in the extracellular region and the two phosphorylatable motifs NPxY and YxxL in the intracellular portion. We previously suggested that Pretaporter, a ligand for Draper, binds to the EGF-like repeat and augments the tyrosine phosphorylation of Draper. In this study, we first tested the binding of Pretaporter to various parts of the extracellular region of Draper and found that a single EGF-like sequence is sufficient for the binding. We next determined roles of the two intracellular motifs by forcedly expressing Draper proteins, in which tyrosine residues within the motifs had been substituted with phenylalanine, in hemocytes of Draper-lacking flies. We found that Draper proteins with Y-to-F substitution in either motif still underwent tyrosine phosphorylation, suggesting the occurrence of phosphorylation at both motifs. The Draper protein with substitution in the YxxL motif rescued a defect of phagocytosis, as did intact Draper, but the Draper protein with substitution in the NPxY motif did not, indicating a role of the motif NPxY, but not YxxL, in Draper-mediated phagocytosis. This coincides with our previous finding that Ced-6, an NPxY-binding signaling adaptor, is required for Draper's actions in apoptotic cell clearance. In summary, we demonstrated that Draper binds to its ligand Pretaporter using EGF-like sequences, and that the NPxY motif in the intracellular region of Draper plays an essential role in its actions as an engulfment receptor.

Keywords: Apoptosis, phagocytosis, tyrosine phosphorylation

**Address correspondence to:*
Dr. Yoshinobu Nakanishi, Graduate School of Medical Sciences, Kanazawa University, Shizenken, Kakuma-machi, Kanazawa, Ishikawa 920-1192, Japan.
E-mail: nakanaka@p.kanazawa-u.ac.jp

1. Introduction

The cells that constitute our body often become effete or harmful. Such altered own cells are induced to undergo apoptosis and become susceptible to phagocytosis (*1-4*). Most apoptotic cells expose substances that serve as ligands for receptors of phagocytes leading to engulfment (*1-4*). Genetic studies with *Caenorhabditis elegans* have shown the existence of two signaling pathways for the induction of phagocytosis (*5-8*). These pathways, namely, CED-6/CED-7/CED-10 and CED-2/CED-5/CED-12/CED-10, are most likely governed by the engulfment receptors CED-1 (*9*) and INA-1 (*10*), respectively. CED-1 is a single-path membrane protein containing atypical epidermal growth factor (EGF)-like sequences (*9*), and INA-1 is a α-subunit of *C. elegans* integrins (*10*). CED-1 (*11*), integrins (*12*), and the intracellular signaling molecules in the above two pathways (*8,13*) seem to be evolutionarily conserved among species including humans. This suggests the phylogenetic conservation of the mode of apoptotic cell clearance.

We (*14*) and other investigators (*15*) have reported the participation of the CED-1 orthologue Draper in the phagocytic elimination of apoptotic cells by hemocytes and glia of *Drosophila melanogaster*. Draper is also responsible for the remodeling of neural circuits: removal of axons (*16,17*) and dendrites (*18*) of larval neurons during metamorphosis, axons in injury-induced Wallerian degeneration (*17,19*), and presynaptic membranes at neuromuscular junctions (*20*). The extracellular portion of Draper contains three cysteine-rich sequences that are shared with many other proteins, namely, the EMI, NIM, and EGF-like domains (*11,21*). We previously reported that a recombinant Draper protein corresponding to the entire EGF-like repeat binds Pretaporter, an endoplasmic reticulum protein that serves as a ligand for Draper, and that the binding of Pretaporter augments the tyrosine phosphorylation of Draper (*22*). There are two phosphorylatable tyrosine residues, which are contained in the motifs NPxY and YxxL, within the intracellular region of Draper. The NPxY motif serves as a binding site for proteins that possess the phosphotyrosine-binding (PTB) domain. In fact, the human orthologue of CED-6, which contains the PTB domain, interacts

with CED-1 through binding to the NPxY motif (*23*). In addition, we previously showed that Draper requires Ced-6 to induce the phagocytosis of apoptotic cells in embryos (*22*). The other motif YxxL is a part of the immunoreceptor tyrosine-based activation motif and serves as a site for binding of proteins containing the Src homology 2 domain (*24*). The importance of YxxL in Draper has been reported for the phagocytic elimination of injured axons by glia (*25*). It is thus likely that both motifs play roles in Draper-mediated phagocytosis. The present study was carried out to determine which region of the extracellular portion of Draper is responsible for the binding to Pretaporter as well as which of the two intracellular motifs is phosphorylated and required for Draper's actions.

2. Materials and Methods

2.1. *Fly stocks and cell culture*

The following lines of *Drosophila* were used: w^{1118}, $drpr^{\Delta 5}$ (*15,26*), *srpHemoGAL4 UAS-srcEGFP* (*29*), *w*; +; *Dr/TM6B Dfd-GMR-nvYFP* (Bloomington Drosophila Stock Center, Indiana University, Bloomington, IN, USA), and *C(1)DX/FM7*; +; *Sb/TM3* (a gift from T. Awasaki). To establish fly lines expressing Draper proteins with amino acid alterations, the *Drosophila* EST clone GH03529 (Berkeley Drosophila Genome Project and National Institute of Genetics), in which nucleotide sequences had been modified so that tyrosine residues in the NPxY and YxxL motifs were changed to phenylalanine, was placed downstream of the *UAS* sequence and used to generate transgenic flies. The resulting flies together with one possessing intact *draper* were intercrossed with the *draper* null mutant $drpr^{\Delta 5}$ and used for mating with *srpHemoGAL4 UAS-srcEGFP*, a GAL4 driver for the hemocyte-specific expression of *UAS*-transgenes. Other flies used in this study were generated through the mating of existing flies. Genotypes of the fly lines analyzed are shown in the corresponding figure captions. The hemocyte-derived cell line l(2)mbn was maintained at 25°C with Schneider's Drosophila medium (Life Technologies Japan, Tokyo, Japan), as described previously (*14*). Sf9 insect cells were maintained at 29°C with Grace's Insect medium (Life Technologies Japan) supplemented with 10% (v/v) heat-inactivated fetal bovine serum.

2.2. *Assay for protein-protein interaction*

Various regions within the extracellular portion of Draper fused to glutathione *S*-transferase (GST) at the N-terminus were prepared using the baculovirus-based vector system (Life Technologies Japan) and Sf9 cells, and affinity-purified by glutathione-Sepharose chromatography (GE Healthcare Japan, Tokyo, Japan), essentially as described previously (*22*). Pretaporter fused to maltose-binding protein (MBP) was prepared and purified as reported previously (*22*). The GST-fused Draper proteins were mixed with MBP-tagged Pretaporter (at an equal molar concentration) in a buffer consisting of 15 mM PIPES (pH 6.5), 0.1 M NaCl, 20 mM KCl, 20 mM MgSO$_4$, and 10 mM CaCl$_2$, precipitated with glutathione-sepharose, and analyzed by Western blotting for the co-precipitation of MBP-Pretaporter using the anti-MBP antibody.

2.3. *Assay for tyrosine phosphorylation*

The EST clone GH03529 and the plasmid pUAST (*28*) were used to prepare vectors to express HA-tagged Draper proteins with altered NPxY and YxxL motifs as well as with unaltered motifs. l(2)mbn cells were transfected with these vectors together with pAct5C-GAL4 (a gift from M. Miura), a GAL4 driver for the ubiquitous expression of *UAS*-transgenes, by lipofection (Cellfectin II; Life Technologies Japan) and cultured for 2 days. The cells were then lysed with a buffer consisting of 40 mM Tris-HCl (pH 7.5), 0.15 M NaCl, 1 mM EDTA, 2% (w/v) CHAPS, protease inhibitors (Nakalai Tesque, Kyoto, Japan), and phosphatase inhibitors (Sigma-Aldrich Japan, Tokyo, Japan). The lysates were incubated with the anti-influenza virus hemagglutinin (HA) antibody, and HA-tagged Draper proteins were precipitated with protein G-sepharose (GE Healthcare Japan) and subjected to Western blotting with the anti-phosphotyrosine antibody. For the analysis of the tyrosine phosphorylation of Draper *in vivo*, pupae of the flies that expressed Draper proteins containing altered NPxY and YxxL motifs with the background of $drpr^{\Delta 5}$ were lysed with a buffer consisting of 20 mM Tris-HCl (pH 8.1), 0.15 M NaCl, 1 mM CaCl$_2$, 1 mM MgCl$_2$, 0.5% (v/v) Nonidet P-40, and 5% (w/v) bovine serum albumin. The resulting lysates were subjected to immunoprecipitation with the anti-Draper antibody, and the precipitates were analyzed by Western blotting with the anti-phosphotyrosine antibody.

2.4. *Immunochemistry*

Cultured l(2)mbn cells were smeared on glass slides, incubated with phosphate-buffered saline (PBS) containing the anti-HA antibody and 1% (v/v) blocking reagent (Roche Diagnostics Japan, Tokyo, Japan), and washed with PBS. They were then successively reacted with biotin-conjugated anti-mouse IgG antibody (Life Technologies Japan) and Alexa488-labeled streptavidin (Life Technologies Japan), and examined by fluorescence microscopy. For the analysis of embryos, dispersed embryonic cells were smeared on glass slides, incubated with PBS containing the anti-Draper antibody and 3% bovine serum albumin, and washed with PBS. The samples were successively reacted with biotin-conjugated anti-rat IgG antibody (Life Technologies Japan) and Alexa546-labeled streptavidin (Life Technologies Japan) followed by microscopic examination.

2.5. Other materials and methods

Generation and use of the anti-Draper and anti-Croquemort rat antibodies were reported previously (*16*). The anti-MBP, anti-GST, anti-HA, and anti-phosphotyrosine (clone RC20) antibodies were purchased from New England Biolabs (Ipswich, MA, USA), Millipore (Billerica, MA, USA), Covance Japan (Tokyo, Japan), and BD Biosciences (San Jose, CA, USA), respectively. The level of phagocytosis of apoptotic cells was cytochemically determined with dispersed embryonic cells as described previously (*29*), and the ratio of hemocytes that had accomplished phagocytosis was exhibited as "phagocytosing hemocytes". Western blotting of lysates of cultured cells (*14*) and flies (*29*) was done essentially as reported previously.

2.6. Data processing and statistical analysis

Results from quantitative analyses were expressed as the mean ± SD of the data from at least three independent experiments. Other data were representative of at least three independent experiments that yielded similar results. Statistical analyses were performed using the two-tailed Student's *t*-test, and *p* values of less than 0.05 were considered significant and are indicated in the figures.

3. Results

3.1. Identification of minimum region of Draper for binding to Pretaporter

We first tried to determine the region of Draper required for the binding to its ligand Pretaporter. The EMI and NIM domains are located close to the N-terminus, and EGF-like sequences appear 15 times occupying the remaining part of the extracellular region (Figure 1A). We previously showed that a recombinant Draper protein lacking the EMI and NIM domains binds Pretaporter (*22*), and thus tested the binding of Pretaporter to Draper proteins with reduced numbers of the EGF-like sequences (Figure 1A). MBP-tagged Pretaporter (MBP-Prtp), portions of the extracellular region of Draper fused with GST (GST-DrprEx), and GST alone as a negative control were purified (Figure 1B) and mixed, and GST-proteins were recovered with glutathione-Sepharose followed by examination for the presence of MBP-Prtp by Western blotting using the anti-MBP antibody. We found that the reduction in the number of EGF-like sequences did not significantly influence the binding to Pretaporter, and that even only a single EGF-like sequence located the closest to the N-terminus effectively bound Pretaporter (Figure 1C, left panels). We next tested single EGF-like sequences located at other parts of Draper for the binding to
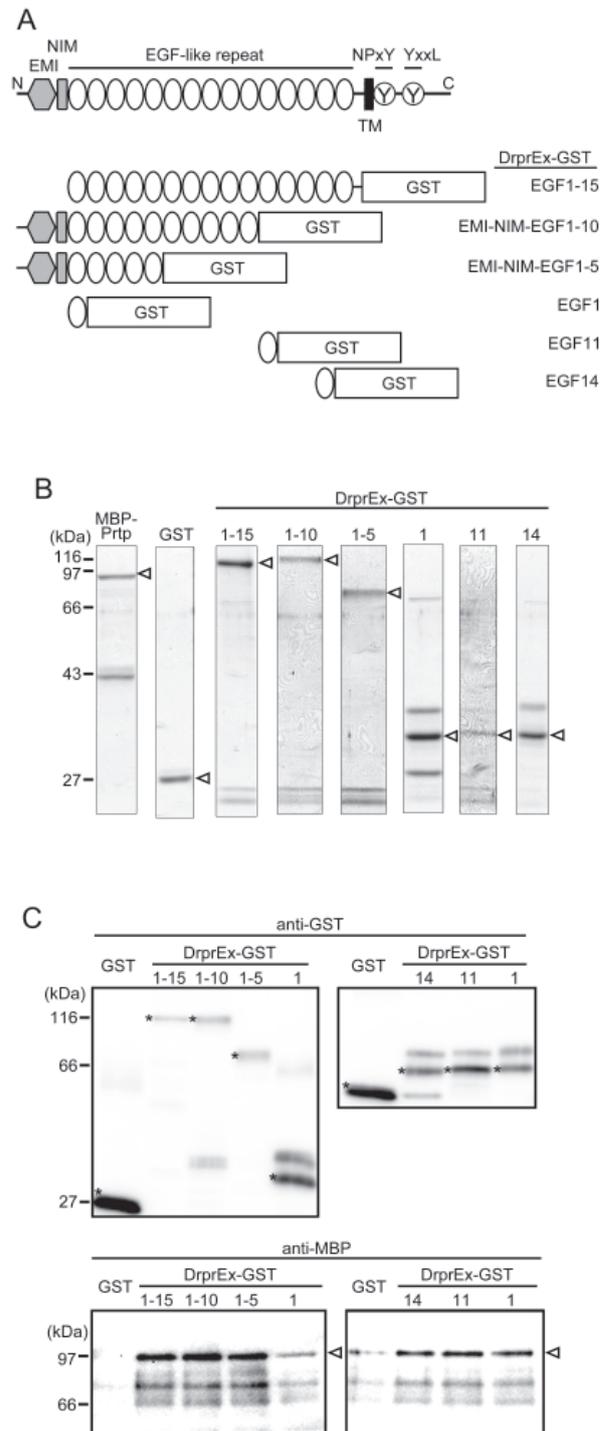
Figure 1. Identification of minimum region of Draper necessary for binding to Pretaporter. Various parts of the extracellular region of Draper were examined for the binding to Pretaporter. (A) Structures of Draper and the Draper proteins analyzed (GST-DrprEx) are schematically drawn not to scale. The positions of the EMI, NIM, EGF-like, NPxY, and YxxL domains together with the transmembrane region (TM) are shown. **(B)** Purified MBP-fused Pretaporter (MBP-Prtp), GST, and GST-DrprEx were analyzed by SDS-PAGE followed by staining with Coomassie brilliant blue. The numbers above the slots correspond to those used to explain the structures of GST-DrprEx in **(A)**. The arrowheads point to the positions of the purified proteins. **(C)** GST-DrprEx and MBP-Prtp were incubated, pulled-down with glutathione-sepharose, and analyzed by Western blotting with anti-GST (top panels) and anti-MBP (bottom panels) antibodies. The asterisks and arrowheads indicate GST-DrprEx and MBP-Prtp, respectively.

Pretaporter, and found that all the sequences examined possessed the activity (Figure 1C, right panels). These results confirmed that EMI and NIM domains are dispensable for the binding of Draper to its ligand Pretaporter and suggested that any single EGF-like sequences of 15 repeats warrant the binding activity of Draper.

3.2. *Tyrosine phosphorylation of Draper with altered NPxY and YxxL motifs*

The cytoplasmic portion of Draper contains two short sequences susceptible to tyrosine phosphorylation, the NPxY and YxxL motifs, which have been presumed to be important for the actions of Draper. To delineate their roles, we first examined the effect of Y-to-F substitution in these motifs on the tyrosine phosphorylation of Draper. Nucleotide sequences of the cDNA of Draper, corresponding to Draper-I (*15*), were altered so that tyrosine residues located in the NPxY and YxxL motifs were changed to phenylalanine (Figure 2A). Draper proteins with Y-to-F substitution were expressed in l(2)mbn cells as proteins fused to HA at the N-terminus (HA-Drpr). When the cells were examined by immunocytochemistry for the surface localization of HA-Drpr using the anti-HA antibody, positive signals were obtained with cells expressing all the three Draper proteins, HA-Drpr-WT (no amino acid alteration), HA-Drpr-Y949F (Y-to-F substitution in YxxL), and HA-Drpr-Y858F (Y-to-F substitution in NPxY) (Figure 2B, left panel). The level of HA-Drpr-Y858F was somewhat higher than those of the other two proteins as examined by Western blotting of whole-cell lysates (Figure 2B, right panel). Under such conditions, the level of tyrosine-phosphorylated HA-Drpr was determined. For this purpose, l(2)mbn cells expressing HA-Drpr were lysed and subjected to immunoprecipitation with the anti-HA antibody followed by Western blotting with the anti-phosphotyrosine antibody (Figure 2C). As we reported previously for endogenous Draper (*22*), HA-Drpr-WT in l(2)mbn cells was already phosphorylated at tyrosine residues. We found that both HA-Drpr-Y858F and HA-Drpr-Y949F underwent tyrosine phosphorylation. These results suggested that Draper is phosphorylated at tyrosine residues in both NPxY and YxxL motifs.

We then conducted similar experiments *in vivo*. Draper with Y-to-F substitution in either NPxY or YxxL were forcedly expressed in hemocytes of *drpr*$^{\Delta 5}$, a null mutant for *draper*, and lysates of pupae were subjected to immunoprecipitation with the anti-Draper antibody followed by Western blotting with the anti-phosphotyrosine antibody (Figure 2D). We found that either Draper protein with the substitution of the tyrosine residue was phosphorylated, suggesting again the occurrence of

tyrosine phosphorylation in both NPxY and YxxL motifs.
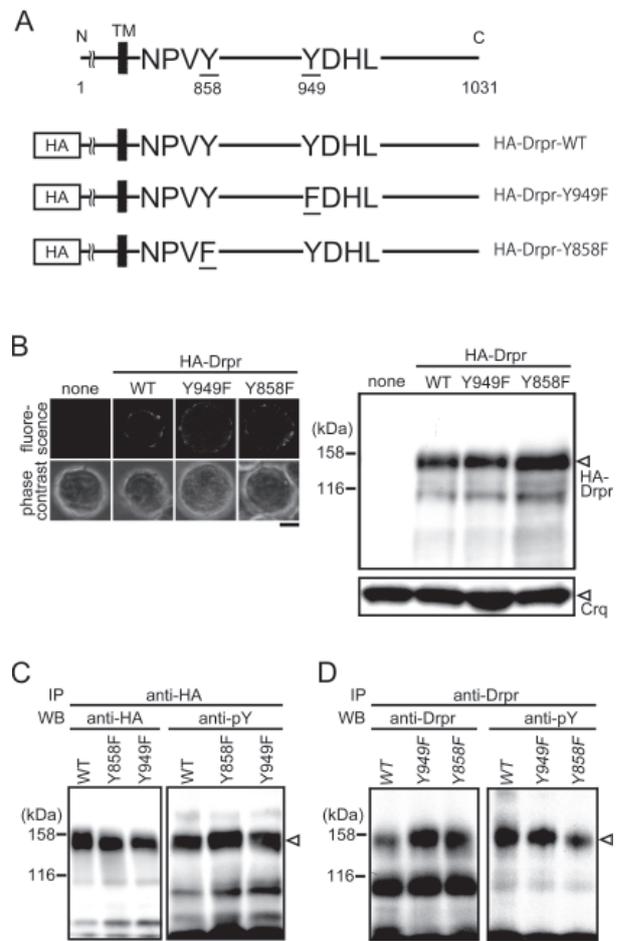
Figure 2. Tyrosine phosphorylation of Draper with altered NPxY and YxxL motifs. The levels of tyrosine-phosphorylated Draper proteins containing the sequences NPxY-YxxL (WT), NPxY-FxxL (Y949F), and NPxF-YxxL (Y858F) were determined. **(A)** Amino acid sequences of the three Draper proteins around NPxY and YxxL motifs are shown. The numbers indicate amino acid positions with the N-terminus as 1. **(B)** Expression of the HA-fused Draper proteins (HA-Drpr) in l(2)mbn cells was determined by immunocytochemistry (left) and Western blotting (right) using anti-HA antibody. In immunocytochemistry, phase contrast and fluorescence views of the same microscopic fields are shown. Scale bar = 5 μm. In Western blotting, the level of hemocyte-specific Croquemort (Crq) was determined for equal loading of the lysates. **(C)** Lysates of l(2)mbn cells expressing HA-Drpr were immunoprecipitated (IP) with anti-HA antibody (anti-HA) followed by Western blotting (WB) with anti-HA and anti-phosphotyrosine antibody (anti-pY). The arrowhead points to the position of HA-Drpr. **(D)** Three Draper proteins with no tags were forcedly expressed in hemocytes of *drpr*$^{\Delta 5}$, and lysates of pupae were immunoprecipitated with anti-Draper antibody (anti-Drpr) followed by Western blotting with anti-Drpr and anti-pY. The arrowhead points to the position of Draper proteins. Note that the intense signals below those of Draper seen in the left panel are derived from immunoglobulin. Genotypes of the fly lines analyzed are: *yw/w* (or *Y*); *UAS-drpr-WT/ srpHemoGAL4 UAS-srcEGFP*; *drpr*$^{\Delta 5}$ (*WT*), *UAS-drpr-Y949F/w* (or *Y*); *srpHemoGAL4 UAS-srcEGFP/+*; *drpr*$^{\Delta 5}$ (*Y949F*), and *UAS-drpr-Y858F/w* (or *Y*); *srpHemoGAL4 UAS-srcEGFP/+*; *drpr*$^{\Delta 5}$ (*Y858F*).

3.3. *Identification of tyrosine residue required for Draper-mediated phagocytosis*

We next determined the importance of the NPxY and YxxL motifs for the actions of Draper in the phagocytosis of apoptotic cells. To do so, a defect of phagocytosis due to a loss of Draper expression in *drpr*[Δ5] was rescued by forced expression of Draper with Y-to-F substitution at the NPxY and YxxL motifs (see Figure 2A) using a hemocyte-specific promoter. To examine the presence of Draper proteins in hemocytes of the transgenic flies, dispersed embryonic cells were immunocytochemically analyzed with the anti-Draper antibody. Most hemocytes, which were identified by the presence of green fluorescent protein (GFP), were positive for the binding of the anti-Draper antibody (Figure 3A, left panel). When lysates of those embryos were examined by Western blotting, the level of intact Draper (*WT*) was lower than those of the other two Draper proteins (Figure 3A, right panel). We then examined the extent of apoptotic cell clearance in the embryos of those flies together with various control flies. The expression of intact Draper, even the least among the three exogenous Draper proteins, sufficiently recovered the level of phagocytosis in *drpr*[Δ5] (Figure 3B). This was the first to genetically confirm the involvement of Draper in the phagocytosis of apoptotic cells by hemocytes. A similar result was obtained for the embryos that expressed the Draper protein with Y-to-F substitution in YxxL (*Y949F*) (Figure 3C). However, the expression of the Draper protein with Y-to-F substitution in NPxY (*Y858F*) failed to rescue the defective phagocytosis caused by a loss of endogenous Draper (Figure 3C). These results collectively indicated that the NPxY motif, but not the YxxL motif, is necessary for Draper to exert actions as a receptor for phagocytosis in hemocytes.

4. Discussion

Draper contains atypical EGF-like sequences and two phosphorylatable motifs, NPxY and YxxL, in the extracellular and intracellular regions, respectively. This study was undertaken to examine the importance of the EGF-like repeat for the binding to the ligand Pretaporter as well as of the NPxY and YxxL motifs for the induction of phagocytosis. The results revealed that a single EGF-like sequence is sufficient for Draper to bind Pretaporter, and that the motif NPxY, but not YxxL, is required for Draper to induce phagocytosis. In general, the NPxY motif, upon tyrosine phosphorylation, binds proteins that contain the PTB domain. In fact, we previously reported that Ced-6, a PTB domain-containing adaptor, is located downstream of Draper (*22*). Our data provide a molecular basis for the idea that Draper activates the pathway CED-6/CED-7/CED-10. The following mechanism is now presumed for Draper-mediated

phagocytosis: Pretaporter binds to Draper through an EGF-like sequence; tyrosine phosphorylation of the NPxY motif is augmented; Ced-6 becomes associated with the phosphorylated NPxY motif; and signals are further transmitted to *Drosophila* orthologues of CED-7 and CED-10 leading to the induction of phagocytosis. On the other hand, Freeman and co-workers reported that the other motif YxxL (*25,30*) together with *Drosophila* components constituting the pathways CED-6/CED-7/CED-10 and CED-2/CED-5/CED-12/CED-10 (*31,32*) are all required for the Draper-mediated phagocytosis of injured axons by glia. Therefore, Draper appears to differentially use the two intracellular motifs for transmitting signals to induce the phagocytosis of apoptotic cells and injured axons. This difference in the mode of Draper's actions could be due to a difference in ligands for Draper and/
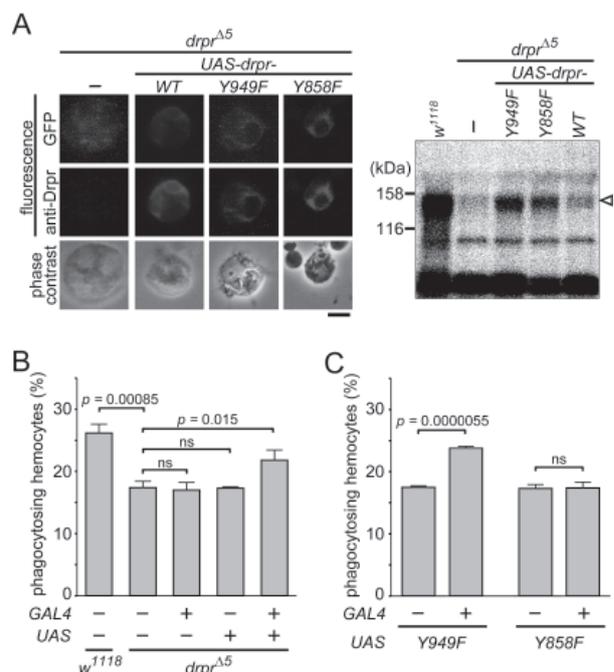
Figure 3. Rescue of defect in apoptotic cell clearance in Draper-lacking flies by expression of Draper with altered NPxY and YxxL motifs. Three Draper proteins containing the sequences NPxY-YxxL (WT), NPxY-FxxL (Y949F), and NPxF-YxxL (Y858F) were expressed in hemocytes of *drpr*[Δ5], and the level of phagocytosis was determined. **(A)** Expression of the Draper proteins was determined by immunocytochemistry (left) and Western blotting (right) using anti-Draper antibody. In immunocytochemistry, phase contrast and fluorescence views of the same microscopic fields that contain GFP-expressing hemocytes are shown. Scale bar = 5 μm. In Western blotting, lysates of whole embryos were analyzed. **(B)** Dispersed embryonic cells obtained from the indicated flies were subjected to an assay for phagocytosis. The fly line *w*[1118] was used as a *draper*[+] control. ns, not significant. Genotype of the fly line (*GAL4+* and *UAS+* with *drpr*[Δ5]) is *yw/w* (or *Y*); *UAS-drpr-WT/srpHemoGAL4 UAS-srcEGFP; drpr*[Δ5]. **(C)** The level of phagocytosis was determined as in **(B)**. Genotypes of the fly lines analyzed are: *UAS-drpr-Y949F/w* (or *Y*); *srpHemoGAL4 UAS-srcEGFP/+*; *drpr*[Δ5] (*GAL4+* with *Y949F*) and *UAS-drpr-Y858F/w* (or *Y*); *srpHemoGAL4 UAS-srcEGFP/+*; *drpr*[Δ5] (*GAL4+* with *Y858F*).

or types of phagocytes. It is necessary to further clarify the mechanism by which Draper transmits signals to downstream molecules, particularly focusing on the roles of the two phosphorylatable motifs located in the cytoplasmic portion of this receptor.

Integrin β-subunits contain the motif NPxY in their cytoplasmic region, which serves as a binding site for various adaptor molecules possessing the PTB domain (*33*). Mammalian $\alpha_V\beta_3$ and $\alpha_V\beta_5$ (*34*), *Drosophila* αPS3βυ ((*29*) and our unpublished observation), and *C. elegans* INA-1-PAT-3 (*10*) act as receptors in the phagocytosis of apoptotic cells. However, $\alpha_V\beta_5$ (*35*) and INA-1-PAT-3 (*10*) seem to reside at the point furthest upstream in the pathway CED-2/CED-5/CED-12/CED-10, not CED-6/CED-7/CED-10. In addition, the NPxY motif contained in β_5 integrin was shown to be dispensable for $\alpha_V\beta_5$-mediated phagocytosis (*36*). In contrast, mammalian stabilin-2, a phosphatidylserine-binding engulfment receptor, uses its NPxY motif to recruit the mammalian orthologue of CED-6 (*37*). Interestingly, stabilin-2 may also activate the CED-2/CED-5/CED-12/CED-10 pathway through physical association with $\alpha_V\beta_5$ (*38*). Therefore, which of the two conserved signaling pathways is used by NPxY motif-containing engulfment receptors seemingly depends on the ligand-receptor combination and/or the receptor repertoire in phagocytes.

Acknowledgements

References

1. Savill J, Fadok V. Corpse clearance defines the meaning of cell death. Nature. 2000; 407:784-788.
2. Lauber K, Blumenthal SG, Waibel M, Wesselborg S. Clearance of apoptotic cells: Getting rid of the corpses. Mol Cell. 2004; 14:277-287.
3. Ravichandran KS, Lorenz U. Engulfment of apoptotic cells: Signals for a good meal. Nat Rev Immunol. 2007; 7:964-974.
4. Ravichandran KS. Beginning of a good apoptotic meal: The find-me and eat-me signaling pathways. Immunity. 2011; 35:445-455.
5. Reddien PW, Horvitz HR. The engulfment process of programmed cell death in *Caenorhabditis elegans*. Annu Rev Cell Dev Biol. 2004; 20:193-221.
6. Kinchen JM, Hengartner MO. Tales of cannibalism, suicide, and murder. Programmed cell death in *C. elegans*. Curr Top Dev Biol. 2004; 65:1-45.
7. Mangahas PM, Zhou Z. Clearance of apoptotic cells in Caenorhabditis elegans. Semin Cell Dev Biol. 2005; 16:295-306.
8. Lettre G, Hengartner MO. Developmental apoptosis in *C. elegans*: A complex CEDnario. Nat Rev Mol Cell Biol. 2006; 7:97-108.
9. Zhou Z, Hartwieg E, Horvitz HR. CED-1 is a transmembrane receptor that mediates cell corpse engulfment in *C. elegans*. Cell. 2001; 104:43-56.
10. Hsu T-Y, Wu Y-C. Engulfment of apoptotic cells in *C. elegans* is mediated by integrin α/SRC signaling. Curr Biol. 2010; 20:477-486.
11. Callebaut I, Mignotte V, Souchet M, Mornon J-P. EMI domains are widespread and reveal the probable orthologs of the *Caenorhabditis elegans* CED-1 protein. Biochem Biophys Res Commun. 2003; 300:619-623.
12. Brown NH. Cell-cell adhesion via the ECM: Integrin genetics in fly and worm. Matrix Biol. 2000; 19:191-201.
13. Kinchen JM, Ravichandran KS. Journey to the grave: Signaling events regulating removal of apoptotic cells. J Cell Sci. 2007; 120:2143-2149.
14. Manaka J, Kuraishi T, Shiratsuchi A, Nakai Y, Higashida H, Henson P, Nakanishi Y. Draper-mediated and phosphatidylserine-independent phagocytosis of apoptotic cells by *Drosophila* hemocytes/macrophages. J Biol Chem. 2004; 279:48466-48476.
15. Freeman MR, Delrow J, Kim J, Johnson E, Doe CQ. Unwrapping glial biology: Gcm target genes regulating glial development, diversification, and function. Neuron. 2003; 38:567-580.
16. Awasaki T, Tatsumi R, Takahashi K, Arai K, Nakanishi Y, Ueda R, Ito K. Essential role of the apoptotic cell engulfment genes *draper* and *ced-6* in programmed axon pruning during *Drosophila* metamorphosis. Neuron. 2006; 50:855-867.
17. Hoopfer ED, McLaughlin T, Watts RJ, Schuldiner O, O'Leary DDM, Luo L. Wld^S protection distinguishes axon degeneration following injury from naturally occurring developmental pruning. Neuron. 2006; 50:883-895.
18. Williams DW, Kondo S, Krzyzanowska A, Hiromi Y, Truman JW. Local caspase activity directs engulfment of dendrites during pruning. Nat Neurosci. 2006; 9:1234-1236.
19. MacDonald JM, Beach MG, Porpiglia E, Sheehan AE, Watts RJ, Freeman MR. The *Drosophila* cell corpse engulfment receptor Draper mediates glial clearance of severed axons. Neuron. 2006; 50:869-881.
20. Fuentes-Medel Y, Logan MA, Ashley J, Ataman B, Budnik V, Freeman MR. Glia and muscle sculpt neuromuscular arbors by engulfing destabilized synaptic boutons and shed presynaptic debris. PLoS Biol. 2009; 7: e1000184. Doi:10.1371/journal.ibio.1000184.
21. Kurucz É, Márkus R, Zsámboki J, Folkl-Medzihradszky K, Darula Z, Vilmos P, Udvardy A, Krausz I, Lukacsovich T, Gateff E, Zettervall C-J, Hultmark D, Andó I. Nimrod, a putative phagocytosis receptor with EGF repeats in *Drosophila* plasmatocytes. Curr Biol. 2007; 17:649-654.
22. Kuraishi T, Nakagawa Y, Nagaosa K, Hashimoto Y, Ishimoto T, Moki T, Fujita Y, Nakayama H, Dohmae N, Shiratsuchi A, Yamamoto N, Ueda K, Yamaguchi M, Awasaki T, Nakanishi Y. Pretaporter, a *Drosophila* protein serving as a ligand for Draper in the phagocytosis of apoptotic cells. EMBO J. 2009; 28:3868-3878.
23. Su HP, Nakada-Tsukui K, Tosello-Trampont A-C, Li

Y, Bu G, Henson PM, Ravichandran KS. Interaction of CED-6/GULP, an adaptor protein involved in engulfment of apoptotic cells with CED-1 and CD91/low density lipoprotein receptor-related protein (LRP). J Biol Chem. 2002; 277:11772-11779.

24. Underhill DM, Goodridge HS. The many faces of ITAMs. Trends Immunol. 2007; 28:66-73.

25. Ziegenfuss JS, Biswas R, Avery MA, Hong K, Sheehan AE, Yeung Y-G, Stanley ER, Freeman MR. Draper-dependent glial phagocytic activity is mediated by Src and Syk family kinase signalling. Nature. 2008; 453:935-939.

26. Kurant E, Axelrod S, Leaman D, Gaul U. Six-microns-under acts upstream of Draper in the glial phagocytosis of apoptotic neurons. Cell. 2008; 133:498-509.

27. Brückner K, Kockel L, Duchek P, Luque CM, Rørth P, Perrimon N. The PDGF/VEGF receptor controls blood cell survival in *Drosophila*. Dev Cell. 2004; 7:73-84.

28. Brand AH, Perrimon N. Targeted gene expression as a means of altering cell fates and generating dominant phenotypes. Development. 1993; 118:401-415.

29. Nagaosa K, Okada R, Nonaka S, Takeuchi K, Fujita Y, Miyasaka T, Manaka J, Ando I, Nakanishi Y. Integrin $\beta\upsilon$-mediated phagocytosis of apoptotic cells in *Drosophila* embryos. J Biol Chem. 2011; 286:25770-25777.

30. Logan MA, Hackett R, Doherty J, Sheehan A, Speese SD, Freeman MR. Negative regulation of glial engulfment activity by Draper terminates glial responses to axon injury. Nat Neurosci. 2012; 15:722-730.

31. Doherty J, Logan MA, Taşdemir ÖE, Freeman MR. Ensheathing glia function as phagocytes in the adult *Drosophila* brain. J Neurosci. 2009; 29:4768-4781.

32. Ziegenfuss JS, Doherty J, Freeman MR. Distinct molecular pathways mediate glial activation and engulfment of axonal debris after axotomy. Nat Neurosci. 2012; 15:979-987.

33. Legate KR, Fässler R. Mechanisms that regulate adaptor binding to β-integrin cytoplasmic tails. J Cell Sci. 2009; 122:187-198.

34. Wu Y, Tibrewal N, Birge RB. Phosphatidylserine recognition by phagocytes: A view to a kill. Trends Cell Biol. 2006; 16:189-197.

35. Akakura S, Singh S, Spataro M, Akakura R, Kim JI, Albert ML, Birge RB. The opsonin MFG-E8 is a ligand for the $\alpha_V\beta_5$ integrin and triggers DOCK180-dependent Rac1 activation for the phagocytosis of apoptotic cells. Exp Cell Res. 2004; 292:403-416.

36. Singh S, D'mello V, van Bergen en Henegouwen P, Birge RB. A NPxY-independent β_5 integrin activation signal regulates phagocytosis of apoptotic cells. Biochem Biophys Res Commun. 2007; 364:540-548.

37. Park SY, Kang KB, Thapa N, Kim SY, Lee SJ, Kim IS. Requirement of adaptor protein GULP during stabilin-2-mediated cell corpse engulfment. J Biol Chem. 2008; 283:10593-10600.

38. Kim S, Park SY, Kim SY, Bae DJ, Pyo JH, Hong M, Kim IS. Cross talk between engulfment receptors stabilin-2 and integrin $\alpha_V\beta_5$ orchestrates engulfment of phosphatidylserine-exposed erythrocytes. Mol Cell Biol. 2012; 32:2698-2708.

Original Article

In vitro free radical scavenging and anti-hyperglycemic activities of *Achyranthes aspera* extract in alloxan-induced diabetic mice

Fatema Zohura Talukder[1], Kousik Ahmed Khan[1], Riaz Uddin[1], Nusrat Jahan[1], Md. Ashraful Alam[1,2,*]

[1] *Pharmacognosy and Pharmacology Laboratory, Department of Pharmacy, Stamford University Bangladesh, Dhaka, Bangladesh;*
[2] *School of Biomedical Sciences, The University of Queensland, Brisbane, QLD, Australia.*

ABSTRACT: Medicinal plants have played an important role in the treatment and prevention of diseases since ancient times. They are also potential sources of nutrients and drugs. This study evaluated *Achyranthes aspera* ethanolic extracts for their *in vitro* antioxidant activity and anti-hyperglycemic effects on alloxan-induced diabetic mice. Diabetes was induced in Swiss albino mice through intra-peritoneal administration of alloxan and their blood glucose levels and weight were measured weekly. At the end of the experiment, all animals were sacrificed and tissue samples were collected. *A. aspera* extracts had potent antioxidant activity compared to reference standard compounds. Treatment with an *A. aspera* extract at doses of 200 mg/kg and 400 mg/kg significantly reduced blood glucose levels in alloxan-induced diabetic mice. *A. aspera* extract also prevented lipid peroxidation as gauged by thiobarbituric acid reactive substances (TBARS) and hydroperoxides. Moreover, *A. aspera* extract increased the activity of catalase and reduced NO levels in alloxan-induced diabetic mice. Results revealed significant anti-hyperglycemic activity of *A. aspera* extracts in alloxan-treated mice that may be mediated by diminished oxidative stress.

Keywords: *Achyranthes aspera*, anti-hyperglycemia, oxidative stress, antioxidant, diabetes

1. Introduction

Hyperglycemia induces glucose auto-oxidation and protein glycation, and subsequent oxidative degradation of glycated proteins leads to enhanced production of reactive oxygen species (*1*). In diabetes, endogenous antioxidants and scavenging protectors such as vitamin E and glutathione are depleted and antioxidant enzymes such as superoxide dismutase (SOD) and catalase are less active (*2*). Thus, supplementation with a natural antioxidant from a plant source would help to prevent organ damage. *Achyranthes aspera* (Amaranthaceae) is commonly found as a weed throughout Bangladesh and the Indian subcontinent (*3,4*). The ethanol extract of the plant contains alkaloids and saponins (*5*). Various parts of the plant, seeds, stem, leaves, and root are reported to contain ecdysterone (*6,7*). Phytochemical investigations of this plant also revealed the presence of long-chain fatty acids, triterpenoids, saponins, and flavonol glycosides (*8,9*). Upon acidic hydrolysis, it yields an aglycone in the form of oleanolic acid or quercitin (*8,9*).

Several pharmacological studies also investigated *A. aspera*. *A. aspera* extracts were reported to have thyroid-stimulating and antiperoxidative properties (*10*). Recent reports suggest that *A. aspera* may benefit wound healing (*11*) and prevent obesity in mice (*12*). The aqueous and methanol extracts of the plant also decreased blood glucose levels in normal and alloxan-induced diabetic rabbits (*13*). *A. aspera* is also used by traditional healers to treat diabetes (*3*). However, literature on the effect of *A. aspera* extracts on oxidative stress in diabetes is lacking. Previous pharmacological studies encouraged the current authors to explore the therapeutic value of *A. aspera* in the face of oxidative stress. In continuation with phytochemical and pharmacological investigations of Bangladeshi medicinal plants (*14-17*), the current study reports on the antioxidant and anti-hyperglycemic activities of *A. aspera* extracts in diabetic mice.

2. Materials and Methods

2.1. Reagents

Alloxan, 2,2-diphenyl-1-picrylhydrazyl (DPPH), naphthyl ethylene diamine dihydrochloride, Folin-Ciocalteu reagent, gallic acid, and thiobarbituric acid were purchased from Sigma-Aldrich, St. Louis, MO, USA. All other reagents are of standard laboratory grade.

*Address correspondence to:
Md. Ashraful Alam, Lecturer (On study leave), Department of Pharmacy, Stamford University Bangladesh, 51 Siddeshwari Road, Dhaka, Bangladesh.
E-mail: sonaliagun@yahoo.com

2.2. *Plant material*

A. aspera was collected from the Bangladesh Agricultural University campus in July 2007 and identified by an expert at the National Herbarium, Mirpur, Dhaka, Bangladesh. Accession No. 32067 was retained there for further reference and a specimen has been preserved in the Pharmacognosy Laboratory, Stamford University Bangladesh.

2.3. *Extraction*

An extract was yielded by placing a dried powder of stem and leaves (200 g) in 80% ethanol in a Soxhlet apparatus at an elevated temperature. The extract was concentrated by evaporation under reduced pressure at 40°C using a Buchi rotary evaporator to yield a gummy concentrate that was greenish in color.

2.4. *Animals used*

Male Swiss albino mice, 3-4 weeks of age, weighing between 20-30 g were used for *in vivo* pharmacological screening. The mice were collected from the Animal Research Branch of the International Center for Diarrheal Disease and Research, Bangladesh (ICDDR, B). They were housed in five groups in stainless steel cages with dimensions of $28 \times 22 \times 13$ in. Soft wood shavings were used as bedding. The mice were acclimatized to the new environment for one week prior to the investigation and lived at constant room temperature (24.0 ± 1.0ºC), humidity 55-65%, and 12 h light/12 h dark cycles. Remaining feed and excreta were removed from cages daily. Rat feed pellets from ICDDR, B were given to the mice with fresh water *ad libitum*. The University's Animal Research Ethical Committee approved the study protocol.

2.5. *In vitro antioxidant activity test*

2.5.1. *DPPH radical scavenging activity*

The free radical scavenging capacity of the extracts was determined using DPPH *(14-16,18)*. A DPPH solution (0.004%, w/v) was prepared in 95% ethanol. *A. aspera* extracts were mixed with ethanol to prepare a stock solution (5 mg/mL). A freshly prepared DPPH solution (0.004%, w/v) was placed in test tubes and *A. aspera* extracts were added followed by serial dilution (1 μg to 500 μg) of every test tube to reach a final volume of 3 mL. After 10 min, absorbance was read at 515 nm using a spectrophotometer (HACH 4000 DU UV–visible spectrophotometer). Ascorbic acid was used as a reference standard and dissolved in distilled water to prepare a stock solution with the same concentration (5 mg/mL). Control samples were prepared with the same volume of distilled water without any extract and reference ascorbic acid. Ninety-five percent ethanol served as the blank. The % scavenging of the DPPH free radical was measured using the following equation:

% Scavenging activity $=100 \times$ (Absorbance of the control – Absorbance of the test sample)/Absorbance of the control

The inhibition curve was plotted for two experiments and was expressed as the % of the mean inhibition ± standard deviation (SD). IC_{50} values were obtained by probit analysis.

2.5.2. *Reducing power*

The reducing power of *A. aspera* was determined by the method previously described by Oyaizu (1986) (*19*). Different concentrations of *A. aspera* extracts (100 to 1,000 μg) in 1 mL of distilled water were mixed with phosphate buffer (2.5 mL, 0.2 M, pH 6.6) and potassium ferricyanide $[K_3Fe(CN)_6]$ (2.5 mL, 1%). The mixture was then incubated at 50°C for 20 min. A portion (2.5 mL) of trichloroacetic acid (10%) was added to the mixture, which was then centrifuged at 3,000 rpm for 10 min. The upper layer of the solution (2.5 mL) was mixed with distilled water (2.5 mL) and $FeCl_3$ (0.5 mL, 0.1%) and the absorbance was measured at 700 nm. Increased absorbance of the reaction mixture indicated increased reducing power. Ascorbic acid served as the standard. Phosphate buffer (pH 6.6) served as the blank solution. The absorbance of the final reaction mixture of two parallel experiments was read and expressed as mean ± standard deviation (SD).

2.5.3. *Nitric oxide (NO) radical inhibition assay*

NO radical inhibition was estimated using a Griess-Illosvoy reaction (*16,20*). In this investigation, Griess-Illosvoy reagent was modified by using naphthyl ethylene diamine dihydrochloride (0.1%, w/v) instead of 1-napthylamine (5%). The reaction mixture (3 mL) containing sodium nitroprusside (10 mM, 2 mL), phosphate buffer saline (0.5 mL), and *A. aspera* extract (10 to 320 μg) or standard solution (ascorbic acid, 0.5 mL) was incubated at 25°C for 150 min. After incubation, 0.5 mL of the reaction mixture was mixed with 1 mL of sulfanilic acid reagent (0.33% in 20% glacial acetic acid) and allowed to stand for 5 min to complete diazotization. Then, 1 mL of naphthyl ethylene diamine dihydrochloride was added. After mixing, the mixture was allowed to stand for 30 min at 25°C. A pink colored chromophore formed in diffused light. The absorbance of these solutions was measured at 540 nm against the corresponding blank solutions.

2.5.4. *Scavenging of hydrogen peroxide (H_2O_2)*

The ability of the extracts to scavenge H_2O_2 was

determined by the method described by Ruch *et al.* (*21*). H_2O_2 (43 mM) was prepared in phosphate buffered saline (pH 7.4). Standard (ascorbic acid) and extract solutions were prepared at concentrations of 50 to 250 mM. Aliquots of standard or extract solutions (3.4 mL) were added to 0.6 mL of H_2O_2 solution. The reaction mixture was incubated at room temperature for 10 min, and the absorbance was determined at 230 nm. The percentage of scavenging was calculated as follows: % H_2O_2 scavenging = 100 × (Absorbance of control − absorbance of sample)/Absorbance of control.

2.5.5. *Assay for total phenolic content*

The concentration of total phenols in extracts was measured with a UV spectrophotometer based on a colorimetric oxidation/reduction reaction (*22*). The oxidizing reagent used was Folin-Ciocalteu reagent. Gallic acid served as the standard. Two-point-five mL of Folin-Ciocalteu reagent (diluted 10 times with water) and 2 mL of Na_2CO_3 (75 g/L) were added to 0.5 mL of diluted extract (1 mg in 4 mL distilled water). The sample was incubated for 20 min at room temperature. A control sample was prepared with 0.5 mL of distilled water. The absorbance was measured at 760 nm. These data were used to estimate the phenolic content based on a standard curve obtained with various concentrations of gallic acid. The results were expressed as μg of gallic acid per mg of extract.

2.6. *Glucose tolerance test*

Animals fasted overnight and were then divided into three groups with five mice each. Control animals were given 1 mL of distilled water orally (Group I). *A. aspera* extracts were administered orally using a feeding syringe at concentrations of 100 and 200 mg/kg (Groups II and III, respectively). After the *A. aspera extract* administration, all groups were given glucose (2 g/kg) orally. Blood samples were collected from the tail vein just prior to and 60, 120, and 240 min after the glucose challenge. Blood glucose concentrations were assayed with a glucometer. Results of the glucose tolerance test served as a hypothetical reference to extrapolate the dose levels that would be used to evaluate short- and long-term effects of *A. aspera* extracts on diabetic mice.

2.7. *Experimental design of a model of alloxan-induced diabetes*

2.7.1. *Animal treatment*

A total of 25 mice (20 diabetic surviving mice, 5 normal mice) were used in the experiment. Group 1 consisted of normal mice, Group 2 consisted of diabetic control mice (alloxan, 150 mg/kg, *i.p.*, in citrate buffer, pH 4.4), Group 3 consisted of diabetic mice given metformin (600

μg/kg body weight) in aqueous solution daily for 3 weeks *via* intraperitoneal administration, Group 4 consisted of diabetic mice given *A. aspera* plant extract (200 mg/kg body weight) in aqueous solution daily for 3 weeks *via* an intragastric tube, and Group 5 consisted of diabetic mice given *A. aspera* (400 mg/kg, body weight) in aqueous solution daily for 3 weeks *via* an intragastric tube.

The diabetic state was assessed by determining the blood glucose concentration 3 and 5 days after alloxan treatment. No detectable irritation or restlessness was observed after each drug or vehicle administration. No noticeable adverse effects (*i.e.*, respiratory distress, abnormal locomotion, and catalepsy) were observed in any of the animals after the drug administration.

2.7.2. *Blood sample collection*

Blood samples were drawn at weekly intervals till the end of study (*i.e.* 3 weeks) by the tail tip method and were used to assay glucose levels in plasma. At the end of the 3rd week, all mice were sacrificed by decapitation after they were anaesthetized with pentobarbitone sodium (60 mg/kg).

2.7.3. *Brain and liver sample collection*

The brain and liver were completely removed and washed in ice-cold saline to remove blood. The brains were weighed and 10% tissue homogenate was prepared with 0.025 M Tris-HCl buffer, pH 7.5. After centrifugation at 8,000 rpm for 15 min, the supernatant was used to measure thiobarbituric acid reactive substances (TBARS), hydroperoxides, NO levels, and catalase activity.

2.7.4. *Estimation of blood glucose*

Glucose was measured in the serum of non-fasting mice. Blood was sampled by the tail tip method and then analyzed with a Reflotron Plus auto analyzer (Roche, Germany) using a commercial kit.

2.7.5. *Estimation of lipid peroxidation*

Lipid peroxidation in the brain and liver was estimated colorimetrically using TBARS by the method previously described by Niehius and Samuelsson (*23*). In brief, 0.1 mL of tissue homogenate (Tris-HCl buffer, pH 7.5) was treated with 2 mL of (1:1:1 ratio) TBA-TCA-HCl reagent (thiobarbituric acid 0.37%, 0.25 M HCl, and 15% TCA) and placed in a water bath for 15 min. It was then allowed to cool. The absorbance of the clear supernatant was measured against a reference blank at 535 nm.

2.7.6. *Estimation of hydroperoxide*

Hydroperoxide levels were estimated by the method previously described by Jiang *et al.* (*24*). Specifically,

Table 1. Scavenging of free radicals by a crude hydroethanolic extract of *A. aspera* and ascorbic acid according to DPPH, NO, and H₂O₂ scavenging assays

Sample	IC$_{50}$ (µg/mL)			Total phenolic content (µg/mg)[a]
	DPPH scavenging assay	NO scavenging assay	H₂O₂ scavenging assay	
A. aspera extract	243.7	39.0	92.0	80.4
Ascorbic acid	55.9	69.9	158.9	--

[a] Data is presented as µg of gallic acid per mg of extract.

0.1 mL of tissue homogenate was treated with 0.9 mL of Fox reagent (88 mg butylated hydroxytoluene (BHT), 7.6 mg xylenol orange, and 9.8 mg ammonium iron sulphate were added to 90 mL of methanol and 10 mL of 250 mM sulphuric acid) and incubated at 37°C for 30 min. The color that developed was read colorimetrically at 560 nm. Hydroperoxide was expressed as mM/100 g tissue.

2.7.7. *Assay of catalase*

Catalase activity was assayed colorimetrically at 620 nm and expressed as µmoles of H₂O₂ consumed/min/mg protein using the method described by Sinha (*25*). The reaction mixture (1.5 mL, vol) contained 1.0 mL of 0.01 M phosphate buffer (pH 7.0), 0.1 mL of tissue homogenate (supernatant), and 0.4 mL of 2 M H₂O₂. The reaction was stopped by the addition of 2.0 mL of dichromate-acetic acid reagent (5% potassium dichromate and glacial acetic acid mixed at a 1:3 ratio).

2.7.8. *Assay of NO*

NO in the form of nitrate and nitrite was determined according to the method described by Tracy *et al.* (*26*). In the current study, Griess-Illosvoy reagent was modified by using naphthyl ethylene diamine dihydrochloride (0.1%, w/v) instead of 1-napthylamine (5%). The reaction mixture (3 mL) containing liver homogenate (2 mL) and phosphate buffer saline (0.5 mL) was incubated at 25°C for 150 min. The remaining steps of the NO scavenging assay were as previously described. A pink chromophore formed in diffused light. The absorbance of these solutions was measured at 540 nm against the corresponding blank solutions. The NO level was measured using a standard curve and was expressed as nmol/g of tissue.

2.8. *Statistical analysis*

All data sets were presented as mean ± SD. Comparison between groups was done by statistical analysis of data sets using one-way analysis of variance (ANOVA) followed by a Newman-Keuls multiple-comparison post hoc test. A *p*-value of < 0.05 was considered statistically significant. All statistical analyses were performed using Graph Pad Prism version 5.00 for Windows.
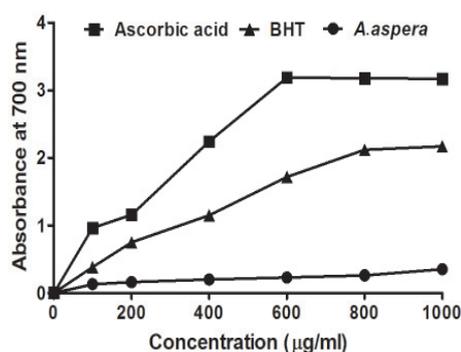

Figure 1. Reducing power of ascorbic acid, BHT, and an extract of *A. aspera*. Values are given for duplicate experiments.
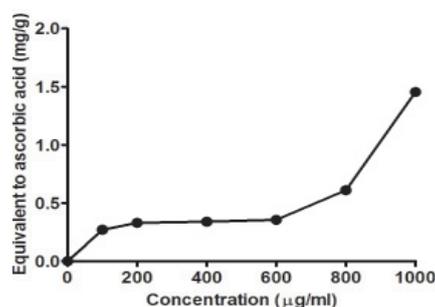

Figure 2. Total antioxidant capacity of an extract of *A. aspera*. Values are given for two consecutive experiments.

3. Results

3.1. *Antioxidant activity of A. aspera extracts*

A. aspera extracts had strong free radical scavenging activity *in vitro* according to various antioxidant assays. Significant antioxidant activity was evident in terms of NO scavenging (IC$_{50}$: 39.0 µg/mL) and H₂O₂ scavenging (IC$_{50}$: 92.0 µg/mL) (Table 1). However, DPPH scavenging (Table 1) and reducing power assays revealed that the extracts had little to no activity (Figure 1). Total antioxidant capacity also increased with an increase in the concentration of the assay medium (Figure 2).

3.2. *Total phenolic content*

The total phenolic content in the extracts of *A. aspera* was determined using Folin-Ciocalteu regents. Phenolic content was calculated based on a regression equation for the calibration curve (y = 0.0162x + 0.0232, R^2 =

0.9985) and was expressed as gallic acid equivalents (80.4 µg/mg extract) (Table 1).

3.3. Effect of A. aspera on plasma glucose levels in normal mice

The oral glucose tolerance test of non-diabetic mice revealed a dose-dependent decrease in plasma glucose over a period of 3 h after administration of the extract of *A. aspera*, as summarized in Figure 3. The maximum reduction in glucose levels was noted with both doses in the second hour of the study. Control animals had increased glucose levels in the first hour that returned to normal within three hours. This is attributed to glucose homeostasis.

3.4. Body weight after 3 weeks of A. aspera administration

The body weight of the diabetic group decreased significantly ($p < 0.05$) compared to that of the normal control. The body weight of diabetic rats treated with *A. aspera* at a dose of 200 and 400 mg/kg body weight almost returned to normal (Figure 4). Alloxan administration caused significant weight loss after 3 weeks of treatment whereas mice in the normal group continued to gain weight. Treatment with a 200 or 400 mg/kg dose of *A. aspera* remedied the weight loss.
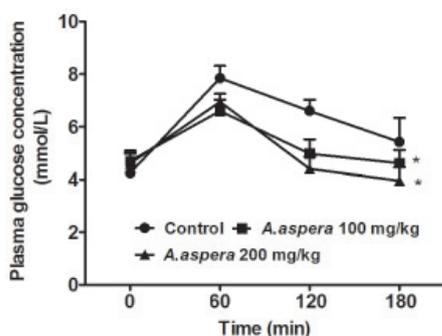
Figure 3. Glucose tolerance test of non-diabetic mice with an extract of *A. aspera*. Values are expressed as mean ± SD. *Statistical significance was defined as $p < 0.05$ in all cases *vs.* control.
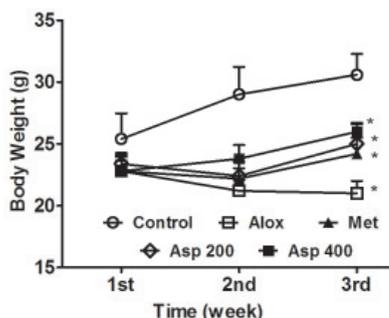
Figure 4. Effect of the hydroalcoholic extract of *A. aspera* on the body weight of mice. Values are expressed as mean ± SD. * Statistical significance was defined as $p < 0.05$ in all cases *vs.* control. Alox, alloxan; Met, metformin; Asp 200, *A. aspera* 200 mg/kg; Asp 400, *A. aspera* 400 mg/kg.

3.5. Effect of A. aspera extracts on glucose levels in alloxan-treated rats

As shown in Figure 5, a single intraperitoneal injection of alloxan at a dose of 150 mg/kg body weight increased glucose levels > 8 mM after 5 days. *A. aspera* extracts significantly decreased blood glucose levels. Serum glucose levels in normal mice (Group 1) were unaltered throughout the study but increased significantly ($p < 0.05$) in the diabetic control group (Group 2) during the second and third week of the study. Glucose levels in the metformin treatment group (Group 3) were almost normal during the study period. Administration of *A. aspera* extracts at a dose of 400 mg/kg significantly reduced elevated glucose levels in the second week after alloxan administration; in the third week, glucose levels were almost normal. Like the higher dose, a lower dose of *A. aspera* also reduced blood glucose levels (Figure 5). Findings were similar to those for the metformin treatment group.

3.6. TBARS, catalase, hydroperoxide, and NO levels

The level of malondialdehyde (MDA) as a lipid peroxidation product was gauged by TBARS (42.0 ± 9.3 nmol/g tissue) and hydroperoxides (28.8 ± 3.3 mM/g tissue) in the liver of alloxan-induced diabetic control mice, which are significantly higher ($p < 0.05$) than those of normal mice (14.0 ± 1.6 nmol/g tissue and 24.1 ± 2.5 mM/g tissue, respectively) (Table 2). TBARS (32.2 ± 2.2 nmol/g tissue) and hydroperoxides (19.4 ± 2.8 mM/g tissue) in the brain also increased in alloxan-induced diabetic mice compared to normal mice (11.8 ± 1.5 nmol/g tissue and 15.1 ± 1.5 mM/g tissue, respectively). Treatment with *A. aspera* significantly decreased the level of lipid peroxidation products (TBARS and hydroperoxides) (Table 2).

Moreover, a significant decrease ($p < 0.05$) in the activity of antioxidant enzyme catalase was also observed in the liver of alloxan-induced diabetic mice (22.4 ± 4.4 U/mg of protein) when compared to normal mice (41.0
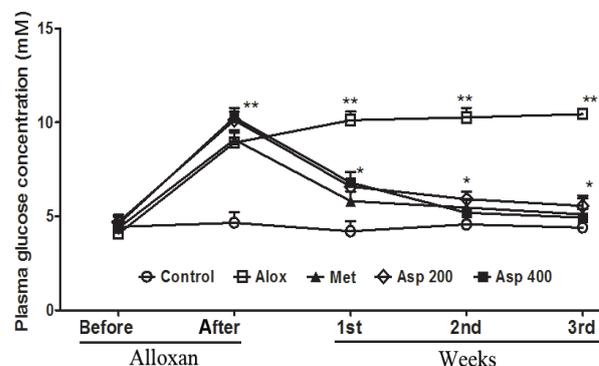
Figure 5. Effect of the hydroethanolic extract of *A. aspera* on blood glucose levels in plasma. Values are expressed as mean ± SD. Statistical significance was defined as $p < 0.05$ in all cases *vs.* control. Alox, alloxan; Met, metformin; Asp 200, *A. aspera* 200 mg/kg; Asp 400, *A. aspera* 400 mg/kg.

Table 2. Effect of an *A. aspera* extract on oxidative markers in brain and liver homogenates from alloxan-induced diabetic mice

Group	TBARS (nmol/g tissue)		Hydroperoxide (mM/g of tissue)		Catalase activity (U^b/mg of protein)	NO (nmol/g of tissue)
	Brain	Liver	Brain	Liver	Liver	Liver
Normal	11.8 ± 1.5^a	14.0 ± 1.6^a	15.1 ± 1.5^a	24.1 ± 2.5^a	41.0 ± 0.6^a	11.5 ± 1.9^a
Diabetes control	32.2 ± 2.2^b	42.0 ± 9.3^b	19.4 ± 2.8^b	28.8 ± 3.3^b	22.4 ± 4.4^b	29.3 ± 1.7^b
Metformin	27.1 ± 2.8^c	27.1 ± 1.7^c	13.1 ± 1.4^c	17.6 ± 1.3^c	31.9 ± 3.9^c	18.3 ± 5.5^c
A. aspera 200 mg/kg	28.5 ± 5.6^c	32.3 ± 4.3^c	16.9 ± 1.1^c	19.5 ± 2.7^c	33.9 ± 1.7^c	22.8 ± 2.4^c
A. aspera 400 mg/kg	21.2 ± 3.1^c	32.0 ± 1.4^c	13.2 ± 1.6^c	9.6 ± 1.2^c	35.3 ± 0.3^c	21.8 ± 2.7^c

Values are expressed as mean ± SD. Differences in means were estimated by means of ANOVA followed by a Newman-Keuls post hoc test ($n = 5$). Statistical significance was defined as $p < 0.05$ in all cases, [a, b] Group normal *vs.* diabetes control, $p < 0.05$; [b, c] Diabetes control *vs.* treatment, $p < 0.05$. $U^b = \mu$mol of H_2O_2 consumed/min.

± 0.6 U/mg of protein) (Table 2). Administration of *A. aspera* extracts restored catalase activity in the liver (33.9 ± 1.7 and 35.3 ± 0.3 U/mg of protein, respectively, for a dose of 200 and 400 mg/kg body weight).

Furthermore, as shown in Table 2, the NO levels also increased in the liver of alloxan-induced diabetic mice (29.3 ± 1.7 nmol/mL) compared to normal mice (11.5 ± 1.9 nmol/mL). Treatment with *A. aspera* significantly decreased the NO levels in diabetic mice (22.8 ± 2.4 and 21.8 ± 2.7 nmol/mL, respectively, for a dose of 200 and 400 mg/kg body weight).

4. Discussion

Oxidative stress in diabetes coexists with a reduction in antioxidant status (*27*). In the current study, *A. aspera* had potent antioxidant activity *in vitro* and lowered blood glucose concentrations and prevented oxidative stress in alloxan-treated diabetic mice. A pancreatic β-cell toxin, alloxan is responsible for oxidative damage to the pancreas. A low dose of alloxan (120 mg/kg) causes partial destruction of pancreatic β-cells in laboratory rodents and thereby produces glucose intolerance and hyperglycemia (*28*).

A. aspera extracts had potent free radical scavenging activity in a dose-dependent manner *in vitro* according to various assays. Phytochemical screening revealed the presence of flavonoids and phenolic compounds in the extracts. Free radical scavenging activity of plant extracts is dependent on the presence of such polyphenolic compounds (*29,30*). In the current study, *A. aspera* extracts had potent inhibitory activity against NO and H_2O_2 generation. NO and H_2O_2 are both strong free radicals in biological systems that are readily converted into more reactive peroxynitrite and superoxide anions (*31*). Previous reports suggest that *A. aspera* has saponin glycosides with aglycones in the form of betaine, oleanolic acid, and quercitin, and these compounds presumably improve diabetes and hyperglycemia (*8,9,32*). Oleanolic acid and quercetin are potent antioxidant compounds (*33,34*). Quercetin is also effective against diabetes in experimental animals and prevents oxidative stress and β-cell damage in streptozotocin-induced diabetic rats (*35,36*). The

current study found that *A. aspera* extracts reduced the elevated blood glucose levels in alloxan-treated diabetic mice in a dose-dependent manner. Lowering of blood glucose levels is probably mediated by improvement or protection of the pancreas' structure in alloxan-treated mice (*37*).

Decreased antioxidant enzyme levels and increased lipid peroxidation were also seen in alloxan-induced diabetic animal (*38*). Thus, supplementation with antioxidants may have a chemoprotective role in diabetes (*39*). The reoxidation of dialurate to alloxan by molecular oxygen yields H_2O_2, which is generally considered to be a cytotoxic agent. The decreased activity of catalase and SOD may be a response to increased H_2O_2 and O_2^- production as a result of the autoxidation of glucose and non-enzymatic glycation (*40*). Catalase is a hemeprotein that catalyzes the reduction of H_2O_2 and protects tissue from highly reactive hydroxyl radicals. SOD and catalase activity decrease in the liver and kidneys during diabetes and are implicated in the accumulation of O_2^- and H_2O_2 (*41*). Administration of *A. aspera* extract increased the activity of catalase and decreased hydroperoxide production by scavenging free radicals because of the presence of phenolic compounds in the extract. Moreover, increased NO production from inducible NO synthase may form peroxynitrite with superoxide and contribute to cellular injury, including lipid peroxidation and nitrosylation of some molecules (*42*). The positive correlation between NO and TBARS concentrations in diabetic mice may be responsible for the direct or indirect effect of NO on increased lipid peroxidation. In this study, alloxan-treated diabetic mice had the largest amounts of NO and TBARS among the groups. *A. aspera* extracts had NO scavenging activity *in vitro* and prevented the production of NO and TBARS in a dose-dependent manner in alloxan-treated diabetic animals.

However, alternate pathways of glucose disposal are also possible with *A. aspera* administration due to the presence of triterpenoid oleanolic acid present in the plant. Oleanolic acid enhances insulin secretion in response to a glucose challenge in both INS-1 832/13 cells and rat islets; no increase in cAMP and intracellular Ca^{2+} ion concentrations has been noted (*43*). Moreover, oleanolic acid inhibits α-glucosidase

and activates TGR5 G-protein-coupled receptors, which may help to lower glucose levels by increasing insulin sensitivity (*44*). This triterpenoid molecule also affects glucose absorption in the gastrointestinal tract by suppressing gastric emptying (GE) in rats and it inhibits the Na^+/glucose co-transport system at the intestinal brush border membrane (*45*). Metformin, a biguanide used in the current study as a standard drug, also had hypoglycemic action (*46*). Metformin acts by decreasing hepatic glucose production and intestinal absorption as well as by increasing peripheral glucose uptake and insulin sensitivity (*46*). Metformin also increases fatty acid oxidation and decreases absorption of glucose from the gastrointestinal tract (*47*).

The current study substantiates the use of *A. aspera* in traditional medicine as a nonspecific hypoglycemic agent. Its hypoglycemic activity is due to its ability to scavenge free radicals and prevent oxidative stress in diabetic mice. Further studies are required to establish the safety of the extract and possibly isolate the active principle responsible for the observed activity of *A. aspera* extracts.

Acknowledgement

References

1. Limaye PV, Raghuram N, Sivakami S. Oxidative stress and gene expression of antioxidant enzymes in the renal cortex of streptozotocin induced diabetic rats. Mol Cell Biochem. 2003, 243:147-152.
2. Watanabe J, Umeda F, Wakasugi H, Ibayashi H. Effect of vitamin E on platelet aggregation in diabetes mellitus. Tohoku J Exp Med. 1984; 143:161-169.
3. Ghani A. Medicinal Plants of Bangladesh with Chemical Constituents and Uses. The Asiatic Society of Bangladesh. 2nd ed., Dhaka, Bangladesh, 2003; pp. 71-72.
4. Datta RM, Mitra JN. Common plants in and around Dacca. Bull Bot Soc Beng. 1953; 7:8-10.
5. Kumar S, Singh JP, Kumar S. Phytochemical screening of some plants of Manipur-I. J Econ Bot Phytochem. 1990; 1:13-16.
6. Banerji A, Chintalwar GJ, Joshi NK, Chadha MS. Isolation of ecdysterone from Indian plants. Phytochemistry. 1971; 10:2225-2226.
7. Banerji A, Chadha MS. Insect moulting hormone from *Achyranthes aspera*. Phytochemistry. 1970; 9:1671.
8. Michl G, Abebe D, Bucar F, Debella A, Kunert O, Schmid MG, Mulatu E, Haslinger E. New Triterpenoid Saponins from *Achyranthes aspera* Linn. Helvetica Chimica Acta. 2000; 83:359-363.
9. Kunert O, Haslinger E, Schmid MG, Reiner J, Bucar F, Mulatu E, Abebe D, Debella A. Three saponins, a steroid, and a flavanol glycoside from *Achyranthes aspera*. Monatshefte für Chemie. 2000; 131:195-204.
10. Tahiliani P, Kar A. *Achyranthes aspera* elevates thyroid hormone level and decrease hepatic lipid peroxidation in male rats. J Ethnopharmacol. 2000; 71:527-532.
11. Edwin S, Jarald EE, Deb L, Jain A, Kinger H, Dutt KR, Raj AA. Wound healing and antioxidant activity of *Achyranthes aspera*. Pharm Biol. 2008; 46:824-828.
12. Rani N, Sharma SK, Neeru Vasudeva N. Assessment of antiobesity potential of *Achyranthes aspera* Linn. seed. Evidence-Based Complementary and Alternative Medicine. 2012. doi:10.1155/2012/715912.
13. Akhtar MS, Iqbal J. Evaluation of the hypoglycaemic effect of *Achyranthes aspera*. J Ethnopharmacol. 1991; 31:49-57.
14. Majumder MM, Mazumder MEH, Alam MA, Akter R, Rahman MM, Sarker SD. Antioxidant and membrane stabilizing properties of *Ichnocarpus frutescens*. J Nat Remedies. 2008; 8:209-215.
15. Alam MA, Ghani A, Subhan N, Rahman MM, Haque MS, Majumder MM, Mazumder MEH, Akter RA, Nahar L, Sarker SD. Antioxidant and membrane stabilizing properties of the flowering tops of *Anthocephalus cadamba*. Nat Prod Commun. 2008; 3:65-67.
16. Alam MA, Nayeem MAB, Awal MA, Mostofa M, Alam MS, Subhan N, Rahman MM. Antioxidant and hepatoprotective action of the crude methanolic extract of the flowering top of *Rosa damascene*. Oriental Pharm Exp Med. 2008; 8:164-170.
17. Subhan N, Alam MA, Ahmed F, Awal MA, Nahar L, Sarker SD. *In vitro* antioxidant property of the extract of *Excoecaria agallocha* (Euphorbiaceae). DARU. 2008; 16:149-154.
18. Braca A, Tommasi ND, Bari LD, Pizza C, Politi M, Morelli I. Antioxidant principles from *Bauhinia terapotensis*. J Nat Prod. 2001; 64:892-895.
19. Oyaizu M. Studies on product of browning reaction prepared from glucose amine. Jpn J Nutr. 1986; 44:307-315.
20. Garrat DC. The Quantitative Analysis of Drugs, vol. 3. Chapman and Hall, Japan, 1964; pp. 456-458.
21. Ruch RJ, Cheng SJ, Klaunig JE. Prevention of cytotoxicity and inhibition of intercellular communication by antioxidant catechins isolated from Chinese green tea. Carcinogenesis. 1989; 10:1003-1008.
22. Majhenic L, Skerget M, Knez Z. Antioxidant and antimicrobial activity of guarana seed extracts. Food Chem. 2007; 104:1258-1268.
23. Niehius WG, Samuelsson D. Formation of malondialdehyde from phospholipids arachidonate during microsomal lipid peroxidation. Eur J Biochem. 1968; 6:126-130.
24. Jiang ZY, Hunt JV, Wolff SP. Ferrous ion oxidation in the presence of xylenol orange for detection of lipid hydroperoxide in low-density lipoprotein. Anal Biochem. 1992; 202:384-387.
25. Sinha KA. Colorimetric assay of catalase. Anal Biochem. 1972; 47:389-394.
26. Tracy WR, Tse J, Carter G. Lipopolysaccharide-induced changes in plasma nitrate and nitrite concentration in rats and mice: Pharmacological evaluation of nitric oxide synthase inhibitors. J Pharmacol Exp Ther. 1995; 272:1011-1015.
27. Collier A, Wilson R, Bradley H, Thomson JA, Small M. Free radical activity in Type II Diabetes. Diabetic Med. 1990; 7:27-30.
28. Yadav JP, Saini S, Kalia AN, Dangi AS. Hypoglycemic and hypolipidemic activity of ethanolic extract of *Salvadora oleoides* in normal and alloxan-induced

diabetic rats. Indian J Pharmacol. 2008; 40:23-27.

29. Osawa T. Protective role of dietary polyphenols in oxidative stress. Mech Ageing Dev. 1999; 111:133-139.

30. Fernandez-Panchona MS, Villanoa D, Troncosoa AM, Garcia-Parrilla MC. Antioxidant activity of phenolic compounds: From *in vitro* results to *in vivo* evidence. Crit Rev Food Sci Nutr. 2008; 48:649-671.

31. Dröge W. Free radicals in the physiological control of cell function. Physiol Rev. 2002; 82:47-95.

32. Blunden G, Yang M, Janicsak G, Mathe I, Carabot-Cuervo A. Betaine distribution in the Amaranthaceae. Biochem Syst Ecol. 1999; 27:87-92.

33. Liu J, Oleanolic acid and ursolic acid: Research perspectives. J Ethnopharmacol. 2005; 100:92-94.

34. Procházková D, Boušová I, Wilhelmová N. Antioxidant and prooxidant properties of flavonoids. Fitoterapia. 2011; 82:513-523.

35. Mahesh T and Menon VP. Quercetin alleviates oxidative stress in streptozotocin-induced diabetic rats. Phytother Res. 2004; 18:123-127.

36. Coskun O, Kanter M, Korkmaz A, Oter S. Quercetin, a flavonoid antioxidant, prevents and protects streptozotocin-induced oxidative stress and β-cell damage in rat pancreas. Pharmacol Res. 2005; 51:117-123.

37. Zambare MR, Bhosale UA, Somani RS, Yegnanarayan R, Talpate KA. *Achyranthes aspera* (Agadha): Herb that improves pancreatic function in alloxan induced diabetic rats. Asian J Pharm Biol Res. 2011; 1:99-104.

38. Sepici-Dincel A, Açıkgöz S, Cevik C, Sengelen M, Yesilada E. Effects of *in vivo* antioxidant enzyme activities of myrtle oil in normoglycaemic and alloxan diabetic rabbits. J Ethnopharmacol. 2007; 110:498-503.

39. Logani MK, Davis RE. Lipid peroxidation in biologic effects and antioxidants: A review. Lipids. 1979; 15:485-493.

40. Aragno M, Brignardello E, Tamagno O, Boccuzzi G. Dehydroepiandrosterone administration prevents the oxidative damage induced by acute hyperglycemia in rats. J Endocrinol. 1997; 155:233-240.

41. Searle AJ, Wilson R. Glutathione peroxide effect of superoxide, hydroxyl and bromine free radicals on enzyme activity. Int J Rad Biol. 1980; 37:213-217.

42. O'Donnell VB, Freeman BA. Interactions between nitric oxide and lipid oxidation pathways. Circ Res. 2001; 88:12-21.

43. Teodoro T, Zhang L, Alexander T, Yue J, Vranic M, Volchuk A. Oleanolic acid enhances insulin secretion in pancreatic β-cells. FEBS Lett. 2008; 582:1375-1380.

44. Sato H, Genet C, Strehle A, Thomas C, Lobstein A, Wagner A, Mioskowski C, Auwerx J, Saladin R. Anti-hyperglycemic activity of a TGR5 agonist isolated from *Olea europaea*. Biochem Biophys Res Commun. 2007; 362:793-798.

45. Matsuda H, Li Y, Murakami T, Yamahara J, Yoshikawa M. Structure-related inhibitory activity of oleanolic acid glycosides on gastric emptying in mice. Bioorg Med Chem. 1999; 7:323-327.

46. Kirpichnikov D, McFarlane SI, Sowers JR. Metformin: An update. Ann Intern Med. 2002; 137:25-33.

47. Collier CA, Bruce CR, Smith AC, Lopaschuk G, Dyck DJ. Metformin counters the insulin-induced suppression of fatty acid oxidation and stimulation of triacylglycerol storage in rodent skeletal muscle. Am J Physiol Endocrinol Metab. 2006; 291:E182-E189.

Neuroprotective and hepatoprotective effects of micronized purified flavonoid fraction (Daflon®) in lipopolysaccharide-treated rats

Omar M.E. Abdel-Salam[1],*, Eman R Youness[2], Nadia A. Mohammed[2], Mehrevan Abd-Elmoniem[2], Enayat Omara[3], Amany A. Sleem[4]

[1] *Department of Toxicology and Narcotics, National Research Centre, Cairo, Egypt;*
[2] *Department of Medical Biochemistry, National Research Centre, Cairo, Egypt;*
[3] *Department of Pathology, National Research Centre, Cairo, Egypt;*
[4] *Department of Pharmacology, National Research Centre, Cairo, Egypt.*

ABSTRACT: Micronized purified flavonoid fraction (MPFF, Daflon®) is a phlebotonic drug widely used in chronic venous or lymphatic insufficiency. We aimed to investigate the effects of MPFF on hepatic and brain oxidative stress and on liver injury caused by lipopolysaccharide (LPS) in rats. MPFF (4.5, 9, or 18 mg/kg) or saline was administered orally for two days prior to intraperitoneal (*i.p.*) LPS (300 μg/kg) and at time of LPS administration. Rats were euthanized 4 h after LPS injection. The administration of LPS increased oxidative stress in brain and liver tissue. Malondialdehyde (MDA) increased by 193.5 and 191.8%, reduced glutathione (GSH) decreased by 73.8 and 70.8% and nitric oxide increased by 118.2 and 151.7% in the brain and liver, respectively. Serum paraoxonase 1 (PON1) activity decreased by 42.6%. Serum aspartate aminotransferase (AST), alanine aminotransferase (ALT) and alkaline phosphatase (ALP) were raised by 101.8, 93.6, and 223.2%, respectively. Rats treated with MPFF at 9 and 18 mg/kg showed decreased brain MDA (27.5-34%), nitrite (25.5-41%) and increased GSH (27.2-74.1%). In the liver, MDA decreased by 16.4-59.8%, nitrite decreased by 54.7-56.7%, and GSH increased by 15.2-70.5% with MPFF at 4.5, 9, or 18 mg/kg, respectively. Serum PON1 activity showed 41-65.9% increments with MPFF. Significant reductions in serum AST, ALT, and ALP were seen after treatment with MPFF. Moreover, the degree of histological damage, expression of the inducible form of nitric oxide synthase and the apoptotic enzyme caspase-3 in the liver were substantially reduced. MPFF thus prevented the increased oxidative stress and inflammation in brain and liver as well as the liver dysfunction caused by endotoxemia in the rat.

**Address correspondence to:*
Dr. Omar M.E. Abdel-Salam, Department of Toxicology and Narcotics, National Research Centre, Tahrir St., Dokki, Cairo, Egypt.
E-mail: omasalam@hotmail.com

1. Introduction

Micronized purified flavonoid fraction (MPFF, Daflon®) is a semisynthetic drug which consists of 90% micronized diosmin (a flavone derivative) and 10% flavonoids expressed as hesperidin (a flavonone derivative). The flavonoid glycosides diosmin and hesperidin occur naturally in citrus fruit (*1*). The drug is widely used in treatment of varicose veins and venous ulcers, lymphatic insufficiency and hemorrhoids (*2,3*). In these conditions, MPFF exerts a venotonic action, decreasing venous reflux, and thereby alleviating edema and providing effective venous drainage (*4*). Moreover, the drug has been shown to provide better outcomes for patients with impaired cardiac function before undergoing cardiac operations that require cardiopulmonary bypass (*5*). These effects of MPFF can be ascribed to the anti-inflammatory, microcirculatory, and antioxidant effects of its flavonoid substances. In this context, MPFF has been shown to decrease the levels of granulocyte and macrophage infiltration into the inflamed tissues as well as leucocyte adhesion to the vascular endothelium. The decrease in release of oxygen free radicals, cytokines, and proteolytic matrix metalloproteinases from activated inflammatory and endothelial cells, results in lower levels of inflammation, decreased microvascular permeability and decreased leukocyte-dependent endothelial damage (*6,7*). MPFF decreases vascular permeability more than any of its single constituents, suggesting that the flavonoids present in its formulation have a synergistic action (*8*). The drug possesses an antioxidant effect, significantly decreasing the level of hydroxyl free radicals (*9*), increasing free SH-group concentration, and natural scavenger capacity (*10*).

Lipopolysaccharide (LPS)-induced endotoxemia is a well-established model for infection with Gram-

negative bacteria. By acting on Toll-like receptor 4 (TLR4) on immune cells such as monocytes, macrophages, neutrophils and dendritic cells, LPS triggers synthesis and release of proinflammatory cytokines and nitric oxide both in the periphery and central nervous system, resulting in peripheral and neuroinflammation (*11,12*). Since neuroinflammation and oxidative stress are important contributors to the pathogenesis and disease progression of some neurodegenerative disorders, including Alzheimer's disease and Parkinson's disease (*13,14*), LPS-endotoxemia represents a useful model for studying the effect of systemic inflammation on brain function (*15*).

The present study was therefore designed to investigate the effects of MPFF on oxidative stress in brain and liver of rats subjected to endotoxemia and systemic inflammation caused by *Escherichia coli* LPS injection. In addition, this study aimed to investigate whether treatment of LPS-rats with MPFF would protect against endotoxemic liver injury.

2. Materials and Methods

2.1. *Animals*

Sprague-Dawley rats of both sexes, weighing 120-130 g were used throughout the experiments and fed with standard laboratory chow and water *ad libitum*. All animal procedures were performed in accordance with the Institutional Ethics Committee and in accordance with the recommendations for the proper care and use of laboratory animals (NIH publication No. 85-23, revised 1985).

2.2. *Drugs and chemicals*

A purified lyophilized *E. coli* endotoxin (Serotype 055:B5, Sigma, St Louis, MO, USA) was used and dissolved in sterile saline, aliquoted, and frozen at −20°C. MPFF, (Daflon®, Servier, Paris, France) consisting of 90% diosmin and 10% hesperidin, was dissolved in isotonic (0.9% NaCl) saline solution immediately before use. The doses of MPFF were based upon the human dose after conversion to that of the rat according to Paget and Barnes (*16*) conversion tables.

2.3. *Study design*

Rats were randomly divided into 5 equal groups (6 rats each). Rats were treated with vehicle (group 1) or MPFF (4.5, 9, or 18 mg/kg) once daily orally for 2 days prior to and at the time of endotoxin administration (LPS: 300 μg/kg, *i.p.*). The fifth group (*n* = 6) received only the vehicle (control). Four hours after LPS or vehicle injection, blood samples were obtained from the retro-orbital venous plexus under ether anesthesia. Rats were then euthanized by decapitation under ether anesthesia, livers and brains were then removed, and washed with ice-cold phosphate buffered saline (PBS,

pH7.4), and parts of the tissues were preserved in formalin 10% for further histopathological and immunohistochemical examination. Other parts were weighed and stored at −80ºC for biochemical analyses. The tissues were homogenized with 0.1 M phosphate buffered saline at pH 7.4, to give a final concentration of 10% (w/v) for the biochemical assays. The time selected for tissue sampling (4 h after *i.p.* administration of LPS) was based on previous studies that indicated the rise in plasma and tissue cytokines and inflammatory mediators (interleukin (IL)-1β, IL-6, tumor necrosis factor (TNF)-α, inducible nitric oxide synthase (iNOS) mRNA expression, nitric oxide, and myeloperoxidase activity) in rats receiving *i.p.* LPS by that time (*17,18*).

2.4. *Determination of lipid peroxidation*

Lipid peroxidation was assayed by measuring the level of malondialdehyde (MDA) in the tissue homogenates. Malondialdehyde was determined by measuring thiobarbituric reactive species using the method of Ruiz-Larrea *et al.* (*19*), in which the thiobarbituric acid reactive substances react with thiobarbituric acid to produce a red colored complex having a peak absorbance at 532 nm (UV-VI8 Recording Spectrophotometer, Shimadzu, Kyto, Japan).

2.5. *Determination of reduced glutathione*

Reduced glutathione (GSH) was determined in tissue by Ellman's method (*20*). The procedure is based on the reduction of Ellman's reagent by –SH groups of GSH to form 2-nitro-5-mercaptobenzoic acid, the nitromercaptobenzoic acid anion has an intense yellow color which can be determined spectrophotometrically.

2.6. *Determination of nitric oxide*

Nitric oxide measured as nitrite was determined by using Griess reagent, according to the method of Moshage *et al.* (*21*), where nitrite, stable end product of the nitric oxide radical, is mostly used as an indicator for the production of nitric oxide.

2.7. *Determination of paraoxonase activity*

Arylesterase activity of paraoxonase was measured spectrophotometrically in serum following the procedure described by Higashino *et al.* (*22*) and Watson *et al.* (*23*) using phenyl acetate (Sigma) as substrate.

2.8. *Determination of serum liver enzymes*

The activities of aspartate aminotransferase (AST) and alanine aminotransferase (ALT) enzymes, indicators of liver damage, were measured in serum according to the Reitman-Frankel colorimetric transaminase procedure (*24*), whereas colorimetric determination of

alkaline phosphatase (ALP) activity was done according to the method of Belfield and Goldberg (*25*), using commercially available kits (BioMérieux, France).

2.9. *Histological assessment of liver injury*

Liver sections from each rat were fixed in freshly prepared 10% neutral buffered formalin, processed routinely, and embedded in paraffin. Five μm thick paraffin sections were prepared and stained with hematoxylin and eosin (H&E) for histopathological examination. Sections were examined using a light microscope.

2.10. *Immunohistochemical assessment of liver injury*

Immunohistochemical staining of anti-caspase-3 antibody and iNOS was performed with streptavidin-biotin. Sections of four μm thick were deparaffinized and incubated with fresh 0.3% hydrogen peroxide in methanol for 30 min at room temperature. The specimens were then incubated with anti-caspase-3 and iNOS antibody as the primer antibody at a 1:100 dilution. The specimens were counterstained with H&E. Negative controls were prepared by substituting normal mouse serum for each primary antibody.

2.11. *Statistical analysis*

Data are expressed as mean ± SE. Statistical analysis of the data was done using one way ANOVA followed by the Duncan test for multiple group comparison tests, using SPSS software (SAS Institute Inc., Cary, NC, USA). Probability levels of $p < 0.05$ were considered statistically significant.

3. Results

3.1. *Biochemical results*

3.1.1. *Effect of MPFF on brain oxidative stress*

The administration of LPS significantly increased brain MDA by 193.4% (91.6 ± 3.4 *vs.* 31.2 ± 2.2 nmol/g, $p < 0.05$). GSH decreased by 73.8% (0.896 ± 0.03 *vs.* 3.42 ± 0.18 μmol/g, $p < 0.05$), while nitric oxide (the level of nitrite) increased by 118.2% (48.0 ± 2.7 *vs.* 22.0 ± 1.0 μmol/g, $p < 0.05$) after LPS injection compared with the saline control group. Brain MDA was significantly decreased by 21.7, 27.5, and 34% after MPFF at 4.5, 9, or 18 mg/kg, respectively (71.7 ± 3.1, 66.4 ± 4.2, and 60.4 ± 3.9 *vs.* 91.6 ± 3.4 nmol/g, $p < 0.05$) (Figure 1A). The administration of MPFF at 9 and 18 mg/kg resulted in a 27.2 and 73.1% increase in GSH (1.14 ± 0.08 and 1.56 ± 0.06 *vs.* 0.896 ± 0.03 μmol/g, $p < 0.05$) (Figure 1B). The level of nitric oxide decreased by 25.5 and 41.0% after MPFF at 9 and 18 mg/kg (38.1 ± 2.1 and 28.3 ± 1.4 *vs.* 48.0 ± 2.7 μmol/g, $p < 0.05$) (Figure 1C).

3.1.2. *Effect of MPFF on liver oxidative stress*

Liver MDA was increased significantly by 191.8% following endotoxin injection (151.2 ± 6.4 *vs.* 51.8 ± 2.5 nmol/g, $p < 0.05$). A significant decrease in GSH by 70.8% (1.05 ± 0.06 *vs.* 3.6 ± 0.18 μmol/g, $p < 0.05$) as well as markedly raised nitric oxide (40.3 ± 2.2 *vs.* 16.0 ± 1.3 μmol/g, $p < 0.05$) were observed after LPS treatment. The administration of MPFF at 9 and 18 mg/kg resulted in a significant decrease in liver MDA by 16.4 and 59.7% compared to the LPS control group (122.1 ± 4.1 and 60.9 ± 3.8 *vs.* 151.2 ± 6.4 nmol/g, $p < 0.05$) (Figure 2A). There was a dose-dependent increase in liver GSH by 15.2, 43.8,
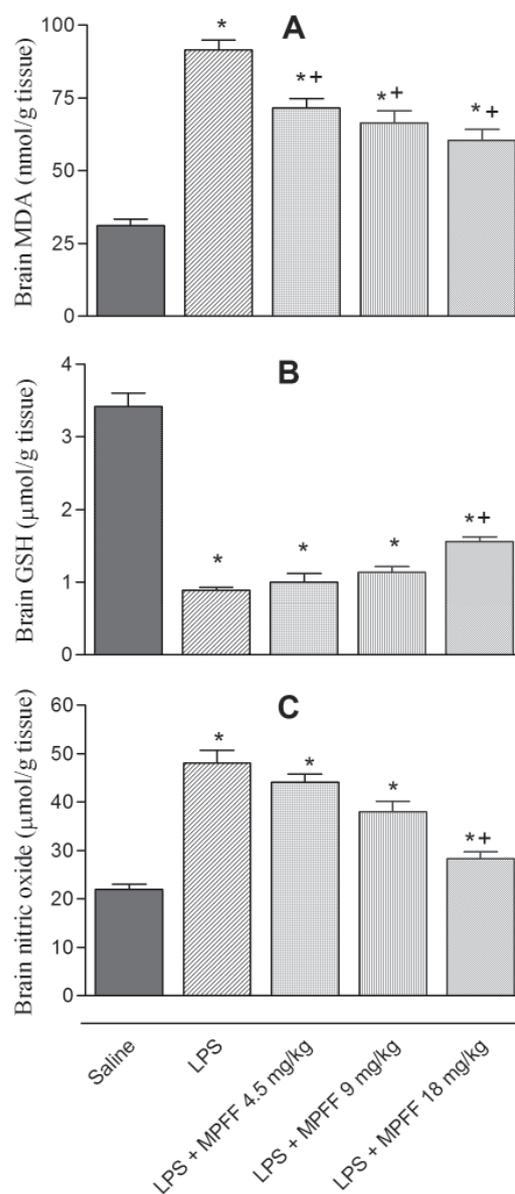

Figure 1. Effect of MPFF on LPS-induced changes in brain MDA (A), GSH (B), and nitric oxide (C). Data are expressed as mean ± SE, $n = 6$. * $p < 0.05$ *versus* saline control; + $p < 0.05$ *versus* LPS (one-way analysis of variance and Duncan multiple range test).

and 70.5% (1.21 ± 0.03, 1.51 ± 0.08, and 1.79 ± 0.06 *vs.* 1.05 ± 0.06 μmol/g, *p* < 0.05) as well as a dose-dependent decrease in nitrite by 54.7, 55.3, and 56.7% (18.2 ± 1.0, 18.0 ± 1.2, and 16.5 ± 0.9 *vs.* 40.3 ± 2.2 μmol/g, *p* < 0.05) after treatment with MPFF at 4.5, 9, or 18 mg/kg, respectively (Figure 2C).

3.1.3. *Effect of MPFF on serum liver enzymes*

In rats treated with only LPS, the levels of ALT, AST, and ALP in plasma were markedly raised by 93.6% (36.6 ± 2.0 *vs.* 18.9 ± 1.2 U/L), 101.8% (123.1 ± 7.2 *vs.* 61.0 ± 3.4 U/L) and 223.2% (446.0 ± 12.8 *vs.* 138 ± 6.9 U/L), respectively. Significant reduction in serum AST, ALT,

and ALP were observed in rats treated with MPFF. Thus, ALT decreased by 17.2, 33.9, and 45.3% after treatment with MPFF at 4.5, 9, or 18 mg/kg, respectively; AST decreased by 17 and 20% by MPFF at 9 or 18 mg/kg, respectively; ALP decreased by 29.1, 37.8, and 44% by MPFF at 4.5, 9, or 18 mg/kg, respectively (Figures 3).

3.1.4. *Effect of MPFF on serum paraoxonase 1 (PON1) activity*

Serum PON1 activity decreased by 42.6% following endotoxin administration (83.8 ± 4.6 *vs.* 146.1 ± 7.8 kU/L, *p* < 0.05). The administration of MPFF resulted in a significant and a dose-related increase in PON1
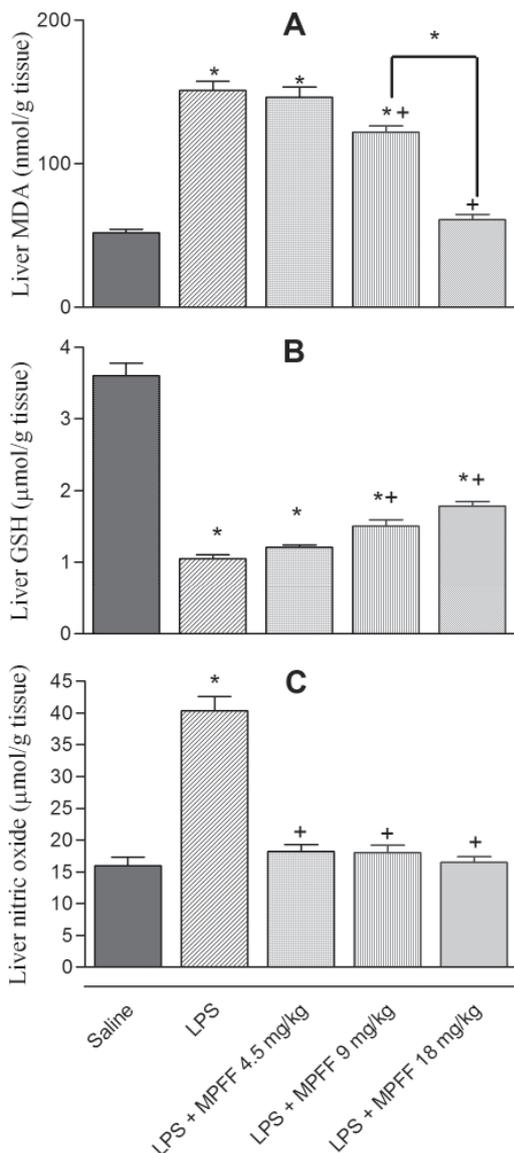

Figure 2. Effect of MPFF on LPS-induced changes in liver MDA (A), GSH (B), and nitric oxide (C). Data are expressed as mean ± SE, *n* = 6. * *p* < 0.05 *versus* saline control and between different groups as indicated in the figure; + *p* < 0.05 *versus* LPS (one-way analysis of variance and Duncan multiple range test).
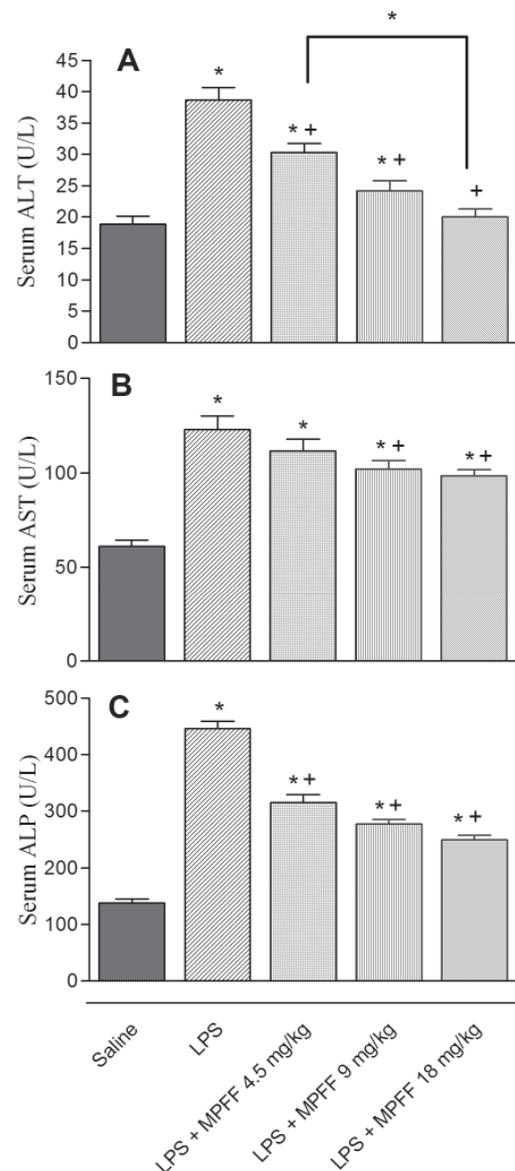
Figure 3. Effect of MPFF on LPS-induced elevation in serum ALT (A); AST (B), and ALP (C). Data are expressed as mean ± SE, *n* = 6. * *p* < 0.05 *versus* saline control and between different groups as indicated in the figure; + *p* < 0.05 *versus* LPS (one-way analysis of variance and Duncan multiple range test).

activity in serum by 41, 56.7, and 65.9% (118.2 ± 6.0, 131.3 ± 5.1, and 139.1 ± 4.8 *vs*. 83.8 ± 4.8 kU/L, *p* < 0.05) after treatment with MPFF at 4.5, 9, or 18 mg/kg, respectively (Figure 4).

3.2. *Histopathological results*

The liver of the control (saline-treated) rats showed normal hepatic architecture with distinct hepatic cells, sinusoidal spaces and a central vein (Figure 5A). Examination of liver sections from LPS-treated rats revealed inflammatory leukocytic cell infiltration around the central vein, and hydropic degeneration with pykontic nuclei (Figure 5B). Focal necrotic areas with inflammatory cell reaction, sinusoidal dilation and activated Kupffer cells were seen (Figure 5C). The administration of MPFF resulted in a significant decrease in liver inflammation and necrosis compared to the LPS control group. The effect was dose-dependent. Thus, liver sections of rats treated with LPS and MPFF at 4.5 mg/kg showed apparently normal tissues with congestion of the central vein and dilation of sinusoids. Minimal focal necrotic areas were also visible (Figure 5D). After treatment with MPFF at 9 mg/kg, sections revealed apparently normal tissues with a mildly congested central hepatic vein and some of the sinusoids. Focal necrotic areas were not seen (Figure 5E). Liver sections of rats treated with LPS and MPFF at 18 mg/kg showed almost normal liver with very mild dilation of sinusoids and no congestion. The nuclei were normal indicating the recovery of the liver tissues (Figure 5F).

3.3. *Immunohistochemical results*

3.3.1. *Caspase-3 expression*

Expression of caspase-3 was not observed in control
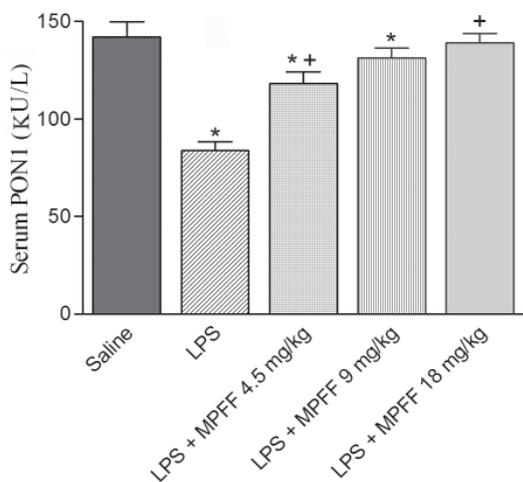
Figure 4. Effect of MPFF on serum PON1 activity in LPS-treated rats. Data are expressed as mean ± SE, *n* = 6.* *p* < 0.05 *versus* saline control; + *p* < 0.05 *versus* LPS (one-way analysis of variance and Duncan multiple range test).

liver (Figure 6A). By comparison, strong expression of caspase-3 was observed in the LPS control group as shown in Figure 6B and gradually decreased in rats treated with MPFF in a dose-dependent manner as shown in Figures 6C-6E.

3.3.2. *iNOS expression*

In the liver tissue of control rats there was a weakly localized iNOS immunohistochemical staining (Figure 7A). In rats treated with LPS, a much more intense expression of iNOS was detected in the hepatocytes of the centrilobular zone in the surface of hepatocytes. A number of hepatocyte nuclei showed iNOS immunoreaction (Figure 7B). In hepatocytes of rats treated with LPS and MPFF, iNOS immunoreactivity showed a dose-dependent decrease compared with the LPS control group (Figures 7C-7E).

4. Discussion

The results of the present study indicate that pretreatment with MPFF was able to ameliorate brain
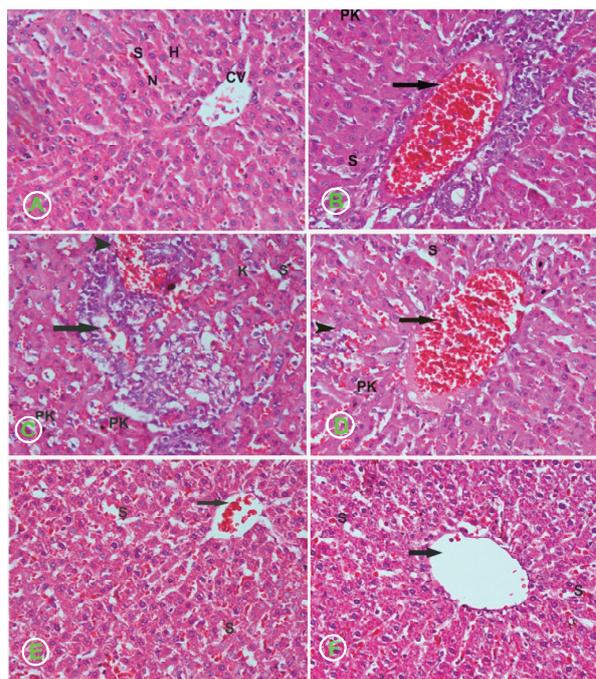

Figure 5. H&E stained liver sections from: (A) control (saline-treated) rat showing central vein (CV), hepatic cells (H), sinusoidal space (S), and nucleus (N); **(B)** LPS-treated rat showing inflammatory leukocytic cell infiltration around central vein (arrow), sinusoidal dilation (S), and pyknotic nuclei (PK); **(C)** LPS-treated rat showing focal necrotic area (arrow) with inflammatory cell reaction (arrow head), congestion and sinusoidal dilation (S), activated Kupffer cell (K) and pyknotic cells; **(D)** LPS + MPFF 4.5 mg/kg-treated rat showing severly congested hepatic central vein and focal area of mild mononuclear cells; **(E)** LPS + MPFF 9 mg/kg-treated rat showing moderately normal tissue with mildly congested central hepatic vein and some of the sinusoids. Focal necrotic areas were not visible; **(F)** LPS + MPFF 18 mg/kg-treated rat showing almost normal liver with very mild dilation of sinusoids and no congestion. The nuclei were normal indicating the recovery of the liver tissues (H&E, ×400).
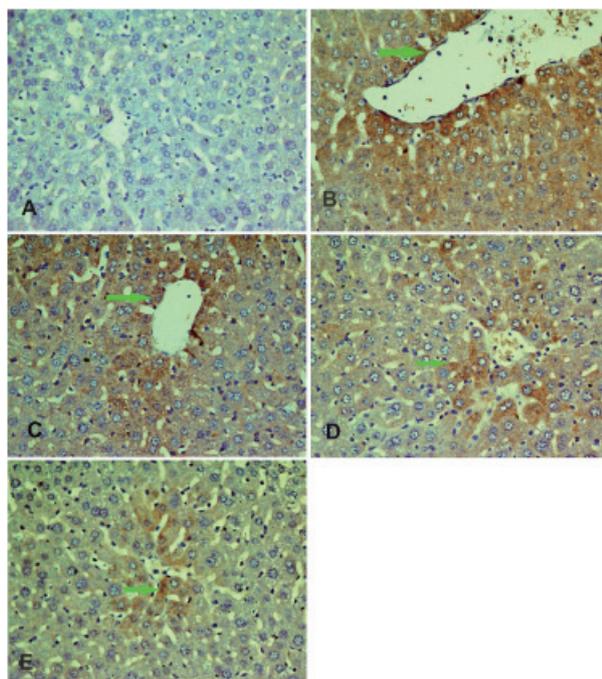
Figure 6. Effect of MPFF on LPS-induced caspase-3 expression in liver: caspase-3 immunohistochemistry of liver from a rat treated with **(A)** saline (control): caspase-3-immunolabeled cells were rarely present; **(B)** only LPS: an increased number of caspase-3 immunolabeled hepatocytes were observed around central veins compared to control animals, suggesting increased apoptosis; **(C)** LPS + MPFF 4.5 mg/kg: caspase-3-immunolabeled cells were slightly decreased compared to LPS control group; **(D)** LPS + MPFF 9 mg/kg: caspase-3-immunolabeled cells were slightly decreased compared to LPS control group; **(E)** LPS + MPFF 18 mg/kg: caspase-3-immunolabeled cells were obviously decreased compared to LPS control group (caspase-3 immune staining, ×400).

Figure 7. Effect of MPFF on LPS-induced iNOS protein expression in liver: iNOS immunohistochemistry of liver from a rat treated with **(A)** saline (control): iNOS-immunolabeled cells were weakly present in the liver of control rats; **(B)** only LPS: a marked increased number of iNOS immunolabeled hepatocytes was observed around central veins compared to normal animals; **(C)** LPS + MPFF 4.5 mg/kg: iNOS immunolabeled cells were slightly decreased compared to LPS control group; **(D)** LPS + MPFF 9 mg/kg: iNOS immunolabeled cells were slightly decreased compared to LPS control group; **(E)** LPS + MPFF 18 mg/kg: iNOS immunolabeled cells were markedly decreased compared to LPS control group (iNOS immune staining, ×400).

and liver oxidative stress induced by the intraperitoneal administration of LPS. The drug lessened the elevation in MDA, a marker of increased oxidative stress, which indicates a free radical attack on polyunsaturated fatty acids of biological membranes (*26*). The increase in nitric oxide in response to LPS was also decreased by treatment with MPFF. Nitric oxide generated by the inducible form of nitric oxide synthase (iNOS) is most often associated with inflammatory conditions in which it is produced in large amounts by monocyte/macrophage lineage cell types. The induction of NOS has been demonstrated in response to a number of stimuli including LPS, IL-1, and TNF-α (*27*). Glutathione is an intracellular tripeptide (γ-glutamyl-cysteinyl-glycine) common in all tissues and is the most important thiol antioxidant in the cell (*28*). The administration of LPS endotoxin was associated with decreased levels of GSH in the brain and liver. This decline in GSH decreased following treatment with MPFF. Collectively, these data suggest a beneficial effect for MPFF during systemic inflammatory illness.

Studies have indicated that the brain is affected during systemic inflammation. Thus, peripheral inflammation induced by intraperitoneal LPS injection produces brain inflammation and oxidative injury (*15*). This is also evident in the present study which shows increased

brain MDA and nitrite levels after LPS. Inflammatory cytokines *e.g.*, IL-1, IL-6, and TNF-α secreted by peripheral innate immune cells during endotoxemia, use neural (*29*) and blood brain barrier pathways (*30*) to relay inflammatory signals to the brain resulting in activation of macrophages and microglia to produce cytokines and free radicals. Such events can induce neuronal dysfunction/degeneration (*15,31*). Studies also suggested that peripheral inflammatory stimuli can aggravate underlying brain pathology *e.g.*, exacerbate brain ischemic injury (*31*) and facilitate microtubule-associated protein (tau) phosphorylation, one of the key pathologies in the brain of patients with Alzheimer's disease (*32*). There is also ample evidence suggesting that increased levels of oxidative stress in brain is linked with aging (*33*) and with development of several neurodegenerative diseases *e.g.*, Parkinson's disease, Alzheimer's disease (*13*), and multiple sclerosis (*34*) as well as in psychiatric diseases *e.g.*, schizophrenia (*35*). Drugs that cause reduction in oxidative damage therefore represent an important therapeutic strategy to slow or halt these disease processes and hence, emphasize the importance of the findings of the present study.

In the present study, the administration of LPS was associated with liver damage. A significant rise in serum

hepatocellular enzymes ALT and AST as well as of the cell wall enzyme ALP was observed. Histologically, focal necrotic areas, inflammatory cell infiltration and hydropic degeneration were seen. Pretreatment of LPS-rats with MPFF significantly attenuated this liver dysfunction. The release of liver enzymes into the circulation was decreased by the drug in a dose-dependent manner and the histological degree of hepatic injury due to endotoxemia was markedly improved by pretreatment with MPFF. Studies have indicated increased iNOS mRNA expression in several organs (*18,36,37*) 4 h after *i.p.* administration of LPS. In the present study, iNOS inmmunoreactivity in the liver increased after LPS where an intense expression of iNOS was detected in the hepatocytes of the centrilobular zone in the surface of hepatocytes. iNOS immunolabeled cells were markedly decreased by the higher dose of MPFF. Caspases are involved in the process of apoptosis or programmed cell death. Caspase-3 is a frequently activated death protease, which disassembles the cell by catalyzing the specific cleavage of many key cellular proteins leading to rapid cell death (*38*). In the present study apoptosis was assessed in liver sections using antibodies that specifically recognize activated caspase-3 (*39*). Increased immunoreactivity of caspase-3 was observed in the cytoplasm of the hepatocytes following LPS challenge. This decreased after pretreatment with MPFF, thereby, indicating decreased apoptosis by the drug. These data clearly indicate hepatic protective effects for MPFF against the deleterious effects of systemic endotoxemia.

The present study also showed that pretreatment with MPFF protected against the decline in serum PON1 induced by endotoxemia. PON1 is a calcium-dependent serum esterase that is synthesized by the liver and released into the circulation, where it binds mainly to high-density lipoproteins and is thought to play an important role in the protection of low-density lipoprotein against oxidative modification (*23*). PON1 also plays an important role in the metabolism of many xenobiotic compounds (*40*). The enzyme is likely to serve an antioxidant function and PON1 activity has been shown to be decreased in several pathologic states such as rheumatoid arthritis (*41*), coronary heart disease (*42*), chronic hepatitis, liver cirrhosis (*43*), and multiple sclerosis in relapse (*44*). In the present study serum PON1 activity decreased following endotoxin administration. In their study, Feingold *et al.* (*45*) observed decreased serum PON1 activity within 24 h following LPS treatment and at doses as low as 100 ng/kg. LPS also induced a marked decrease in PON1 mRNA in the liver as early as 4 h after a single LPS treatment. Paraoxonase might also represent an early defense mechanism against elevated levels of oxidative stress (*46*). In the present study, the administration of MPFF was associated with a dose-dependent increase of PON1 activity in the serum of LPS-treated rats. This

PON1 response is likely to reflect reduction of oxidative stress by MPFF with sparing of the enzyme.

MPFF is a vasotonic drug that is widely used to improve disorders of venous or lymphatic origin (*2,3*). The drug is safe with no or minor side effects being reported (*47*). MPFF owes its beneficial effects to the ability of its content of different flavonoids to decrease leukocytic infiltration and adhesion to the vascular endothelium, resulting in reduced levels of proteolytic enzymes, and decreased microvascular permeability (*7*). The drug possesses antioxidant effects as well (*9,10*). The present study shows that the administration of MPFF is associated with hepatic protective effects. The present study is also the first to demonstrate the inhibitory effect of MPFF pretreatment on the brain oxidative stress in an *in vivo* model of systemic inflammation induced by LPS endotoxin. These findings derive their significance from the evidence that oxidative stress and neuroinflammation are important contributors in the pathogenesis of several neurodegenerative disorders. Oxidative stress also contributes to age-associated neurodegeneration. Orally administered MPFF, therefore, might be a useful adjunct in the treatment of these disorders.

References

1   Katsenis K. Micronized purified flavonoid fraction (MPFF): A review of its pharmacological effects, therapeutic efficacy and benefits in the management of chronic venous insufficiency. Curr Vasc Pharmacol. 2005; 3:1-9.

2   Jiang ZM, Cao JD. The impact of micronized purified flavonoid fraction on the treatment of acute hemorrhoidal episodes. Curr Med Res Opin. 2006; 22:1141-1147.

3   Gohel MS, Davies AH. Pharmacological agents in the treatment of venous disease: An update of the available evidence. Curr Vasc Pharmacol. 2009; 7:303-308.

4   Jantet G. Chronic venous insufficiency: Worldwide results of the RELIEF study. Reflux assessment and quality of life improvement with micronized Flavonoids. Angiology. 2002; 53:245-256.

5   Sirlak M, Akar AR, Eryilmaz S, Cetinkanat EK, Ozcinar E, Kaya B, Elhan AH, Ozyurda U. Micronized purified flavonoid fraction in pretreating CABG patients. Tex Heart Inst J. 2010; 37:172-177.

6   Friesenecker B, Tsai AG, Intaglietta M. Cellular basis of inflammation, edema and the activity of Daflon 500 mg. Int J Microcirc Clin Exp. 1995; 15 (Suppl 1):17-21.

7   Cyrino FZ, Bottino DA, Lerond L, Bouskela E. Micronization enhances the protective effect of purified flavonoid fraction against post ischaemic microvascular injury in the hamster cheek pouch. Clin Exp Pharmacol Physiol. 2004; 31:159-162.

8   Paysant J, Sansilvestri-Morel P, Bouskela E, Verbeuren TJ. Different flavonoids present in the micronized purified flavonoid fraction (Daflon 500 mg) contribute to its anti-hyperpermeability effect in the hamster cheek pouch microcirculation. Int Angiol. 2008; 27:81-85.

9   Delbarre B, Delbarre G, Calinon F. Effect of Daflon 500 mg, a flavonoid drug, on neurological signs, levels of free radicals and electroretinogram in the gerbil after

ischemia-reperfusion injury. Int J Microcirc Clin Exp. 1995; 15 (Suppl. 1):27-33.

10 Rapavi E, Kocsis I, Fehér E, Szentmihályi K, Lugasi A, Székely E, Blázovics A. The effect of citrus flavonoids on the redox state of alimentary-induced fatty liver in rats. Nat Prod Res. 2007; 21:274-281.

11 Quan N, Stern EL, Whiteside MB, Herkenham M. Induction of pro-inflammatory cytokine mRNAs in the brain after peripheral injection of subseptic doses of lipopolysaccharide in the rat. J Neuroimmunol. 1999; 93:72-80.

12 Turrin NP, Gayle D, Ilyin SE, Flynn MC, Langhans W, Schwartz GJ, Plata-Salaman CR. Pro-inflammatory and anti-inflammatory cytokine mRNA induction in the periphery and brain following intraperitoneal administration of bacterial lipopolysaccharide. Brain Res Bull. 2001; 54:443-453.

13 Halliwell B. Role of free radicals in the neuro-degenerative diseases: Therapeutic implications for antioxidant treatment. Drugs Aging. 2001; 18:685-716.

14 Minghetti L. Role of inflammation in neurodegenerative diseases. Curr Opin Neurol. 2005; 18:315-321.

15 Qin L, Wu X, Block ML, Liu Y, Breese GR, Hong JS, Knapp DJ, Crews FT. Systemic LPS causes chronic neuroinflammation and progressive neurodegeneration. Glia. 2007; 55:453-462.

16 Paget GE, Barnes JM. Toxicity testing. In: Evaluation of Drug Activities Pharmacometics (Laurence DR, Bacharach AL, eds.). Academic, London, UK, 1964; pp. 1-135.

17 Vona-Davis L, Wearden P, Hill J, Hill R. Cardiac response to nitric oxide synthase inhibition using aminoguanidine in a rat model of endotoxemia. Shock. 2002; 17:404-410.

18 Beurel E, Jope RS. Lipopolysaccharide-induced interleukin-6 production is controlled by glycogen synthase kinase-3 and STAT3 in the brain. J Neuroinflammation. 2009; 11:6-9.

19 Ruiz-Larrea MB, Leal AM, Liza M, Lacort M, de Groot H. Antioxidant effects of estradiol and 2-hydroxyestradiol on iron-induced lipid peroxidation of rat liver microsomes. Steroids. 1994; 59:383-388.

20 Ellman GL. Tissue sulfhydryl groups. Arch Biochem. 1959; 82:70-77.

21 Moshage H, Kok B, Huizenga JR, Jansen PL. Nitrite and nitrate determination in plasma: A critical evaluation. Clin Chem. 1995; 41:892-896.

22 Higashino K, Takahashi Y, Yamamura Y. Release of phenyl acetate esterase from liver microsomes by carbon tetrachloride. Clin Chim Acta. 1972; 41:313-320.

23 Watson AD, Berliner JA, Hama SY, La Du BN, Faull KF, Fogelman AM, Navab M. Protective effect of high density lipoprotein associated paraoxonase. Inhibition of the biological activity of minimally oxidized low density lipoprotein. J Clin Invest. 1995; 96:2882-2891.

24 Crowley LV. The Reitman-Frankel colorimetric transaminase procedure in suspected myocardial infarction. Clin Chem. 1967; 13:482-487.

25 Belfield A, Goldberg DM. Human serum glucose-6 phosphatase activity: Confirmation of its presence and lack of diagnostic value. Clin Chim Acta. 1971; 31:81-85.

26 Gutteridge JM. Lipid peroxidation and antioxidants as biomarkers of tissue damage. Clin Chem. 1995; 41:1819-1828.

27 Moncada S, Palmer RM, Higgs EA. Nitric oxide: Physiology, pathophysiology, and pharmacology. Pharmacol Rev. 1991; 43:109-142.

28 Wang W, Ballatori N. Endogenous glutathione conjugates: Occurrence and biological functions. Pharmacol Rev. 1998; 50:335-356.

29 Dantzer R, O'Connor JC, Freund GG, Johnson RW, Kelley KW. From inflammation to sickness and depression: When the immune system subjugates the brain. Nat Rev Neurosci. 2008; 9:46-56.

30 Marques F, Falcao AM, Sousa JC, Coppola G, Geschwind D, Sousa N, Correia-Neves M, Palha JA. Altered iron metabolism is part of the choroid plexus response to peripheral inflammation. Endocrinology. 2009; 150:2822-2828.

31 Spencer SJ, Mouihate A, Pittman QJ. Peripheral inflammation exacerbates damage after global ischemia independently of temperature and acute brain inflammation. Stroke. 2007; 38:1570-1577.

32 Lee DC, Rizer J, Selenica ML, Reid P, Kraft C, Johnson A, Blair L, Gordon MN, Dickey CA, Morgan D. LPS-induced inflammation exacerbates phospho-tau pathology in rTg4510 mice. J Neuroinflammation. 2010; 7:56.

33 Poon HF, Calabrese V, Scapagnini G, Butterfield DA. Free radicals and brain aging. Clin Geriatr Med. 2004; 20:329-359.

34 Haider L, Fischer MT, Frischer JM, Bauer J, Höftberger R, Botond G, Esterbauer H, Binder CJ, Witztum JL, Lassmann H. Oxidative damage in multiple sclerosis lesions. Brain. 2011; 134:1914-1924.

35 Behrens MM, Sejnowski TJ. Does schizophrenia arise from oxidative dysregulation of parvalbumin interneurons in the developing cortex? Neuropharmacology. 2009; 57:193-200.

36 Galea E, Reis DJ, Feinstein DL. Cloning and expression of inducible nitric oxide synthase from rat astrocytes. J Neurosci Res. 1994; 37:406-414.

37 Duval DL, Miller DR, Collier J, Billings RE. Characterization of hepatic nitric oxide synthase: Dentification as the cytokine-inducible form primarily regulated by oxidants. Mol Pharmacol. 1996; 50:277-284.

38 Porter AG, Jänicke RU. Emerging roles of caspase-3 in apoptosis. Cell Death Differ. 1999; 6:99-104.

39 Duan WR, Garner DS, Williams SD, Funckes-Shippy CL, Spath IS, Blomme EA. Comparison of immunohistochemistry for activated caspase-3 and cleaved cytokeratin 18 with the TUNEL method for quantification of apoptosis in histological sections of PC-3 subcutaneous xenografts. J Pathol. 2003; 199:221-228.

40 Costa LG, Cole TB, Vitalone A, Furlong CE. Measurement of paraoxonase (PON1) status as a potential biomarker of susceptibility to organophosphate toxicity. Clin Chim Acta. 2005; 352:37-47.

41 Tanimoto N, Kumon Y, Suehiro T, Ohkubo S, Ikeda Y, Nishiya K, Hashimoto K. Serum paraoxonase activity decreases in rheumatoid arthritis. Life Sci. 2003; 72:2877-2885.

42 Kotur-Stevuljevic J, Spasic S, Jelic-Ivanovic Z, Spasojevic-Kalimanovska V, Stefanovic A, Vujovic A, Memon L, Kalimanovska-Ostric D. PON1 status is influenced by oxidative stress and inflammation in coronary heart disease patients. Clin Biochem. 2008; 41:1067-1073.

43   Ferre N, Camps J, Prats E, Vilella E, Paul A, Figuera L, Joven J. Serum paraoxonase activity: A new additional test for the improved evaluation of chronic liver damage. Clin Chem. 2002; 48:261-268.

44   Jamroz-Wisniewska A, Beltowski J, Stelmasiak Z, Bartosik-Psujek H. Paraoxonase 1 activity in different types of multiple sclerosis. Mult Scler. 2009; 15:399-402.

45   Feingold KR, Memon RA, Moser AH, Grunfeld C. Paraoxonase activity in the serum and hepatic mRNA levels decrease during the acute phase response.

Atherosclerosis. 1998; 139:307-315.

46   Abdel-Salam OME, Khadrawy YA, Mohammed NA. Neuroprotective effect of nitric oxide donor isosorbide-dinitrate against oxidative stress induced by ethidium bromide in rat brain. EXCLI J. 2012; 11:125-141.

47   Meyer O. Safety of use of Daflon 500 mg confirmed by acquired experience and new research. Phlebology. 1992; 7 (Suppl 2):64-68.

Original Article

The synergistic effect of SaOS-2 cell extract and other bone-inducing agents on human bone cell cultivation

Ashraf Saif[1,*], Kristian Wende[2], Ulrike Lindequist[2]

[1] *Al-Leith University College, Umm Al-Qura University, Makkah, Saudi Arabia;*
[2] *Institute of Pharmacy, Ernst-Moritz-Arndt-University of Greifswald, Greifswald, Germany.*

ABSTRACT: Human osteosarcoma cell line SaOS-2 is an osteoblastic cell model that contains factors like bone morphogenetic proteins necessary for initiating bone formation. The cell line also expresses high levels of osteoinductive activity. In contrast to highly complicated and expensive ways to identify, purify, and separate specific bone-inducing agents from SaOS-2 cells, lysate can be used as an alternative to isolated bone-stimulating factors. Lysates of SaOS-2 stimulate the activity of the alkaline phosphatase of human osteoblastic cells HOS 58 *in vitro*. In other words, they probably possess osteoinductive activity. Different serial concentrations of substances like dexamethasone and insulin were tested with and without a lysate of SaOS-2 cells to assay their synergistic action. Results showed that a lysate of the SaOS-2 cell line acts as a synergistic agent and increases the osteoinductive activity of known bone-inducing agents. SaOS-2 cell lysate could be used in the future as a clinical agent to promote bone repair and possibly enhance osteointegration. Using SaOS-2 total cellular extract offers the possibility of lowering the effective dose of other bone-inducing agents.

Keywords: Osteoinduction, bone alkaline phosphatase, SaOS-2 cell lysate, osteointegration, human osteosarcoma cells HOS 58, bone morphogenetic proteins, tissue-engineered bone

1. Introduction

The loss of bone tissue can occur through infection, loss of blood supply, diseases such as osteoporosis, or as a complication of a fracture or genetic disorders, *e.g.* osteogenesis imperfecta. Current management of bone defects includes tissue replacement with transplanted autografts or allografts or synthetic devices. However, each of these therapies has its own serious risks and constraints. Harvesting autografts, typically from the iliac crest, is constrained by anatomical limitations and associated with donor-site morbidity (*1*). The problems and risks associated with the use of allografts include not only disease transmission but also the risk of tissue rejection. In addition, the loss of osteoinductive factors during allograft processing may impact tissue quality. A synthetic prosthesis such as bone cement and metal, *e.g.* titanium and its alloys or stainless steel, often results in insufficient osseous integration and stress-shielding of the surrounding bone or fatigue failure of the implant (*1*). These shortcomings highlight the need for greater use and further study of bone-inducing agents to increase the osteogenic character of tissue-engineered bone.

Bone alkaline phosphatase (ALP) is located on the surface of osteoblasts and is thought to play a major role in bone formation and mineralization. Its levels are considered to reflect osteoblastic activity (*2*). Bone ALP levels can therefore be used as a biochemical marker to assess metabolic bone diseases (*e.g.* osteoporosis), bone disorders as a late complication of diabetes, and even bone metastasis. Moreover, bone morphogenetic proteins (BMPs), which are members of the transforming growth factor (TGF)-β superfamily (*3-6*), appear to play an important role in the initiation of osteogenesis during development (*7-10*) and in bone repair (*6,11-14*).

Human osteosarcoma cell line SaOS-2 is an osteoblastic cell model that expresses high levels of tissue ALP activity (*15*). According to reports, its lysate should have osteoinductive activity (*16,17*). SaOS-2 cells may be osteoinductive because they contain several BMPs including BMP-1, 2, 3, 4, and 6, any or all of which may support bone induction (*18,19*). These cells apparently produce factors necessary for initiating bone formation.

The current study sought to investigate the effect of lysate from SaOS-2 cells alone and in combination with other bone-enhancing agents on the ALP activity of the HOS 58 cell line. This investigation should pave the way for more pharmacological, toxicological, and medical studies of this cell lysate to allow its use in medicine as a drug additive.

Address correspondence to:
Dr. Ashraf Saif, Al-Leith University College, Umm Al-Qura University, Makkah 311, Saudi Arabia.
E-mail: aaa_saif@hotmail.com

2. Materials and Methods

2.1. *Materials*

Cell culture plastics, fetal bovine serum (FBS), phosphate-buffered saline (PBS), L-glutamine, trypsine, and antibiotics were purchased from Biochrom KG (Berlin, Germany). Bovine serum albumin (BSA; fraction V) and Iscove's modified Dulbecco's medium (IMDM) with or without phenol red were purchased from Invitrogen (Karlsruhe, Germany). All other reagents were obtained from Sigma (Deisenhofen, Germany). HOS 58 cells were donated by A. Battmann (University of Giessen, Institute of Pathology, Germany). SaOS-2 cells were purchased from DSZM (Braunschweig, Germany).

2.2. *Cell lines and culture*

Both the HOS 58 cell line and SaOS-2 cell line were grown as a monolayer in IMDM with 10% FBS, 2 mM L-glutamine, and 1% penicillin-streptomycin solution (penicillin 10,000 IE/mL; streptomycin 10,000 μg/mL). Both cell lines were grown in 95% humidity and 5% CO_2 at 37°C and routinely sub-cultured.

2.3. *Preparation of SaOS-2 lysate*

To prepare a cell lysate, cells were washed with 3×10 mL phosphate buffer and scraped from the surface of tissue culture flasks using a cell scraper. Approximately 2.5×10^8 cells were freeze-dried and suspended in 50 mL extraction buffer consisting of 0.1 M Tris-HCl buffer (pH 8.0). Cells were then incubated with gentle stirring for 1 h at room temperature and centrifuged at 4,000 rpm for 15 min to remove cellular debris. The resulting supernatant served as a stock solution (5×10^6 cells/mL).

2.4. *Standardization of the ALP activity of SaOS-2 cell lysate*

The crude lysate was standardized based on its ALP activity. Crude ALP activity was determined by the release of 4-nitrophenol (4-NP) from 4-nitrophenyl phosphate (4-NPP, see Section 2.8).

2.5. *Assay of bone-inducing activity*

For assays, HOS 58 cells were grown to confluence in 96-well plates for 48 h. After they were washed twice with PBS, medium was changed to IMDM without phenol red supplemented with 0.05% BSA, 2 mM L-glutamine, and 1% antibiotics (assay medium). Different concentrations of crude SaOS-2 cell lysate in assay medium were prepared using a stock solution (5×10^6 cells/mL in PBS). The final PBS concentration did not exceed 0.05%. Different serial concentrations of substances like dexamethasone (Dexa) and insulin were used with and without 20 μL of a stock

(5×10^6 cells/mL in PBS) crude extract of SaOs-2 cells to assay their synergistic action. Further procedures are indicated below.

2.6. *Cell disruption*

Cultivated HOS 58 cells were washed with PBS and disrupted by adding 100 μL of 0.1% Triton X-100 in 0.1 M Tris-HCl, pH 9.8 (lysis buffer) followed by freeze/thawing and vigorous mixing. The resulting suspension was centrifuged and the supernatant (cell lysate) was assayed for its protein content and ALP activity.

2.7. *Determination of total cellular protein*

Total cellular protein was determined using Roti-Nanoquant reagent (Roth GmbH, Karlsruhe, Germany), a modified Bradford method, according to the manufacturer's instructions (*20*). Briefly, 10 μL cell lysate was diluted with PBS (1:4) in a microtiter plate. Roti-Nanoquant (200 μL) reagent was added and mixed, and the OD was read out at 405 and 620 nm (Anthos Labtec, Salzburg, Austria). The total protein content was calculated from a standard curve using BSA.

2.8. *ALP activity*

Cellular ALP activity was determined by the release of 4-NP from 4-NPP. An aliquot of cell lysate was mixed with 0.2 M amino propanol buffer (pH 9.8, AMP) and 24 mM 4-NPP in AMP. After incubation (37°C), the reaction was stopped with 0.5 M NaOH (50 μL) and the OD was read out at 405 nm. The concentration was calculated from a calibration curve for 4-NP.

2.9. *Cell vitality and cell proliferation assays (MTT assay)*

The MTT assay was used to measure the cell proliferation rate and cell viability. HOS 58 cells (see Section 2.2) were incubated with different concentrations of normalized SaOS-2 cell lysate (0.9-1.1 U/mL – 0.007-0.008 U/mL) for 43 h. After cells were washed, 20 μL MTT in IMDM (5 mg/mL, Sigma, Deisenhofen, Germany) was added to each well. Plates were incubated at 37°C in 95% humidity and 5% CO_2 for another 5 h. Finally, the MTT solution was removed and crystals were dissolved in 200 μL DMSO. After thorough mixing, plates were incubated for 5 min and absorbance was measured at 590 nm. Cell viability was calculated as a percent of vehicle control (*21,22*).

2.10. *Statistical analysis*

For each experiment, three independent experiments were carried out and results were expressed as mean ± SD. Statistical differences were analyzed using single-tailed ANOVA. A p values < 0.05 was considered significant.

3. Results and Discussion

3.1. *Extraction of SaOS-2 cells*

The SaOS-2 cell line was established in culture in 1975 (*16*). These cells produce a large amount of ALP but little or no matrix *in vitro* and are unable to grow when transplanted into athymic mice. SaOS-2 cells contain several BMPs including BMP-1, 2, 3, 4, 6, and 7, any or all of which may support bone induction (*18,19*). Moreover, BMPs, which are members of the TGF-β super family (*3-6*), appear to play an important role in the initiation of osteogenesis during development (*7*) and in bone repair (*6,11-14*).

An important question with respect to bone repair or bone tissue engineering is whether a combination of BMPs will be more cost-effective in clinical practice than a single recombinant BMP. Although individual BMPs, and especially recombinant BMP-2 (*23,24*) or recombinant BMP-7 (*25*), have been used to successfully accelerate bone regeneration in large defects, the required concentration of a specific recombinant BMP is up to 1,000-fold higher than that of the native BMP complex (*4*). The combination of several BMPs and other factors might be more cost-effective at enhancing new bone formation than individual recombinant human BMPs. Thus, a total cellular extract of SaOS-2 cells was tested for its bone-inducing ability. The cellular extract was standardized based on its ALP activity.

Cultivation of 10^5 SaOS-2 cells consistently yielded approximately 1 U of bone tissue ALP crude lysate (cALP) (Figure 1 and Table 1), given that one unit (U) of ALP activity is the quantity of enzyme that catalyzes the hydrolysis of 1 μmol substrate in 1 min. Results show that the residual activity of ALP in the crude lysate of SaOS-2 cells (freeze-dried/thawing) was 10.1 U/mL (Figure 1 and Table 1), which was equivalent to the level reported previously (*18*). In comparison to bone ALP made from human bone, the specific activity would be 500 times greater because SaOS-2 cells contain 40-50 times more ALP activity than TE-85 cells (*8,26*).

3.2. *Effect of SaOS-2 lysate on the ALP activity and total protein content of HOS 58 cells*

ALP activity is commonly used as an indicator of osteoblastic cell maturation. The enzyme is considered to mark the middle stage of bone formation and generally appears during the matrix maturation phase. It plays an unclear but crucial role in matrix mineralization (*2*). Figure 2 clearly shows a significant increase ($p < 0.01$) in the level of ALP activity of HOS 58 cells to almost 200% in the presence of a crude extract of SaOS-2 cells (0.1 U/mL ALP).

Figure 3 shows that the SaOS-2 cell lysate in concentrations up 10 U/mL did not affect protein production by HOS 58 cells. Above that concentration, protein production drops, reaching only 80% of that
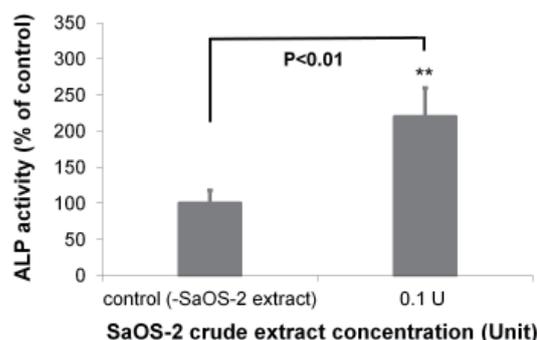
Figure 2. Effect of SaOS-2 cell lysate (normalized to 0.1 U/mL ALP) on the ALP activity of HOS 58 cells.
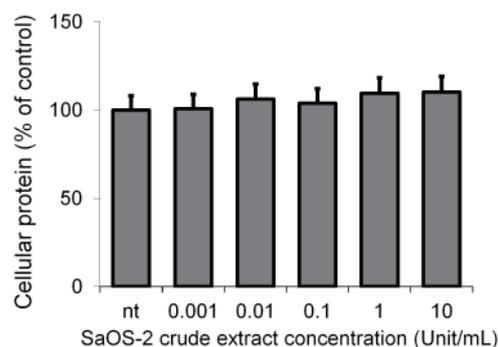
Figure 3. Effect of different concentrations of an extract of SaOS-2 cells on the total protein activity of HOS 58 cells. No significant toxicity was observed up to 10 unit/mL, suggesting that the cells continued to be viable in the experimental setup. Three independent experiments were performed.

Figure 1. Quantification of the ALP activity in a crude extract of SaOS-2 cells.

Table 1. ALP activity from a crude extract of SaOS-2 cells

	Working solution volume (mL)	Cell number/mL of working solution	ALP (U/mL)	Average protein (mg/mL)
Crude extract	49	$0.9\text{-}1.1 \times 10^6$	10.1	1.86
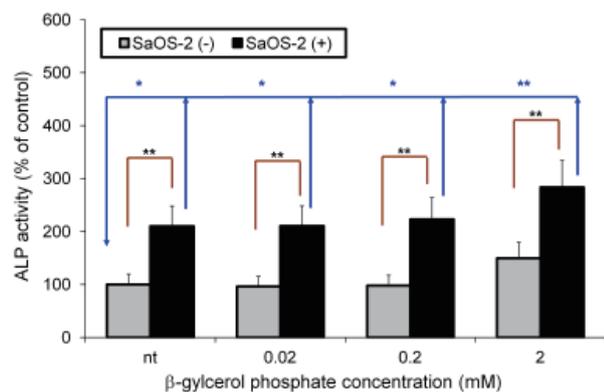
Figure 4. Synergistic effect of SaOS-2 cell lysate (normalized to 0.1 U/mL ALP) with β-glycerol phosphate on the ALP activity of HOS 58 cells. * $p < 0.05$, ** $p < 0.01$.

Figure 5. Synergistic effect of SaOS-2 cell lysate (normalized to 0.1 U/mL ALP) with Dexa on ALP activity of HOS 58 cells. * $p < 0.05$, ** $p < 0.01$.

of the vehicle control (data not shown). Because cytotoxicity is lacking, cell maturation must have been stimulated. Had it not, extracellular matrix (ECM) production would have decreased and thus the protein content of the cell (and matrix) lysate would have decreased. No increase in cellular protein was noted at any of the concentrations tested. This corroborates the contention that SaOS-2 cell lysate promotes cell maturation and reduces cell proliferation and ECM production.

3.3. *Synergistic effect with β-glycerol phosphate*

Figure 4 clearly shows a significant increase ($p < 0.01$, *vs.* vehicle control) in the level of cellular ALP activity of HOS 58 cells to almost 130% at a 2 mM β-glycerol phosphate (bGP) concentration alone. Synergistic use of SaOS-2 cell lysate (normalized to 0.1 U/mL ALP) respectively increased ALP activity to 210%, 225%, and 280% with 0.02, 0.2, and 2 mM bGP (+ 0.1 U cALP).

The most rational explanation for the observed synergistic action of bGP with SaOS-2 extract is that bGP hydrolyzed to glycerol and inorganic phosphate ions (Pi). Glycerol inhibits cell proliferation (*27*), so bone-inducing agents from SaOS-2 extracts accelerate cell maturation and lead to increased ALP activity. The hydrolysis of bGP also leads to a greater concentration of inorganic Pi in the culture medium, which may react with more BMPs from the SaOS-2 extract (phosphorylation) and result in increased formation of phosphoproteins (*28,29*). These phosphoproteins increase bone-inducing activity.

3.4. *Synergistic effect with Dexa*

The ALP activity of HOS 58 cells increased with greater Dexa concentrations from 10^{-12} M to 10^{-8} M. Higher concentrations (from 10^{-7} M to 10^{-5} M) led to decrease in ALP activity. Figure 5 shows that synergistic use of SaOS-2 cell lysate (normalized to 0.1 U/mL ALP) and Dexa respectively increased ALP activity from 102%,
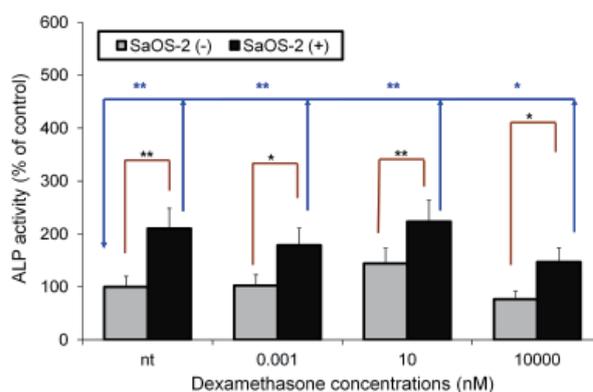
144%, and 77% with 10^{-12} M, 10^{-8} M, and 10^{-5} M Dexa to 178%, 223%, and 147% with 10^{-12} M, 10^{-8} M, and 10^{-5} M of Dexa plus SaOS-2 cell lysate.

Results show that Dexa and the SaOS-2 cell extract act synergistically on ALP activity. Dexa concentrations that decrease ALP activity have less impact when combined with the SaOS-2 cell extract. Concentrations of Dexa that increase ALP activity further increase ALP activity when combined with the SaOS-2 cell extract.

Given these findings, lower concentrations of Dexa appear to stimulate the proliferative activity of bone-like cell cultures and increase the number of osteoblastic cells in culture. Osteoblastic cells in the presence of excessive amounts of BMPs from an SaOS-2 extract promote early maturation of cells and therefore cause an increase in ALP activity. In addition, higher concentrations of Dexa appear to inhibit cell proliferation and reduce the number of osteoblastic cells, thus decreasing ALP activity.

Prolonged physiological levels of Dexa are clearly associated with deleterious effects on the skeleton and are a major cause of osteoporosis (*30,31*). One advantage of the synergistic effect of Dexa and an SaOS-2 cell extract would be that lower concentrations of Dexa could be used to avoid prolonged exposure and avoid its negative impact on bones.

3.5. *Synergistic effect with insulin*

Figure 6 clearly shows a significant increase ($p < 0.01$, *vs.* vehicle control) in the level of ALP activity of HOS 58 human cells to almost 190% at an insulin concentration of 20 μg/mL. ALP activity is affected by the insulin concentration and respectively increased to 120%, 155%, and 190% with 0.2, 2, and 20 μg/mL insulin. Synergistic use of SaOS-2 cell lysate (normalized to 0.1 U/mL ALP) respectively increased ALP activity to 190%, 205%, and 260% with 0.02, 0.2, and 2 mM insulin (+ 0.1 U cALP).

Synergistic action with insulin may be because insulin, like insulin-like growth factor (IGF)-I, increases
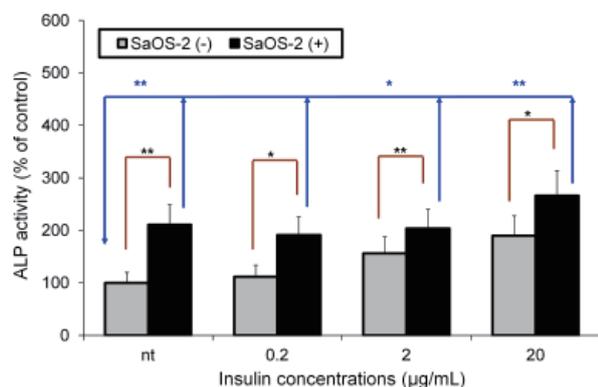
Figure 6. Synergistic effect of SaOS-2 cell lysate (normalized to 0.1 U/mL ALP) with insulin on ALP activity of HOS 58 cells. $* p < 0.05$, $** p < 0.01$.

cell proliferation. The combinations of IGF and TGF-β, IGF and platelet-derived growth factor (PDGF), and PDGF and TGF-β enhance murine osteoblast activity and proliferation (*32*). As mentioned earlier, BMPs in SaOS-2 extract caused early maturation of an increased number of osteoblastic cells, changing their phase of differentiation phase and causing ALP to accumulate in cell culture.

4. Conclusion

In conclusion, SaOS-2 lysate increases the ALP activity of human osteoblastic cells *in vitro*, presumably indicating that it has bone-inducing activity. SaOS-2 lysate may have the potential to serve as a clinical agent to promote bone repair and possibly enhance osteointegration. Evidence is not clear as to whether a single factor is responsible for SaOS-2 osteoinductivity. The mechanism of osteoinductivity seems to be multifactorial, so a total lysate of SaOS-2 cells may be better than isolated compounds. The mechanism of its activity (both *in vitro* and *in vivo*), its possible toxicity, its chemical composition, and its standardized quality must be studied further.

References

1. Rose FR, Oreffo RO. Bone tissue engineering: Hope vs hype. Biochem Biophys Res Commun. 2002; 292:1-7.
2. Perizzolo D, Lacefield WR, Brunette DM. Interaction between topography and coating in the formation of bone nodules in culture for hydroxyapatite- and titanium-coated micromachined surfaces. J Biomed Mater Res. 2001; 56:494-503.
3. Wang EA, Rosen V, Cordes P, Hewick RM, Kriz MJ. Purification and characterization of other distinct bone-inducing factors. Proc Natl Acad Sci U S A. 1988; 85:9484-9488.
4. Luyten FP, Cunningham NS, Vukicevic S, Pralkar V, Ripamonti U Reddi AH. Advances in osteogenin and related bone morphogenetic proteins in bone induction and repair. Acta Orthop Belg. 1992; 58:263-267.
5. Reddi AH. Role of morphogenetic proteins in skeletal

tissue engineering and regeneration. Nat Biotechnol. 1998; 16:247-252.
6. Reddi AH. BMPs: From bone morphogenetic proteins to body morphogenetic proteins. Cytokine Growth Factor Rev. 2005; 16:249-250.
7. Lyons KM, Pelton RW, Hogan BM. Organogenesis and pattern formation in the mouse: RNA distribution patterns suggest a role for bone morphogenetic protein-2A (BMP-2A). Development. 1990; 109:833-844.
8. Jones CM, Lyons KM, Hogan BM. Involvement of bone morphogenetic protein-4 (BMP-4) and Vgr-1 in morphogenesis and neurogenesis in the mouse. Development. 1991; 111:531-542.
9. Ozkaynak E, Schnegelsberg PJ, Jin DF, Clifford GM, Warren FD, Drier EA, Oppermann H. Osteogenic protein-2. A new member of the transforming growth factor-β; superfamily expressed early in embryogenesis. J Biol Chem. 1992; 267:25220-25227.
10. Vukicevik S, Latin V, Chen P, Batorsky R, Reddi AH, Sampath TK. Localization of osteogenic protein-1 (bone morphogenetic protein-7) during human embryonic development: High affinity binding to basement membranes. Biochem. Biophys. Res Commun.1994; 198:693-700.
11. Rosen V, Thies RS. The BMP proteins in bone formation and repair. Trends Genet. 1992; 8:97-102.
12. Nakase T, Nomura S, Yoshikawa H, Hashimoto J, Hirota S. Transient and localized expression of bone morphogenetic protein 4 messenger RNA during fracture healing. J Bone Mineral Res. 1994; 9:651-659.
13. Bessa PC, Casal M, Reis RL. Bone morphogenetic proteins in tissue engineering: The road from laboratory to clinic, part II (BMP delivery). J Tissue Eng. Regenerative Med. 2008; 2:81-96.
14. Bragdon B, Moseychuk O, Saldanha S, King D, Julian J, Nohe A. Bone morphogenetic proteins: A critical review Cell Signalling. 2011; 23:609-620.
15. Murray E, Provvedini D, Curran D, Catherwood B, Sussman H, Manolagas S. Characterization of a human osteoblastic osteosarcoma cell line (SAOS-2) with high bone alkaline phosphatase activity. J Bone Mineral Res.1987; 2:231-238.
16. Anderson HC, Sugamoto K, Morris DC, Hsu HH, Hunt T. Bone-inducing agent (BIA) from cultured human Saos-2 osteosarcoma cells. Bone Mineral. 1992; 16:49-62.
17. Hunt TR, Schwappach JR, Anderson HC. Healing of a segmental defect in the rat femur with use of an extract from a cultured human osteosarcoma cell-line (Saos-2). A preliminary report. J Bone Joint Surg Am. 1996; 78:41-48.
18. Anderson HC, Hsu HT, Raval P, Reynold PR, Gurley DJ. The bone-inducing agent in Saos-2 cell extracts and secretions. Cells Mater.1998; 8:89-98.
19. Anderson HC, Reynolds PR, Hsu HT, Missana L, Masuhara K, Moylan PE, Roach HI. Selective synthesis of bone morphogenetic proteins-1, -3, -4 and bone sialoprotein may be important for osteoinduction by Saos-2 cells. J Bone Mineral Metab. 2002; 20:73-82.
20. Zor T, Selinger Z. Linearization of the Bradford protein assay increases its sensitivity: Theoretical and experimental studies. Anal Biochem. 1996; 236:302-308.
21. Mosmann T. Rapid colorimetric assay for cellular growth and survival: Application to proliferation and cytotoxicity assays. J Immunol Methods. 1983; 65:55-63.
22. Ciapetti G, Cenni E, Pratelli L, Pizzoferrato A. *In vitro* evaluation of cell/biomaterial interaction by MTT assay. Biomaterials. 1993; 14:359-364.

23. Barboza E, Caula A, Machado F. Potential of recombinant human bone morphogenetic protein-2 in bone regeneration. Implant Dent. 1999; 8:360-367.

24. Bostrom MP, Camacho NP. Potential role of bone morphogenetic proteins in fracture healing. Clin Orthop Related Res. 1998; 355:S274-S282.

25. Cook SD. Preclinical and clinical evaluation of osteogenic protein-1 (BMP-7) in bony sites. Orthopedics. 1999; 22:669-671.

26. Farley JR, Kyeyune-Nyombi E, Tarbaux NM, Hall SL, Strong DD. Alkaline phosphatase activity from human osteosarcoma cell line SaOS-2: An isoenzyme standard for quantifying skeletal alkaline phosphatase activity in serum. Clin Chem.1989; 35:223-229.

27. Wiebe JP, Dinsdale CJ. Inhibition of cell proliferation by glycerol. Life Sci. 1991; 48:1511-1517.

28. Lussi A, Crenshaw MA, Linde A. Induction and inhibition of hydroxyapatite formation by rat dentine phosphoprotein *in vitro*. Arch Oral Biol. 1988; 33:685-691.

29. Glimcher MJ. Mechanism of calcification: Role of collagen fibrils and collagen-phosphoprotein complexes *in vitro* and *in vivo*. Anatomical Rec.1989; 224:139-153.

30. Lukert BP, Kream BE. Clinical and basic aspects of glucocorticoid action in bone. In: Principles of Bone Biology (Bilezikian JP, Raisz JG, Rodan GA, eds.). Academic Press, San Diego, CA, USA, 1996; pp. 533-548.

31. Ishida Y, Heersche JM. Glucocorticoid-induced osteoporosis: Both *in vivo* and *in vitro* concentrations of glucocorticoids higher than physiological levels attenuate osteoblast differentiation. J Bone Mineral Res. 1998; 13:1822-1826.

32. Mott DA, Mailhot J, Cuenin MF, Sharawy M, Borke J. Enhancement of osteoblast proliferation *in vitro* by selective enrichment of demineralized freeze-dried bone allograft with specific growth factors. J Oral Implantol. 2002; 28:57-66.

Original Article

Separation of the enantiomers of naringenin and eriodictyol by amylose-based chiral reversed-phase high-performance liquid chromatography

Xiaojiang Guo, Chao Li, Linlin Duan, Lijuan Zhao, Hongxiang Lou, Dongmei Ren*

Department of Natural Product Chemistry, Key Lab of Chemical Biology of Ministry of Education, Shandong University, Ji'nan, Shandong, China.

ABSTRACT: Naringenin and eriodictyol are chiral flavanones widely present in citrus fruits and herbal products. Pharmacological interest in the two flavanones is well known. Due to the chiral carbon atom, the compounds always exist in the racemic form. The present study reported a stereospecific HPLC method for the enantioseparation of naringenin and eriodictyol, which was performed on an amylose-based chiral stationary phase (CSP), Chiralpak AD-RH, in the reversed-phase mode. The effects of the mobile phase on retention, enantioseparation, and elution order were investigated. The different 3',4' substituent pattern of the two compounds affected the enantioselectivity. An online coupling HPLC-CD method was used for elution order determination. Both the CD sign of the eluted peaks at a single wavelength and complete CD spectra of the eluted enantiomers were obtained by the method.

Keywords: Naringenin, eriodictyol, HPLC-CD, enantioseparation

1. Introduction

Naringenin (5,7,4'-trihydroxyflavanone, **1**) and eriodictyol (5,7,3',4'-tetrahydroxyflavanone, **2**) (Figure 1) are chiral flavanones present in citrus fruits and herbal products. Pharmacological interest in the two flavanones is well known. Both compounds have long been realized as antioxidants and chemopreventive agents (*1*). Recent studies have shown that naringenin also possesses activities such as anti-inflammatory (*2*), anti-cancer (*3,4*), anti-metastasis (*5*), normalizing lipids (*6,7*), anti-hyperglycemia (*8*), and anti-hypercholesterolemia (*9*). Eriodictyol can provide a cytoprotective effect in ultraviolet (UV)-irradiated keratinocytes (*10*), induce long-term protection in ARPE-19 cells (*11*), and prevent early retinal and plasma abnormalities in streptozotocin induced diabetic rats (*12*). Deriving from the stereogenic center at C-2, the two flavanones are chiral. It is well known that interactions with enzymes are often stereospecific, so enantiomers should have different behaviors in pharmacological action and metabolic process, but due to the lack of readily available pure flavanone enantiomers, most bioactivity studies were carried out using a racemic mixture. For the separation of enantiomers of compounds **1** and **2**, a couple of methods have been previously reported, such as capillary electrophoresis (*13*), micellar electrokinetic chromatography (*14*), and high performance liquid chromatography (HPLC) under normal-phase conditions (*15*). With respect to normal phase and polar organic mobile phase, the reversed-phase mode is particularly advantageous in the direct analysis of biological matrices without a batch sample preparation step and in coupling with mass spectrometry. There were also reports about the enantioseparation of compounds **1** and **2** using reversed-phase HPLC. The only validated reversed-phase HPLC method reported for the stereospecific separation of **2** was separation on a Chiralpak OJ-RH column (*16*), while **1** could be enantioseparated using a Chiralcel OD-RH column (*17*). Both the Chiralpak OJ-RH column and Chiralcel OD-RH column are cellulose-derived columns. In this article, we report the enantioseparation of compounds **1** and **2** using an isocratic reversed-phase HPLC with two amylose-based chiral stationary phases (CSP), Chiralpak AD-RH and Chiralpak AS-RH. Chiralpak AD-RH provided better enantioseparation of the two analytes.

*Address correspondence to:
Dr. Dongmei Ren, School of Pharmaceutical Sciences, Shandong University, 44 Wenhuaxi Road, Ji'nan 250012, China.
E-mail: rendom@sdu.edu.cn
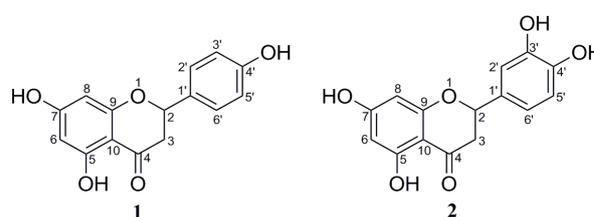
Figure 1. Structures of compounds 1 and 2.

Moreover, the online coupling HPLC-circular dichroism (CD) method makes possible direct absolute configuration assignment of the eluted enantiomers.

2. Materials and Methods

2.1. *Chemicals and reagents*

Racemic naringenin (**1**) and eriodictyol (**2**) were purified from *Dracocephalum rupestre*. The purity was proved to be above 98% by HPLC analysis. The structure identification was carried out using ^{1}H and ^{13}C nuclear magnetic resonance (NMR). HPLC-grade methanol, ethanol and acetonitrile were from Burdick & Jackson (SK Chemicals, Seoul, Korea).

2.2. *Chromatographic system and conditions*

The HPLC-UV was performed on an Agilent 1260 HPLC system, equipped with quaternary pump, diode array detector and an autosampler (Agilent, Palo Alto, LA, USA). The HPLC-CD was performed on a JASCO LC-Net II/ADC HPLC system, equipped with a PU-2089 plus pump, CD-2095 plus CD detector and a 7125 Rheodyne injector with 20 μL sample loop (Jasco, Tokyo, Japan). The columns (150 mm × 4.6 mm) were amylose tris(S)-α-methylbenzyl carbamate (Chiralpak AS-RH), amylose tris-3,5-dimethylphenyl carbamate (Chiralpak AD-RH) both coated on 5 μm silica gel. The above columns were obtained from Daicel (Tokyo, Japan). Experiments were performed at ambient temperature. All solvents were degassed in an ultrasonic bath prior to use. To eliminate some unexpected memory effects, a column regeneration procedure according to the vendor's instruction was performed when a new organic modifier was utilized. Once a new chromatographic condition was adopted, the column was equilibrated for at least 1 h before injection. Samples of naringenin and eriodictyol were diluted in methanol to a concentration of 0.1 mg/mL for HPLC-UV and 0.5 mg/mL for HPLC-CD. The prepared HPLC sample solutions were filtered through a nonsterile 0.45 μm PTEE syringe filter. UV and CD detection were performed at 284 nm. The CD spectra of the enantiomers were obtained by stopped-flow scanning at each chromatographic peak by CD detector in the

wavelength range of 220-420 nm. Column void volume (t_0) was measured by injection of tri-*tert*-butylbenzene as a non-retained marker. The retention factor (k) was calculated as $k_1 = (t_1 - t_0)/t_0$ and $k_2 = (t_2 - t_0)/t_0$ where t_1 and t_2 are the retention times for the first and second eluting enantiomers, respectively. The separation factor (α) was calculated as $\alpha = k_2/k_1$. The resolution factor was evaluated according to $R_s = 2(t_2 - t_1)/(w_1 + w_2)$, *i.e.* the peak separation divided by the mean value of the baseline widths. Retention times (t) were mean values of two replicate determinations.

3. Results and Discussion

3.1. *Optimization of chromatographic conditions*

The effect of two amylose-based CSP, Chiralpak AD-RH and Chiralpak AS-RH, on the chiral recognition of compounds **1** and **2** was first studied. The effect of mobile-phase on the separation process was examined by modifying the percentage of water (doped with 0.1% trifluoroacetic acid, TFA) and type of organic cosolvent (methanol, ethanol, or acetonitrile) in the reversed-phase mixtures. The chromatographic parameters, capacity factor (k), separation factor (α), and resolution factor (R_s) for the resolved compounds **1** and **2** are given in Tables 1 and 2 for Chiralpak AD-RH and Chiralpak AS-RH, respectively.

These tables showed that both compounds **1** and **2** could be resolved with good separation factors (α) and resolution factors (R_s) on the Chiralpak AD-RH column by optimizing the mobile phase composition. For the enantioseparation on the Chiralpak AS-RH column, although a variation in the chromatographic parameters was optimized to obtain the best resolution, the two compounds could not be separated very well. Only a partial resolution of compound **1** was achieved using methanol and ethanol as organic modifiers or using acetonitrile as organic modifier for compound **2** (Figure 2). Thus, the results suggested the use of Chiralpak AD-RH to study the enantioseparation of compounds **1** and **2** is better. Chemically, Chiralpak AD-RH is amylose tris (3,5-dimethylphenyl carbamate), while Chiralpak AS-RH is amylose tris (S-α-methylbenzyl carbamate). Therefore, it may be concluded that the presence

Table 1. Chromatographic results for enantiomeric resolution of compounds 1 and 2 on Chiralpak AD-RH CSP

Eluent	k_1		k_2		α		R_s	
	1	**2**	**1**	**2**	**1**	**2**	**1**	**2**
Methanol-H$_2$O[a], 95:5	3.14	2.41	4.26	2.86	1.36	1.19	3.76	2.48
Methanol-H$_2$O[a], 90:10	5.37	3.57	6.91	5.26	1.29	1.47	3.43	4.39
Methanol-H$_2$O[a], 85:15	9.21	5.73	11.42	9.43	1.24	1.65	2.98	5.90
Ethanol-H$_2$O[a], 80:20	0.61	1.14	0.61	1.69	1.00	1.48	0	3.30
Ethanol-H$_2$O[a], 70:30	2.20	2.20	2.35	3.33	1.07	1.65	0.80	4.60
Acetonitrile-H$_2$O[a], 50:50	1.55	0.94	1.70	1.04	1.10	1.11	1.10	0.82
Acetonitrile-H$_2$O[a], 35:65	7.02	3.57	8.01	3.95	1.14	1.11	2.86	1.16

[a] H$_2$O doped with 0.1% TFA.

Table 2. Chromatographic results for enantiomeric resolution of compounds 1 and 2 on Chiralpak AS-RH CSP

Eluent	k_1		k_2		α		R_s	
	1	2	1	2	1	2	1	2
Methanol-H$_2$O^a, 80:20	1.73	0.92	1.97	0.92	1.21	1.00	1.47	0
Methanol-H$_2$O^a, 65:35	6.83	3.34	7.67	3.34	1.12	1.00	1.57	0
Methanol-H$_2$O^a, 60:40	11.67	-	12.89	-	1.10	-	1.50	-
Ethanol-H$_2$O^a, 55:45	3.56	1.95	3.86	1.95	1.08	1.00	1.23	0
Ethanol-H$_2$O^a, 40:60	23.85	9.33	25.29	9.33	1.06	1.00	1.87	0
Acetonitrile-H$_2$O^a, 25:75	14.17	5.44	14.17	5.76	1.00	1.06	0	1.40
Acetonitrile-H$_2$O^a, 20:80	-	12.76	-	13.61	-	1.07	-	1.83
Acetonitrile-H$_2$O^a, 15:85	-	36.88	-	39.81	-	1.08	-	2.96

^{a} H$_2$O doped with 0.1% TFA.
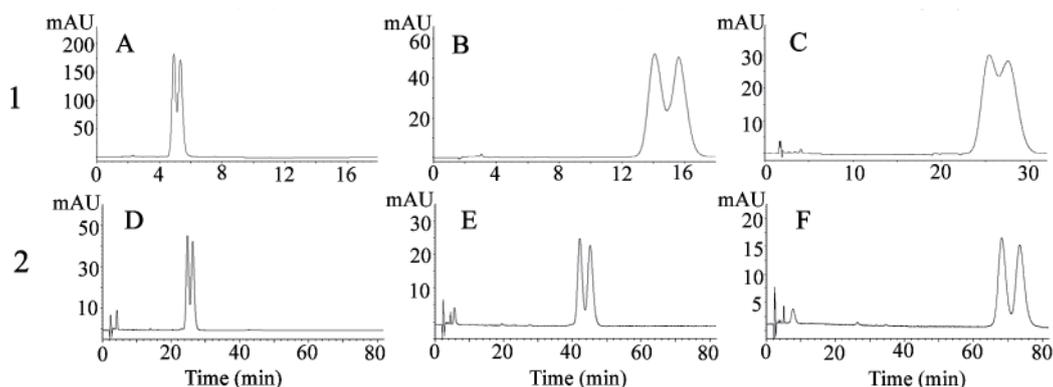
Figure 2. Typical HPLC chromatograms of enantiomeric resolution of compounds 1 and 2 on Chiralpak AS-RH column.
Mobile phase: **(A)** methanol-H$_2$O doped with 0.1% TFA, 80:20 (v/v); **(B)** methanol-H$_2$O doped with 0.1% TFA, 65:35 (v/v); **(C)** ethanol-H$_2$O doped with 0.1% TFA, 45:55 (v/v); **(D)** acetonitrile-H$_2$O doped with 0.1% TFA, 20:80 (v/v); **(E)** acetonitrile-H$_2$O doped with 0.1% TFA, 17:83 (v/v); **(F)** acetonitrile-H$_2$O doped with 0.1% TFA, 15:85 (v/v).

of the two methyl groups on the phenyl moieties of Chiralpak AD-RH CSP increases the π basicity of the phenyl moieties, which results in π-π interactions of greater magnitude in comparison to Chiralpak AS-RH, and hence a better resolution occurred on Chiralpak AD-RH in comparison to Chiralpak AS-RH. Typical enantiomeric separations of flavanones **1** and **2** on Chiralpak AD-RH CSP and mobile phase composition are shown in Figure 3.

Several analytical considerations can be made from the results shown in Table 1 and Figure 3. *i)* As expected for the reversed-phase behavior of the Chiralpak AD-RH column, when the organic cosolvent concentration in the mobile phase increased, the *k*-values of the enantiomers were decreased in all cases. *ii)* The use of a different type of organic cosolvent in the mobile phase yielded quite different stereoselectivities for the two enantiomeric pairs. For both compounds **1** and **2**, the use of methanol as organic modifier gave good selectivity factors (*α*) and resolution factors (*R$_s$*). Thus, a mobile phase composition consisting of a simple mixture of methanol-water 90:10 (v/v) achieved an enantioselectivity factor value of 3.43 and 4.39 for compounds **1** and **2** respectively. *iii)* It can also be noted that for compound **2**, both *α* and *R$_s$* increased significantly by decreasing the percentage of methanol in the mobile phase, while for compound **1**, *α* and *R$_s$* only changed slightly by changing the concentration of

methanol in the mobile phase. *iv)*The use of ethanol as organic modifier of the eluent could reduce the retention time of the enantiomers of compounds **1** and **2**. The resolution of compound **2** was achieved successfully in the ethanol solvent system, but the resolution of compound **1** was poor when ethanol was used as mobile phase. *v)* Compound **1** could be enantioseparated when acetonitrile was used as organic cosolvent in the mobile phase, but the resolution was poor for compound **2** in the same mobile phase. Thus slight modification in the substitution pattern influences heavily affected the behavior of the flavanones on the same CSP.

3.2. *Online coupling HPLC-CD*

Elution order between a pair of enantiomers is a key theme in the field of chiral HPLC, but until now prediction of elution order remains difficult. An online HPLC-CD method is quite useful to trace the elution order between enantiomers in a given selector system. In addition to obtaining a CD signal at a chosen wave length, the method could also afford the complete CD spectrum of the eluting peak in a stop-flow mode. As shown in Figure 4, the CD signals at 284 nm were obtained for compounds **1** and **2** in a continuous flow mode. Although the use of ethanol for compound **1** and acetonitrile for compound **2** as organic modifier did not afford good resolution as detected by UV (Figure 3),
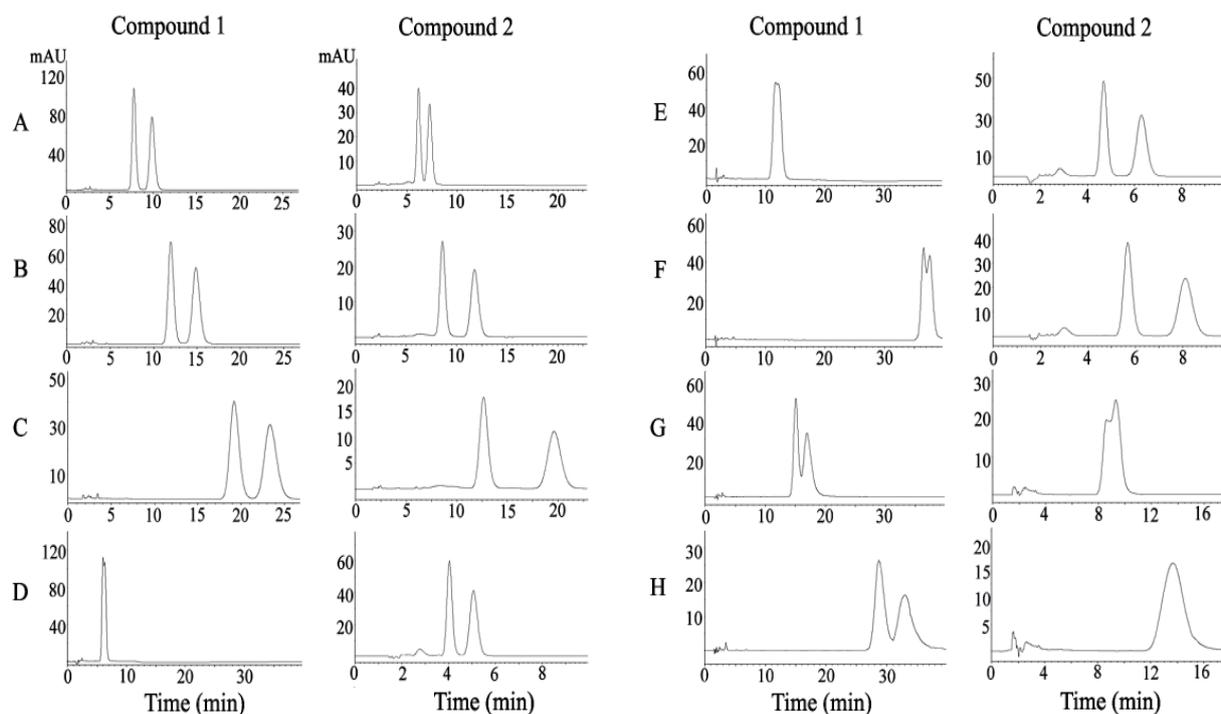
Figure 3. Typical HPLC chromatograms of enantiomeric resolution of compounds 1 and 2 on Chiralpak AD-RH column. Mobile phase: **(A)** methanol-H_2O doped with 0.1% TFA, 95:5 (v/v); **(B)** methanol-H_2O doped with 0.1% TFA, 90:10 (v/v); **(C)** methanol-H_2O doped with 0.1% TFA, 85:15 (v/v); **(D)** ethanol-H_2O doped with 0.1% TFA, 80:20 (v/v); **(E)** ethanol-H_2O doped with 0.1% TFA, 75:25 (v/v); **(F)** ethanol-H_2O doped with 0.1% TFA, 70:30 (v/v); **(G)** acetonitrile-H_2O doped with 0.1% TFA, 35:65 (v/v); **(H)** acetonitrile-H_2O doped with 0.1% TFA, 30:70 (v/v).
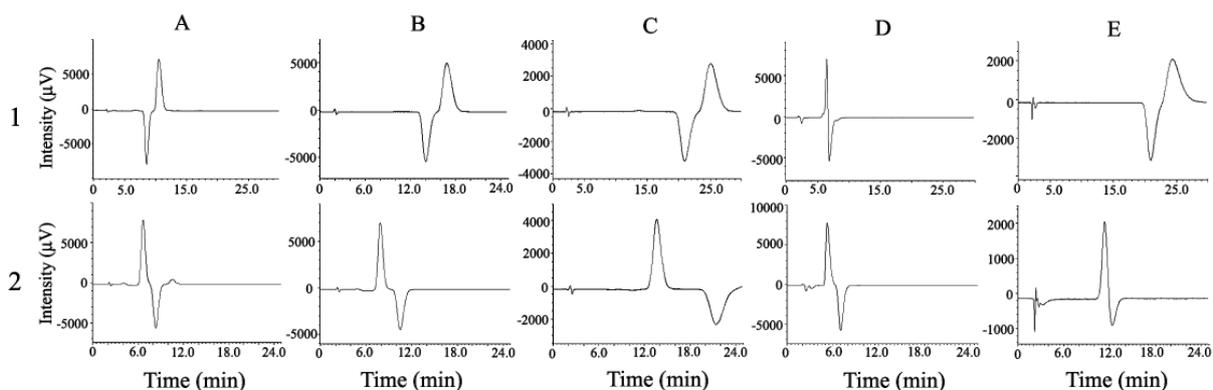
Figure 4. HPLC-CD chromatograms at 284 nm for compounds 1 and 2 on Chiralpak AD-RH. Mobile phase: **(A)** methanol-H_2O doped with 0.1% TFA, 95:5 (v/v); **(B)** methanol-H_2O doped with 0.1% TFA, 90:10 (v/v); **(C)** methanol-H_2O doped with 0.1% TFA, 85:15 (v/v); **(D)** ethanol-H_2O doped with 0.1% TFA, 70:30 (v/v); **(E)** acetonitrile-H_2O doped with 0.1% TFA, 30:70 (v/v).

clear negative signals and positive signals still could be seen in the CD traces.

It has been previously reported that a negative CD signal at 280-290 nm of flavanone is related to the *S*-configuration at C-2, whereas a positive CD signal at 290 nm established an *R*-configuration (*18*). Based on this, the elution order can be easily determined. As evidenced by the positive and negative CD signals at 284 nm, the opposite elution order of compounds **1** and **2** was observed by using methanol and acetonitrile as organic modifiers. For compound **1**, the *S*-enantiomer eluted as the first peak, but eluted as the second for compound **2**. When ethanol was used as organic

modifier, the elution order is the same for the two pairs of enantiomers, *i.e.* the first eluted enantiomers are the *R*-configuration and the second eluted are the *S*-configuration. These phenomena indicated that the introduction of OH in position 3' might increase the possibility of additional hydrogen bonding between the compound and the CSP, and this kind of bonding might play a key role in the chiral recognition process. It has been reported that by changing the percentage of polar alcohol in the mobile phase you could induce an elution order reversal (*19,20*). In this experiment, the solvent-induced elution order reversal only took place by changing the type of organic modifier, no enantiomeric
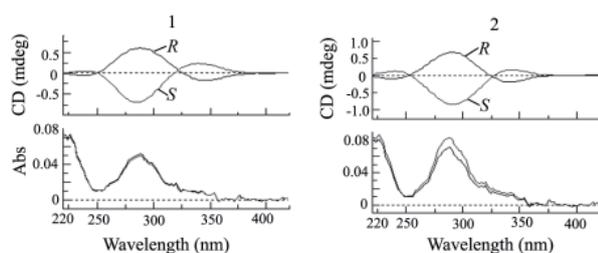
Figure 5. CD spectra of the eluted peaks of compounds 1 and 2 in HPLC-CD online coupling. CSP: Chiralpak AS-RH; mobile phase: methanol-H$_2$O doped with 0.1% TFA, 90:10 (v/v).

elution order reversal was observed by changing the concentration of organic cosolvent (Figure 4).

The online CD spectra of the enantiomers of compounds **1** and **2** were obtained using the stop-flow mode (Figure 5). The complete CD spectra of the two compounds are very similar, with the typical characteristics of a flavanone, *i.e.* as the signs at 280-290 nm for the π→π* absorption band and at 330-340 nm for the n→π* absorption band are related to the absolute configuration.

4. Conclusion

In summary, two amylose-based CSPs, Chiralpak AD-RH and Chiralpak AS-RH, were used for the enantioseparation of naringenin and eriodictyol. The Chiralpak AD-RH column was found to be more selective for the chiral resolution of the two flavanones. The separation of the enantiomers was optimized by varying the chromatographic parameters. The resolution was found to depend on the nature and concentration of organic modifier in the mobile phase. The 3',4' substituent pattern of the compounds affected the enantioselectivity on the same CSP. The HPLC-CD coupling technique was used for the configuration determination of the enantiomers. Elution order reversal was observed by changing the type of organic modifier in the mobile phase.

Acknowledgements

References

1. Cavia-Saiz M, Busto MD, Pilar-Izquierdo MC, Ortega N, Perez-Mateos M, Muñiz P. Antioxidant properties, radical scavenging activity and biomolecule protection capacity of flavonoid naringenin and its glycoside naringin: A comparative study. J Sci Food Agric. 2010; 90:1238-1244.
2. Park HY, Kim GY, Choi YH. Naringenin attenuates the release of pro-inflammatory mediators from lipopolysaccharide-stimulated BV2 microglia by inactivating nuclear factor-κB and inhibiting mitogen-activated protein kinases. Int J Mol Med. 2012; 30:204-210.
3. Sabarinathan D, Mahalakshmi P, Vanisree AJ. Naringenin, a flavanone inhibits the proliferation of cerebrally implanted C6 glioma cells in rats. Chem Biol Interact. 2011; 189:26-36.
4. Sabarinathan D, Mahalakshmi P, Vanisree AJ. Naringenin promotes apoptosis in cerebrally implanted C6 glioma cells. Mol Cell Biochem. 2010; 345:215-222.
5. Qin L, Jin L, Lu L, Lu X, Zhang C, Zhang F, Liang W. Naringenin reduces lung metastasis in a breast cancer resection model. Protein Cell. 2011; 2:507-516.
6. Cho KW, Kim YO, Andrade JE, Burgess JR, Kim YC. Dietary naringenin increases hepatic peroxisome proliferators-activated receptor α protein expression and decreases plasma triglyceride and adiposity in rats. Eur J Nutr. 2011; 50:81-88.
7. Goldwasser J, Cohen PY, Yang E, Balaguer P, Yarmush ML, Nahmias Y. Transcriptional regulation of human and rat hepatic lipid metabolism by the grapefruit flavonoid naringenin: Role of PPAR-α, PPAR-γ and LXR-α. PLoS One. 2010; 5:e12399.
8. Annadurai T, Muralidharan AR, Joseph T, Hsu MJ, Thomas PA, Geraldine P. Antihyperglycemic and antioxidant effects of a flavanone, naringenin, in streptozotocin-nicotinamide-induced experimental diabetic rats. J Physiol Biochem. 2012; 68:307-318.
9. Chanet A, Milenkovic D, Deval C, Potier M, Constans J, Mazur A, Bennetau-Pelissero C, Morand C, Bérard AM. Naringin, the major grapefruit flavonoid, specifically affects atherosclerosis development in diet-induced hypercholesterolemia in mice. J Nutr Biochem. 2012; 23:469-477.
10. Lee ER, Kim JH, Choi HY, Jeon K, Cho SG. Cytoprotective effect of eriodictyol in UV-irradiated keratinocytes via phosphatase-dependent modulation of both the p38 MAPK and Akt signaling pathways. Cell Physiol Biochem. 2011; 27:513-524.
11. Johnson J, Maher P, Hanneken A. The flavonoid, eriodictyol, induces long-term protection in ARPE-19 cells through its effects on Nrf2 activation and phase 2 gene expression. Invest Ophthalmol Vis Sci. 2009; 50:2398-2406.
12. Bucolo C, Leggio GM, Drago F, Salomone S. Eriodictyol prevents early retinal and plasma abnormalities in streptozotocin-induced diabetic rats. Biochem Pharmacol. 2012; 84:88-92.
13. Pan J, Zhang S, Yan L, Tai J, Xiao Q, Zou K, Zhou Y, Wu J. Separation of flavanone enantiomers and flavanone glucoside diastereomers from *Balanophora involucrata* Hook. f. by capillary electrophoresis and reversed-phase high-performance liquid chromatography on a C18 column. J Chromatogr A. 2008; 1185:117-129.
14. Asztemborska M, Miskiewicz M, Sybilska, D. Separation of some chiral flavanones by micellar electrokinetic chromatography. Electrophoresis. 2003; 24:2527-2531.
15. Caccamese S, Caruso C, Parrinello N, Savarino A. High-performance liquid chromatographic separation and chiroptical properties of the enantiomers of naringenin and other flavanones. J Chromatogr A. 2005; 1076:155-162.
16. Yáñez JA, Miranda ND, Remsberg CM, Ohgami Y, Davies NM. Stereospecific high-performance liquid chromatographic analysis of eriodictyol in urine. J Pharm Biomed Anal. 2007; 43:255-262.

17. Yáñez JA, Davies NM. Stereospecific high-performance liquid chromatographic analysis of naringenin in urine. J Pharm Biomed Anal. 2005; 39:164-169.

18. Ren DM, Guo HF, Yu WT, Wang SQ, Ji M, Lou HX. Stereochemistry of flavonoidal alkaloids from *Dracocephalum rupestre*. Phytochemistry. 2008; 69:1425-1433.

19. Cirilli R, Ferretti R, De Santis E, Gallinella B, Zanitti L, La Torre F. High-performance liquid chromatography separation of enantiomers of flavanone and 2'-hydroxy- chalcone under reversed-phase conditions. J Chromatogr A. 2008; 1190:95-101.

20. Xiang C, Liu G, Kang S, Guo X, Yao B, Weng W, Zeng Q. Unusual chromatographic enantioseparation behavior of naproxen on an immobilized polysaccharide- based chiral stationary phase. J Chromatogr A. 2011; 1218:8718-8721.

Attenuation of tumor growth by honokiol: An evolving role in oncology

Shailendra Kapoor*

Mechanicsville, VA, USA.

ABSTRACT: *Honokiol may exert significant anti-neoplastic effects in other systemic tumors besides skin cancers by virtue of modulation of other pathways. For instance, honokiol attenuates tumor growth in mammary malignancies. It mediates its anti-neoplastic role in these tumors by accentuating the phosphorylation of AMPK. As a result, honokiol causes significant mitigation of tumor proliferation and growth.*

Guillermo *et al*. have provided great insight into the role of honokiol in management of skin cancers (*1*). Honokiol may exert significant anti-neoplastic effects in other systemic tumors besides skin cancers by virtue of modulation of other pathways.

Honokiol attenuates tumor growth in mammary malignancies. It mediates its anti-neoplastic role in these tumors by accentuating the phosphorylation of 5' adenosine monophosphate-activated protein kinase (AMPK). AMPK in turn affects the pACC-pS6K pathway (*2*). Nitric oxide (NO) levels are also significantly attenuated. Nuclear factor kappa B (NF-κB) activity is also reduced by honokiol. Besides this, honokiol also augments cytoplasmic translocation of liver kinase B1 (LKB1) resulting in attenuated invasiveness as well as migration of the cancer cells. As a result, honokiol causes significant mitigation of tumor proliferation and growth. Intracellular cGMP levels are also decreased markedly (*3*). Besides these effects honokiol also causes inhibition of cyclooxygenase-2. Interestingly, honokiol also exhibits synergism with chemotherapeutic agents such as rapamycin by accentuating the inhibition of the PI3K/Akt/mTOR pathway (*4*).

Similar effects are seen in gastric carcinomas. Honokiol administration results in attenuated activation of the signal transducer and activator of transcription 3 (STAT3) pathway (*5*). It mediates this effect by up-regulating SPH-1. Honokiol also augments calpain-II-mediated cleavage of GRP94 thus augmenting intra-tumoral apoptosis (*6*). Simultaneous decrease in intra-tumoral production of VEGF is also seen. As a result, intra-tumoral angiogenesis is markedly decreased. Honokiol also decreases growth in colo-rectal malignancies. It mediates this role by modulating the Notch pathway (*7*). Doublecortin-like kinase 1 (DCLK1) expression is markedly down-regulated. Besides this inhibition of γ-secretase is also seen. These effects are especially more pronounced when honokiol is used in conjunction with ionizing radiation. In fact, honokiol increases the radio-sensitivity of colorectal cancer cells. Hes-1 levels are also attenuated (*8*). APH-1 is also decreased. Cyclin D1 expression is down-regulated while the Bax/Bcl-2 ratio is increased. Similar effects are seen in pancreatic malignancies. It mediates this role by increasing p27 levels. On the other hand, Cdk4 expression is down regulated. This results in attenuated IκB-α phosphorylation as well as augmented accumulation of NF-κB in the cytoplasm of the cancerous cells (*9*). Honokiol especially augments and increases the anti-proliferative and apoptotic effects of other chemotherapeutic agents such as gemcitabine.

As is evident from the above examples honokiol exerts significant anti-neoplastic activity in a number of systemic tumors. Hopefully, the coming few years will see increased use of honokiol for mitigating tumor growth.

References

1   Guillermo RF, Chilampalli C, Zhang X, Zeman D, Fahmy H, Dwivedi C. Time and dose-response effects of honokiol on UVB-induced skin cancer development. Drug Discov Ther. 2012; 6:140-146.
2   Nagalingam A, Arbiser JL, Bonner MY, Saxena NK, Sharma D. Honokiol activates AMP-activated protein kinase in breast cancer cells *via* an LKB1-dependent pathway and inhibits breast carcinogenesis. Breast Cancer Res. 2012; 14:

**Address correspondence to:*
Dr. Shailendra Kapoor, 74 crossing, Mechanicsville, VA, USA.
E-mail: shailendrakapoor@yahoo.com

R35.

3   Singh T, Katiyar SK. Honokiol, a phytochemical from Magnolia spp., inhibits breast cancer cell migration by targeting nitric oxide and cyclooxygenase-2. Int J Oncol. 2011; 38:769-776.

4   Liu H, Zang C, Emde A. Anti-tumor effect of honokiol alone and in combination with other anti-cancer agents in breast cancer. Eur J Pharmacol. 2008; 591:43-51.

5   Liu SH, Wang KB, Lan KH. Calpain/SHP-1 interaction by honokiol dampening peritoneal dissemination of gastric cancer in nu/nu mice. PLoS One. 2012; 7:e43711.

6   Sheu ML, Liu SH, Lan KH. Honokiol induces calpain-mediated glucose-regulated protein-94 cleavage and apoptosis in human gastric cancer cells and reduces tumor

growth. PLoS One. 2007; 2:e1096.

7   Ponnurangam S, Mammen JM, Ramalingam S. Honokiol in combination with radiation targets notch signaling to inhibit colon cancer stem cells. Mol Cancer Ther. 2012; 11:963-972.

8   He Z, Subramaniam D, Ramalingam S. Honokiol radiosensitizes colorectal cancer cells: Enhanced activity in cells with mismatch repair defects. Am J Physiol Gastrointest Liver Physiol. 2011; 301:G929-G937.

9   Arora S, Bhardwaj A, Srivastava SK. Honokiol arrests cell cycle, induces apoptosis, and potentiates the cytotoxic effect of gemcitabine in human pancreatic cancer cells. PLoS One. 2011; 6:e21573.

(Received November 20, 2012)

Author Index (*2012*)

Subject Index (2012)

Reviews

Evidence-based research on traditional Japanese medicine, Kampo, in treatment of gastrointestinal cancer in Japan.
Gao JJ, Song PP, Qi FH, Kokudo N, Qu XJ, Tang W
2012; 6(1):1-8. (DOI: 10.5582/ddt.2012.v6.1.1)

Up-frameshift protein 1 (UPF1): Multitalented entertainer in RNA decay.
Imamachi N, Tani H, Akimitsu N
2012; 6(2):55-61. (DOI: 10.5582/ddt.2012.v6.2.55)

Monoamine oxidases in major depressive disorder and alcoholism.
Duncan J, Johnson S, Ou XM
2012; 6(3):112-122. (DOI: 10.5582/ddt.2012.v6.3.112)

Improved treatment of nicotine addiction and emerging pulmonary drug delivery.
Islam N, Rahman S
2012; 6(3):123-132. (DOI: 10.5582/ddt.2012.v6.3.123)

Research progress in the radioprotective effect of superoxide dismutase.
Huang XJ, Song CX, Zhong CQ, Wang FS
2012; 6(4):169-177. (DOI: 10.5582/ddt.2012.v6.4.169)

An overview on antiepileptic drugs.
Das N, Dhanawat M, Shrivastava SK
2012; 6(4):178-193. (DOI: 10.5582/ddt.2012.v6.4.178)

Topoisomerase IIα, rather than IIβ, is a promising target in development of anti-cancer drugs.
Chen W, Qiu J, Shen YM
2012; 6(5):230-237. (DOI: 10.5582/ddt.2012.v6.5.230)

Review of drugs for Alzheimer's disease.
Sun XT, Jin L, Ling PX
2012; 6(6):285-290. (DOI: 10.5582/ddt.2012.v6.6.285)

Brief Reports

Synthesis of solasodine glycoside derivatives and evaluation of their cytotoxic effects on human cancer cells.
Cui CZ, Wen XS, Cui M, Gao J, Sun B, Lou HX
2012; 6(1):9-17. (DOI: 10.5582/ddt.2012.v6.1.9)

Identification and evaluation of agents isolated from traditionally used herbs against *Ophiophagus hannah* venom.
Salama R, Sattayasai J, Gande AK, Sattayasai N, Davis M, Lattmann E
2012; 6(1):18-23. (DOI: 10.5582/ddt.2012.v6.1.18)

Synthesis and anticancer activity of novel 5-(indole-2-yl)-3-substituted 1,2,4-oxadiazoles.
Wang P, Liu JZ, Xing HL, Liu Y, Xie WC, Zhao GS
2012; 6(3):133-139. (DOI: 10.5582/ddt.2012.v6.3.133)

Anti-inflammatory activities of fractions from *Geranium nepalense* and related polyphenols.
Lu CH, Li YY, Li LJ, Liang LY, Shen YM
2012; 6(4):194-197. (DOI: 10.5582/ddt.2012.v6.4.194)

A new boronic acid-based fluorescent sensor for L-dihydroxyphenylalanine.
Wu ZY, Yang XY, Xu WF, Wang BH, Fang H
2012; 6(5):238-241. (DOI: 10.5582/ddt.2012.v6.5.238)

Original Articles

***LKB1*, *TP16*, *EGFR*, and *KRAS* somatic mutations in lung adenocarcinomas from a Chiba Prefecture, Japan cohort.**
Suzuki Y, Oonishi T, Kudo T, Doi H
2012; 6(1):24-30. (DOI: 10.5582/ddt.2012.v6.1.24)

Inhibition of morphine tolerance is mediated by painful stimuli *via* central mechanisms.
Iwai S, Kiguchi N, Kobayashi Y, Fukazawa Y, Saika F, Ueno K, Yamamoto C, Kishioka S
2012; 6(1):31-37. (DOI: 10.5582/ddt.2012.v6.1.31)

Comparison of antioxidant activity of compounds isolated from guava leaves and a stability study of the most active compound.
Nantitanon W, Okonogi S
2012; 6(1):38-43. (DOI: 10.5582/ddt.2012.v6.1.38)

A novel flow-injection analysis system for evaluation of antioxidants by using sodium dichloroisocyanurate as a source of hypochlorite anion.
Ichiba H, Hanami K, Yagasaki K, Tanaka M, Ito H, Fukushima T
2012; 6(1):44-48. (DOI: 10.5582/ddt.2012.v6.1.44)

Stability-indicating HPLC method for the determination of the stability of oxytocin parenteral solutions prepared in polyolefin bags.
Kaushal G, Sayre BE, Prettyman T
2012; 6(1):49-54. (DOI: 10.5582/ddt.2012.v6.1.49)

A facile method for the synthesis of *N*-(α-aminoacyl) sulfonamides.
Wu SL, Chen ML, Wang YT, Hou XB, Yang XY, Su L, Fang H
2012; 6(2):62-68. (DOI: 10.5582/ddt.2012.v6.2.62)

In silico ligand based design of indolylpiperidinyl derivatives as novel histamine H$_1$ receptor antagonists.
Paliwal S, Singh S, Pal M
2012; 6(2):69-77. (DOI: 10.5582/ddt.2012.v6.2.69)

Synthesis, analgesic, anti-inflammatory and ulcerogenic properties of some novel *N'*-((1-(substituted amino)methyl)-2-oxoindolin-3-ylidene)-4-(2-(methyl/phenyl)-4-oxoquinazolin-3(4*H*)-yl)benzohydrazide derivatives.
Saravanan G, Alagarsamy V, Prakash CR
2012; 6(2):78-87. (DOI: 10.5582/ddt.2012.v6.2.78)

Evaluation of innate immune stimulating activity of polysaccharides using a silkworm (*Bombyx mori*) muscle contraction assay.
Fujiyuki T, Hamamoto H, Ishii K, Urai M, Kataoka K, Takeda T, Shibata S, Sekimizu K
2012; 6(2):88-93. (DOI: 10.5582/ddt.2012.v6.2.88)

Regulation of Janus-activated kinase-2 (JAK2) by diindolylmethane in ovarian cancer *in vitro* and *in vivo*.

Kandala PK, Srivastava SK
2012; 6(2):94-101. (DOI: 10.5582/ddt.2012.v6.2.94)

Analyzing global trends of biomarker use in drug interventional clinical studies.
Hayashi K, Masuda S, Kimura H
2012; 6(2):102-107. (DOI: 10.5582/ddt.2012.v6.2.102)

Time and dose-response effects of honokiol on UVB-induced skin cancer development.
Guillermo RF, Chilampalli C, Zhang X, Zeman D, Fahmy H, Dwivedi C
2012; 6(3):140-146. (DOI: 10.5582/ddt.2012.v6.3.140)

Ameliorating effect of DL-α-lipoic acid against cisplatin-induced nephrotoxicity and cardiotoxicity in experimental animals.
Hussein A, Ahmed AAE, Shouman SA, Sharawy S
2012; 6(3):147-156. (DOI: 10.5582/ddt.2012.v6.3.147)

Evaluation of skin surface hydration state and barrier function of stratum corneum of dorsa of hands and heels treated with PROTECT X2 skin protective cream.
Kubota T
2012; 6(3):157-162. (DOI: 10.5582/ddt.2012.v6.3.157)

Effect of surfactant on lycopene-loaded nanostructured lipid carriers.
Riangjanapatee P, Okonogi S
2012; 6(3):163-168. (DOI: 10.5582/ddt.2012.v6.3.163)

Synthesis and structure-activity relationship study of 2-(substituted benzylidene)-7-(4-fluorophenyl)-5-(furan-2-yl)-2*H*-thiazolo[3,2-*a*]pyrimidin-3(7*H*)-one derivatives as anticancer agents.
Selvam TP, Karthick V, Kumar PV, Ali MA
2012; 6(4):198-204. (DOI: 10.5582/ddt.2012.v6.4.198)

Antioxidant and hepatoprotective activity of an ethanol extract of *Syzygium jambos* (L.) leaves.
Islam MR, Parvin MS, Islam ME
2012; 6(4):205-211. (DOI: 10.5582/ddt.2012.v6.4.205)

Antimicrobial screening of some Egyptian plants and active flavones from *Lagerstroemia indica* leaves.
Diab Y, Atalla K, Elbanna K
2012; 6(4):212-217. (DOI: 10.5582/ddt.2012.v6.4.212)

Optimization of cell-wall skeleton derived from *Mycobacterium bovis* BCG Tokyo 172 (SMP-105) emulsion in delayed-type hypersensitivity and antitumor models.
Miyauchi M, Murata M, Fukushima A, Sato T, Nakagawa M, Fujii T, Koseki N, Chiba N, Kashiwazaki Y
2012; 6(4):218-225. (DOI: 10.5582/ddt.2012.v6.4.218)

Cloning and expression analysis of squalene synthase, a key enzyme involved in antifungal steroidal glycoalkaloids biosynthesis from *Solanum nigrum*.
Sun Y, Zhao Y, Wang L, Lou HX, Cheng AX
2012; 6(5):242-248. (DOI: 10.5582/ddt.2012.v6.5.242)

Enhancement of anti-cholinesterase activity of *Zingiber cassumunar* essential oil using a microemulsion technique.
Okonogi S, Chaiyana W
2012; 6(5):249-255. (DOI: 10.5582/ddt.2012.v6.5.249)

Subcutaneous concentrations following topical iontophoretic delivery of diclofenac.
Kasha PC, Anderson CR, Morris RL, Sembrowich WL, Chaturvedula A, Banga AK

Case Report

Commentary

Letters

A comment on: *Research progress in the radioprotective effect of superoxide dismutase.*
Bhandari PR
2012; 6(5):283-284. (DOI: 10.5582/ddt.2012.v6.5.283)

Attenuation of tumor growth by honokiol: An evolving role in oncology.
Kapoor S
2012; 6(6):327-328. (DOI: 10.5582/ddt.2012.v6.6.327)

Guide for Authors

1. Scope of Articles

Drug Discoveries & Therapeutics welcomes contributions in all fields of pharmaceutical and therapeutic research such as medicinal chemistry, pharmacology, pharmaceutical analysis, pharmaceutics, pharmaceutical administration, and experimental and clinical studies of effects, mechanisms, or uses of various treatments. Studies in drug-related fields such as biology, biochemistry, physiology, microbiology, and immunology are also within the scope of this journal.

2. Submission Types

Original Articles should be well-documented, novel, and significant to the field as a whole. An Original Article should be arranged into the following sections: Title page, Abstract, Introduction, Materials and Methods, Results, Discussion, Acknowledgments, and References. Original articles should not exceed 5,000 words in length (excluding references) and should be limited to a maximum of 50 references. Articles may contain a maximum of 10 figures and/or tables.

Brief Reports definitively documenting either experimental results or informative clinical observations will be considered for publication in this category. Brief Reports are not intended for publication of incomplete or preliminary findings. Brief Reports should not exceed 3,000 words in length (excluding references) and should be limited to a maximum of 4 figures and/or tables and 30 references. A Brief Report contains the same sections as an Original Article, but the Results and Discussion sections should be combined.

Reviews should present a full and up-to-date account of recent developments within an area of research. Normally, reviews should not exceed 8,000 words in length (excluding references) and should be limited to a maximum of 100 references. Mini reviews are also accepted.

Policy Forum articles discuss research and policy issues in areas related to life science such as public health, the medical care system, and social science and may address governmental issues at district, national, and international levels of discourse. Policy Forum articles should not exceed 2,000 words in length (excluding references).

Case Reports should be detailed reports of the symptoms, signs, diagnosis, treatment, and follow-up of an individual patient. Case reports may contain a demographic profile of the patient but usually describe an unusual or novel occurrence. Unreported or unusual side effects or adverse interactions involving medications will also be considered. Case Reports should not exceed 3,000 words in length (excluding references).

News articles should report the latest events in health sciences and medical research from around the world. News should not exceed 500 words in length.

Letters should present considered opinions in response to articles published in Drug Discoveries & Therapeutics in the last 6 months or issues of general interest. Letters should not exceed 800 words in length and may contain a maximum of 10 references.

3. Editorial Policies

Ethics: Drug Discoveries & Therapeutics requires that authors of reports of investigations in humans or animals indicate that those studies were formally approved by a relevant ethics committee or review board.

Conflict of Interest: All authors are required to disclose any actual or potential conflict of interest including financial interests or relationships with other people or organizations that might raise questions of bias in the work reported. If no conflict of interest exists for each author, please state "There is no conflict of interest to disclose".

Submission Declaration: When a manuscript is considered for submission to Drug Discoveries & Therapeutics, the authors should confirm that 1) no part of this manuscript is currently under consideration for publication elsewhere; 2) this manuscript does not contain the same information in whole or in part as manuscripts that have been published, accepted, or are under review elsewhere, except in the form of an abstract, a letter to the editor, or part of a published lecture or academic thesis; 3) authorization for publication has been obtained from the authors' employer or institution; and 4) all contributing authors have agreed to submit this manuscript.

Cover Letter: The manuscript must be accompanied by a cover letter signed by the corresponding author on behalf of all authors. The letter should indicate the basic findings of the work and their significance. The letter should also include a statement affirming that all authors concur with the submission and that the material submitted for publication has not been published previously or is not under consideration for publication elsewhere. The cover letter should be submitted in PDF format. For example of Cover Letter, please visit http://www.ddtjournal.com/downcentre.php (Download Centre).

Copyright: A signed JOURNAL PUBLISHING AGREEMENT (JPA) must be provided by post, fax, or as a scanned file before acceptance of the article. Only forms with a hand-written signature are accepted. This copyright will ensure the widest possible dissemination of information. A form facilitating transfer of copyright can be downloaded by clicking the appropriate link and can be returned to the e-mail address or fax number noted on the form (Please visit Download Centre). Please note that your manuscript will not proceed to the next step in publication until the JPA form is received. In addition, if excerpts from other copyrighted works are included, the author(s) must obtain written permission from the copyright owners and credit the source(s) in the article.

Suggested Reviewers: A list of up to 3 reviewers who are qualified to assess the scientific merit of the study is welcomed. Reviewer information including names, affiliations, addresses, and e-mail should be provided at the same time the manuscript is submitted online. Please do not suggest reviewers with known conflicts of interest, including participants or anyone with a stake in the proposed research; anyone from the same institution; former students, advisors, or research collaborators (within the last three years); or close personal contacts. Please note that the Editor-in-Chief may accept one or more of the proposed reviewers or may request a review by other qualified persons.

Language Editing: Manuscripts prepared by authors whose native language is not English should have their work proofread by a native English speaker before submission. If not, this might delay the publication of your manuscript in Drug Discoveries & Therapeutics.

The Editing Support Organization can provide English proofreading, Japanese-English translation, and Chinese-English translation services to authors who want to publish in Drug Discoveries & Therapeutics and need assistance before submitting a manuscript. Authors can visit this organization directly at http://www.iacmhr.com/iac-eso/support.php?lang=en. IAC-ESO was established to facilitate manuscript preparation by researchers whose native language is not English and to help edit works intended for international academic journals.

4. Manuscript Preparation

Manuscripts should be written in clear, grammatically correct English and submitted as a Microsoft Word file in a single-column format. Manuscripts must be paginated and typed in 12-point Times New Roman font with 24-point line spacing. Please do not embed figures in the text. Abbreviations should be used as little as possible and should be explained at first mention unless the term is a well-known abbreviation (*e.g.* DNA). Single words should not be abbreviated.

Title page: The title page must include 1) the title of the paper (Please note the title should be short, informative, and contain the major key words); 2) full name(s) and affiliation(s) of the author(s), 3) abbreviated names of the author(s), 4) full name, mailing address, telephone/fax numbers, and e-mail address of the corresponding author; and 5) conflicts of interest (if you have an actual or potential conflict of interest to disclose, it must be included as a footnote on the title page of the manuscript; if no conflict of interest exists for each author, please state "There is no conflict of interest to disclose"). Please visit Download Centre and refer to the title page of the manuscript sample.

Abstract: A one-paragraph abstract consisting of no more than 250 words must be included. The abstract should briefly state the purpose of the study, methods, main findings, and conclusions. Abbreviations must be kept to a minimum and non-standard abbreviations explained in brackets at first mention. References should be avoided in the abstract. Key words or phrases that do not occur in the title should be included in the Abstract page.

Introduction: The introduction should be a concise statement of the basis for the study and its scientific context.

Materials and Methods: The description should be brief but with sufficient detail to enable others to reproduce the experiments. Procedures that have been published previously should not be described in detail but appropriate references should simply be cited. Only new and significant modifications of previously published procedures require complete description. Names of products and manufacturers with their locations (city and state/country) should be given and sources of animals and cell lines should always be indicated. All clinical investigations must have been conducted in accordance with Declaration of Helsinki principles. All human and animal studies must have been approved by the appropriate institutional review board(s) and a specific declaration of approval must be made within this section.

Results: The description of the experimental results should be succinct but in sufficient detail to allow the experiments to be analyzed and interpreted by an independent reader. If necessary, subheadings may be used for an orderly presentation. All figures and tables must be referred to in the text.

Discussion: The data should be interpreted concisely without repeating material already presented in the Results section. Speculation is permissible, but it must be well-founded, and discussion of the wider implications of the findings is encouraged. Conclusions derived from the study should be included in this section.

Acknowledgments: All funding sources should be credited in the Acknowledgments section. In addition, people who contributed to the work but who do not meet the criteria for authors should be listed along with their contributions.

References: References should be numbered in the order in which they appear in the text. Citing of unpublished results, personal communications, conference abstracts, and theses in the reference list is not recommended but these sources may be mentioned in the text. In the reference list, cite the names of all authors when there are fifteen or fewer authors; if there are sixteen or more authors, list the first three followed by *et al*. Names of journals should be abbreviated in the style used in PubMed. Authors are responsible for the accuracy of the references. Examples are given below:

Example 1 (Sample journal reference):
Nakata M, Tang W. Japan-China Joint Medical Workshop on Drug Discoveries and Therapeutics 2008: The need of Asian pharmaceutical researchers' cooperation. Drug Discov Ther. 2008; 2:262-263.

Example 2 (Sample journal reference with more than 15 authors):
Darby S, Hill D, Auvinen A, *et al*. Radon in homes and risk of lung cancer: Collaborative analysis of individual data from 13 European case-control studies. BMJ. 2005; 330:223.

Example 3 (Sample book reference):
Shalev AY. Post-traumatic stress disorder: Diagnosis, history and life course. In: Post-traumatic Stress Disorder, Diagnosis, Management and Treatment (Nutt DJ, Davidson JR, Zohar J, eds.). Martin Dunitz, London, UK, 2000; pp. 1-15.

Example 4 (Sample web page reference):
World Health Organization. The World Health Report 2008 – primary health care: Now more than ever. *http://www.who.int/whr/2008/whr08_en.pdf* (accessed September 23, 2010).

Tables: All tables should be prepared in Microsoft Word or Excel and should be arranged at the end of the manuscript after the References section. Please note that tables should not in image format. All tables should have a concise title and should be numbered consecutively with Arabic numerals. If necessary, additional information should be given below the table.

Figure Legend: The figure legend should be typed on a separate page of the main manuscript and should include a short title and explanation. The legend should be concise but comprehensive and should be understood without referring to the text. Symbols used in figures must be explained.

Figure Preparation: All figures should be clear and cited in numerical order in the text. Figures must fit a one- or two-column format on the journal page: 8.3 cm (3.3 in.) wide for a single column, 17.3 cm (6.8 in.) wide for a double column; maximum height: 24.0 cm (9.5 in.). Please make sure that artwork files are in an acceptable format (TIFF or JPEG) at minimum resolution (600 dpi for illustrations, graphs, and annotated artwork, and 300 dpi for micrographs and photographs). Please provide all figures as separate files. Please note that low-resolution images are one of the leading causes of article resubmission and schedule delays. All color figures will be reproduced in full color in the online edition of the journal at no cost to authors.

Units and Symbols: Units and symbols conforming to the International System of Units (SI) should be used for physicochemical quantities. Solidus notation (*e.g.* mg/kg, mg/mL, mol/mm^2/min) should be used. Please refer to the SI Guide www.bipm.org/en/si/ for standard units.

Supplemental data: Supplemental data might be useful for supporting and enhancing your scientific research and Drug Discoveries & Therapeutics accepts the submission of these materials which will be only published online alongside the electronic version of your article. Supplemental files (figures, tables, and other text materials) should be prepared according to the above guidelines, numbered in Arabic numerals (*e.g.*, Figure S1, Figure S2, and Table S1, Table S2) and referred to in the text. All figures and tables should have titles and legends. All figure legends, tables and supplemental text materials should be placed at the end of the paper. Please note all of these supplemental data should be provided at the time of initial submission and note that the editors reserve the right to limit the size and length of Supplemental Data.

5. Submission Checklist

The Submission Checklist will be useful during the final checking of a manuscript prior to sending it to Drug Discoveries & Therapeutics for review. Please visit Download Centre and download the Submission Checklist file.

6. Online submission

Manuscripts should be submitted to Drug Discoveries & Therapeutics online at http://www.ddtjournal.com. The manuscript file should be smaller than 5 MB in size. If for any reason you are unable to submit a file online, please contact the Editorial Office by e-mail at office@ddtjournal.com

7. Accepted manuscripts

Proofs: Galley proofs in PDF format will be sent to the corresponding author *via* e-mail. Corrections must be returned to the editor (proof-editing@ddtjournal.com) within 3 working days.

Offprints: Authors will be provided with electronic offprints of their article. Paper offprints can be ordered at prices quoted on the order form that accompanies the proofs.

Page Charge: A page charge of $140 will be assessed for each printed page of an accepted manuscript. The charge for printing color figures is $340 for each page. Under exceptional circumstances, the author(s) may apply to the editorial office for a waiver of the publication charges at the time of submission.

(Revised October 2011)

DD&T
Drug Discoveries & Therapeutics

JOURNAL PUBLISHING AGREEMENT (JPA)

Manuscript No.:

Title:

Corresponding author:

The International Advancement Center for Medicine & Health Research Co., Ltd. (IACMHR Co., Ltd.) is pleased to accept the above article for publication in Drug Discoveries & Therapeutics. The International Research and Cooperation Association for Bio & Socio-Sciences Advancement (IRCA-BSSA) reserves all rights to the published article. Your written acceptance of this JOURNAL PUBLISHING AGREEMENT is required before the article can be published. Please read this form carefully and sign it if you agree to its terms. The signed JOURNAL PUBLISHING AGREEMENT should be sent to the Drug Discoveries & Therapeutics office (Pearl City Koishikawa 603, 2-4-5 Kasuga, Bunkyo-ku, Tokyo 112-0003, Japan; E-mail: office@ddtjournal.com; Tel: +81-3-5840-9697; Fax: +81-3-5840-9698).

1. Authorship Criteria

As the corresponding author, I certify on behalf of all of the authors that:

1) The article is an original work and does not involve fraud, fabrication, or plagiarism.

2) The article has not been published previously and is not currently under consideration for publication elsewhere. If accepted by Drug Discoveries & Therapeutics, the article will not be submitted for publication to any other journal.

3) The article contains no libelous or other unlawful statements and does not contain any materials that infringes upon individual privacy or proprietary rights or any statutory copyright.

4) I have obtained written permission from copyright owners for any excerpts from copyrighted works that are included and have credited the sources in my article.

5) All authors have made significant contributions to the study including the conception and design of this work, the analysis of the data, and the writing of the manuscript.

6) All authors have reviewed this manuscript and take responsibility for its content and approve its publication.

7) I have informed all of the authors of the terms of this publishing agreement and I am signing on their behalf as their agent.

2. Copyright Transfer Agreement

I hereby assign and transfer to IACMHR Co., Ltd. all exclusive rights of copyright ownership to the above work in the journal Drug Discoveries & Therapeutics, including but not limited to the right 1) to publish, republish, derivate, distribute, transmit, sell, and otherwise use the work and other related material worldwide, in whole or in part, in all languages, in electronic, printed, or any other forms of media now known or hereafter developed and the right 2) to authorize or license third parties to do any of the above.

I understand that these exclusive rights will become the property of IACMHR Co., Ltd., from the date the article is accepted for publication in the journal Drug Discoveries & Therapeutics. I also understand that IACMHR Co., Ltd. as a copyright owner has sole authority to license and permit reproductions of the article.

I understand that except for copyright, other proprietary rights related to the Work (*e.g.* patent or other rights to any process or procedure) shall be retained by the authors. To reproduce any text, figures, tables, or illustrations from this Work in future works of their own, the authors must obtain written permission from IACMHR Co., Ltd.; such permission cannot be unreasonably withheld by IACMHR Co., Ltd.

3. Conflict of Interest Disclosure

I confirm that all funding sources supporting the work and all institutions or people who contributed to the work but who do not meet the criteria for authors are acknowledged. I also confirm that all commercial affiliations, stock ownership, equity interests, or patent-licensing arrangements that could be considered to pose a financial conflict of interest in connection with the article have been disclosed.

Corresponding Author's Name (Signature):

Date:

Drug Discoveries & Therapeutics (www.ddtjournal.com)

Pearl City Koishikawa 603, 2-4-5 Kasuga, Bunkyo-ku, Tokyo 112-0003, Japan; E-mail: office@ddtjournal.com; Tel: +81-3-5840-9697; Fax: +81-3-5840-9698